8-2001

Subgrade resilient modulus testing at Tennessee instrumented pavement sites : standard and alternative methods

Jason Ernest Cathey

To the Graduate Council:

I am submitting herewith a thesis written by Jason Ernest Cathey entitled "Subgrade resilient modulus testing at Tennessee instrumented pavement sites : standard and alternative methods." I have examined the final electronic copy of this thesis for form and content and recommend that it be accepted in partial fulfillment of the requirements for the degree of Master of Science, with a major in Civil Engineering.

Eric C. Drumm, Major Professor

We have read this thesis and recommend its acceptance:

Richard M. Bennett, Edwin Burdette

Accepted for the Council:
Carolyn R. Hodges

Vice Provost and Dean of the Graduate School

(Original signatures are on file with official student records.)

To the Graduate Council:

I am submitting herewith a thesis written by Jason Ernest Cathey entitled "Subgrade Resilient Modulus Testing at Tennessee Instrumented Pavement Sites: Standard and Alternative Methods." I have examined the final copy of the thesis for form and content and recommend that it be accepted in partial fulfillment of the requirements for the degree of Master of Science, with a major in Civil Engineering.

Eric C Drumm

Dr. Eric C. Drumm, Major Professor

We have read this thesis and
recommend its acceptance:

Richard M. Bennett

Edwin G. Burdette

Accepted for the Council:

Interim Vice Provost and
Dean of the Graduate School

SUBGRADE RESILIENT MODULUS TESTING AT TENNESSEE INSTRUMENTED PAVEMENT SITES: STANDARD AND ALTERNATIVE METHODS

A Thesis

Presented for the

Master of Science

Degree

The University of Tennessee, Knoxville

Jason Ernest Cathey

August 2001

Dedication

This thesis is dedicated to my parents, Mrs. Rita Ann Cathey and Mr. Ernest Kennedy Cathey. This thesis would have not been possible without their love, support, and encouragement.

Acknowledgments

I would like to thank Dr. Eric C. Drumm for the opportunity to further my education. This degree would not have been possible without his continual patience and encouragement.

I would also like to thank Dr. Richard M. Bennett and Dr. Edwin Burdette for serving on my graduate committee. The Tennessee Department of Transportation is recognized for their generous financial support.

The laboratory work could not have been completed without the help of Mr. N. Randy Rainwater. Randy's patience and friendship was vital in setting up the MTS equipment for resilient modulus testing. Thanks to Mr. Ken Thomas and Mr. Larry Roberts for their help and suggestions for modifying the ATM device and MTS system.

Thanks to Mr. Gang Zuo for writing the Visual Basic program for the ATM and answering numerous off the wall questions. Thanks to Mr. Tik-Hing Choi for modifying the ATM program to perform the double integration calculations.

Abstract

The resilient modulus is a basic material property that is used in the current 1993 AASHTO Pavement Design Guide to characterize subgrade soils under vehicular loading. The resilient modulus is used in the mechanistic empirical design method to determine strains at the top of the soil subgrade and to predict strains developed in the overlying asphalt layer. The new 2002 AASHTO Pavement Design Guide, which is moving toward a more rational mechanistic design method, will continue to use the resilient modulus to characterize the subgrade.

The resilient modulus is often estimated since the standard repeated load triaxial test is time consuming, not always economically feasible, and a limited number of laboratories have the capability to perform the test. Therefore many researchers have made attempts to develop other methods.

A laboratory investigation was conducted on four fine-grained subgrade soils from various instrumented pavement sites across Tennessee. For each of the four site soils, index properties were determined. Several specimens were remolded for each site at optimum moisture and density. Repeated load triaxial tests were performed in accordance with the AASHTO T 307-99 procedure. A log-log equation proposed by Schwartz (2001) and Andrei (1999) was used to model the results. The results from the triaxial tests were found to be consistent and the model was found to have a strong correlation with the data obtained.

The resilient modulus was also determined using the ATM (alternative test method) developed by Li (1992). Improvements were made to the ATM prototype

device and to the data processing. Calculations based on the single degree of freedom mass spring system produced inconsistent and counterintuitive results. The data was reanalyzed by integrating the complete time-acceleration history to find the recoverable strain. The results from the double integration technique produced values of resilient modulus greater than the repeated load triaxial test. However the results were more consistent than those obtained with the previous analysis approach. Loading rate effects and differing states of stress between the repeated load triaxial test and the ATM, can explain the difference in values.

A hammer weight and reduction factor was recommended for using the ATM to estimate resilient modulus. It was suggested that additional testing be performed on ATM specimens without confinement and the effects of sample length be investigated. While it is easy to find resilient modulus values for different stress states with the ATM by using different combinations of drop heights and weights, the model developed in the standardized triaxial test is still preferable and more compatible with pavement design methods. With the automated data collection and analysis system, the need for an alternative method may not be as great.

Table of Contents

Chapter 1 Introduction 1

1.1 Importance of Resilient Modulus Testing 1

1.2 Definition of Resilient Modulus 2

1.3 Factors Affecting Resilient Modulus 4

1.3.1 Confining Pressure 4

1.3.2 Deviator Stress 5

1.3.3 Moisture Content 5

1.3.4 Degree of Saturation 6

1.3.5 Density 6

1.3.6 Compaction Method 6

1.3.7 Thixotropy 7

1.3.8 Freeze-Thaw Action 7

1.3.9 Loading Waveform and Duration 8

1.4 Alternative Test Methods and Improvements to the M_R Test 8

1.4.1 Modifications to the Resilient Modulus Test Procedure 9

1.4.2 Correlations 10

1.5 Resilient Modulus Models 12

1.5.1 Resilient Modulus Models 12

1.6 Recent University of Maryland Research 16

Chapter 2 Resilient Modulus Testing 20

2.1 Materials 20

2.2 Repeated Load Triaxial Test 20
2.3 Sample Preparation 25
2.4 Repeated Load Triaxial Test Results 28
2.5 Differences in Results 32
2.6 Stress Ratio 37
Chapter 3 CBR Testing 42
Chapter 4 Alternative Test Method 51
4.1 Previous ATM Research 51
4.2 Previous ATM Results 53
4.3 Improvements to the ATM 57
4.4 Visual Basic Program for ATM 58
4.5 Resilient Modulus Calculations from ATM 62
4.6 ATM Results for Site Soils 63
4.7 Loading Rate Effects 67
4.7 Loading Rate Effects 67
4.8 Corrected Acceleration 70
4.9 Confining Pressure 70
4.10 Polyurethane 72
4.11 Stress Paths 77
4.12 Reduction Factor 77
4.13 Limitations of the ATM 83
Chapter 5 Conclusions and Recommendations 85

5.1 Conclusions 85

5.2 Recommendations 86

References 88

Appendices 96

Appendix A Soil Information 97

Appendix B Repeated Load Triaxial Test Data 102

Appendix C ATM Data 133

Appendix D MTS Template 147

Appendix E ATM Derivation 176

Appendix F ATM Integration 192

Vita 200

List of Tables

Table 2-1 Soil Properties.....22

Table 2-2 Testing Sequences for Triaxial Testing.....39

Table 3-1 Standard Values for High Quality Crushed Rock (ASTM D 1883).....43

Table 3-2 CBR Test Results.....47

Table 4-1 Confining Pressures for Sumner ATM #2.....73

Table 4-2 Confining Pressures for Small Weight and 10 mm Drop Height.....74

List of Figures

Figure 1-1 Resilient Behavior Under Repeated Loads.....3

Figure 2-1 Locations of Soils for Testing.....21

Figure 2-2 AASHTO T307-99 Testing Sequences.....24

Figure 2-3 Haversine Loading Function.....26

Figure 2-4 Typical Pulse Hold Signal.....29

Figure 2-5 Typical Repeated Load Triaxial Test Results.....30

Figure 2-6 Resilient Modulus Models.....33

Figure 2-7 Resilient Modulus Models for 41.4kPa (6psi) Confining Stress 33

Figure 2-8 Resilient Modulus Models for 27.6kPa (4psi) Confining Stress.....34

Figure 2-9 Resilient Modulus Models for 13.8kPa (2psi) Confining Stress 34

Figure 2-10 Stress Path for Loading Sequences (adopted from Andrei 1999).....38

Figure 3-1 Soil Ratings for Road and Runways (after Liu and Evett 2000).....44

Figure 3-2 Relationships between M_R and CBR for Tennessee Soils.....46

Figure 3-3 CBR Correlation with Blount County.....48

Figure 3-4 CBR Correlation with McNairy County.....48

Figure 3-5 CBR Correlation with Overton County.....49

Figure 3-6 CBR Correlation with Sumner County.....49

Figure 4-1 ATM Setup.....54

Figure 4-2 Typical ATM Signal.....59

Figure 4-3 ATM Signal with Filtering.....61

Figure 4-4 Typical ATM Result for Peak Method.....64

Figure 4-5 Typical ATM Result for Area Method.....64

Figure 4-6 Typical ATM Result Using Double Integration Technique.....66

Figure 4-7 Typical ATM Result Using Double Integration Technique with Corrected Acceleration.....71

Figure 4-8 ATM Result Using Polyurethane with Peak Acceleration.....76

Figure 4-9 ATM Result Using Polyurethane and Acceleration Occurring at Peak Displacement.....76

Figure 4-10 Stress Paths for Sumner ATM #2.....78

Figure 4-11 Stress Paths for Blount ATM #1.....78

Figure 4-12 ATM Versus Traditional Test for Blount County.....80

Figure 4-13 ATM Versus Traditional Test for McNairy County.....80

Figure 4-14 ATM Versus Traditional Test for Overton County.....81

Figure 4-15 ATM Versus Traditional Test for Sumner County.....81

Figure 4-16 Sumner ATM #2 with Reduction Factor = 0.30.....82

Chapter 1 Introduction

1.1 Importance of Resilient Modulus Testing

Mechanistic-empirical methods are used to predict the performance of multilayered pavement systems. Mechanistic design procedures relate an input and output, loading and response. "In true mechanistic design, loads are carefully calculated and the pavement's response to those loads are determined based solely on the pavement material properties" (FHWA 1994). In practice, laboratory data and field observations are used to obtain the response of a pavement system because theory by itself has not proven to be sufficient for design (Huang 1993). Mechanistic design procedures are based on the assumption that a pavement can be modeled as a multi-layered elastic or visco-elastic structure on an elastic or visco-elastic foundation (AASHTO 1993). In the mechanistic-empirical design procedure, the mechanistic models are calibrated with observations of actual pavement performance.

There is a national and international trend that is moving toward mechanistic-empirical methods (Harichandran et al. 2001). Efforts are, however, being made to establish a more rational mechanistic-based design method. The new 2002 AASHTO Pavement Design Guide will incorporate new design specifications for this reason and will be entirely mechanistic (FHWA 2000; Schwartz 2001).

The 1986 AASHTO Guide for Design of Pavement Structures introduced the resilient modulus into the design procedure. The resilient modulus replaced the soil support value used in previous editions because it is a basic material property that can be used in mechanistic analysis (AASHTO 1986). The current 1993 Design Guide uses the

resilient modulus as the basis for material characterization in the mechanistic-empirical design method (AASHTO 1993). The resilient modulus is an important component of mechanistic-empirical pavement design method. It was found in the AASHO Road Test that 60-80% of pavement deflections were a result of the strains developed in the subgrade (AASHO 1962). Therefore, increasing resilient modulus in the subgrade decreases the strain and increases the fatigue life of the asphalt layer (Elliot and Thornton 1988a).

1.2 Definition of Resilient Modulus

The importance of the resilient characteristics of soils in pavement design was first recognized in the 1950's by Hveem, whose work indicated how pavement fatigue failures were caused by the resilience in the supporting soils (Hveem 1955). The concept of resilient modulus was originally introduced by Seed et al. (1962). Seed et al. (1962) developed a triaxial compression test that applied a confining pressure and subjected specimens to a series of constant deviator stress loads, which simulated a stress condition from a wheel load. The resilient modulus was calculated by dividing the deviator stress by the resilient strain.

"It is well known that most paving materials are not elastic but experience some permanent deformation after each loading application. However, if the load is small compared to the strength of the material and is repeated for a large number of load times, the deformation under each load repetition is nearly completely recoverable and proportional to the load and can be considered elastic" (Huang 1993). Figure 1-1 demonstrates this relationship. As the number of load repetitions increase, the plastic

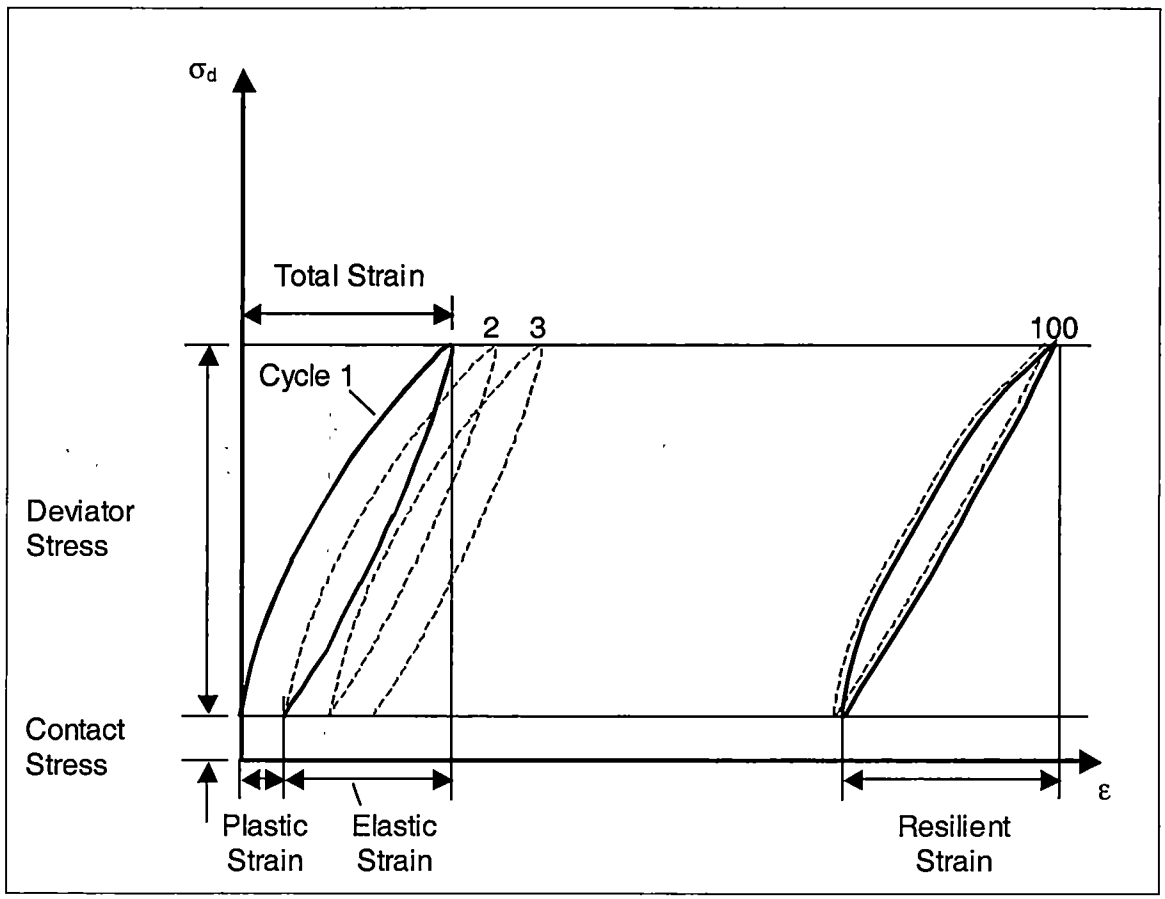

Figure 1-1 Resilient Behavior Under Repeated Loads

strains become smaller and the curves tend to stabilize. The resilient modulus is an elastic modulus and can be defined as the secant modulus of the stabilized portion of the stress-strain curve:

$$M_R = \frac{\sigma_d}{\varepsilon_r} \tag{1-1}$$

Where:

M_R = resilient modulus

σ_d = deviator stress ($\sigma_1 - \sigma_3$)

σ_1 = major principle stress (axial stress)

σ_3 = minor principle stress (confining stress)

ε_r = resilient or recoverable strain

1.3 Factors Affecting Resilient Modulus

Many researchers have investigated the factors which affect the results of repeated load triaxial testing for fine-grained soils. These factors include confining pressure, deviator stress, moisture content, density, sample preparation, thixotropy, freeze-thaw action, loading waveform, and duration.

1.3.1 Confining Pressure

It has been observed that the resilient modulus of fine-grained soils increases with increasing confining pressure (Jones and Witczak 1977; Thornton and Elliott 1986; Andrei 1999; Kim and Kweon 2000). Tennessee soils have displayed this behavior also (Hudson 1992; Madgett 1994; Reeves 1995). At higher deviator stresses, the effect of confining stress is reduced and the modulus appears to be relatively constant.

It should be noted that others have found there is little to no effect of confining pressure in fine-grained soils (Fredlund et al. 1977; Hudson 1992).

1.3.2 Deviator Stress

As the magnitude of the deviator stress increases, the resilient modulus decreases for fine-grained soils (Seed et al. 1962; Monismith et al. 1967; Thompson and Robnett 1976; Jones and Witczak 1977; Elliot and Thornton 1988a; Drumm et al. 1990; Pezo et al. 1991; Hudson 1992; Monismith 1992; Drumm et al. 1997; Andrei 1999; Kim and Kweon 2000). This typical type of response is known as "stress softening." The opposite is true for granular materials as they experience an increase in modulus with increasing deviator stress.

1.3.3 Moisture Content

Increases in compaction moisture content, for a given value of dry density, increase the amount of resilient deformation, thereby reducing the resilient modulus (Seed et al. 1962; Monismith et al. 1967; Thornton and Elliott 1986; Elliott and Thornton 1988a). The opposite is also true. Decreases in moisture content reduce the amount of resilient strain, thereby increasing the resilient modulus.

For samples compacted dry of optimum moisture content, the resilient modulus response starts off by demonstrating a "stress softening" behavior, but after a certain point in increasing deviator stress, it will display a "stress hardening" behavior (Monismith 1992; Hudson 1992). That is to say that the sample will experience an increase in modulus with increased deviator stress.

1.3.4 Degree of Saturation

Studies have shown how moisture content and density affect the resilient modulus. It is of interest to understand how the resilient modulus is affected by increasing moisture content after compaction since the moisture content of most pavements increases over time. Reeves (1995) showed that the resilient modulus of Tennessee subgrade soils decreased with increasing saturation. Others have also shown that resilient modulus decreases as the result of saturation (Thornton and Elliott 1986; Thompson and Robnett 1979; Monismith et al. 1967; Seed et al. 1962).

1.3.5 Density

Increases in dry density lead to increased stiffness and decreases lead to decreased stiffness (Seed et al. 1962; Monismith 1992). Thornton and Elliot (1986) found this to be true. However, they found the difference to be small in specimens compacted to 95% and 100% of optimum dry density. Several Tennessee subgrade soils were found to exhibit this behavior also, with the exception of two A-4 soils, which contained more silt (Hudson 1992).

1.3.6 Compaction Method

Monismith (Monismith et al.1967; Monismith 1992) reported that static compaction wet of the line of optimum creates essentially the same soil structure as kneading dry of the line of optimum. He warned that dispersed and flocculated compacted soil structures can have significant differences in mechanical properties, even at the same water content and dry density (Monismith 1992, Monismith 1967).

Specimens compacted by kneading compaction and those prepared by static compaction have about the same resilient strain characteristics when compacted below optimum water content. However when compacted above optimum, they have significantly different responses (Seed et al. 1962). Overall, specimens compacted by static compaction have higher resilient modulus than those compacted by kneading (Thornton and Elliott 1986).

Thompson and Robnett (1979) used kneading type compaction in preparing specimens, because they believed this method better simulated compaction conditions in the field. They found that there was a tendency for specimens statically compacted to have a higher resilient modulus than those compacted by kneading.

1.3.7 Thixotropy

The term thixotropy is used to describe an increase of stress-strain modulus over time in a soil at constant composition (Lamb and Whitman 1969). The gain in strength is due to changes in particle arrangement and pore pressure over time (Seed et al. 1962). A few researchers have documented this phenomenon (Seed et al. 1962; Monismith 1967; Pezo et al. 1991). Thomson and Robnett (1976, 1979) cured all test specimens 7 days to minimize the effects of thixotropic strength gain.

1.3.8 Freeze-Thaw Action

Freeze thaw-action influences the stiffness of fine-grained soils. Frozen soils increase in stiffness. However, when they thaw, the stiffness is reduced substantially (Monismith 1992). It has been found that one freeze-thaw cycle causes a dramatic reduction in resilient modulus whereas subsequent cycles caused minor reductions

(Thornton and Elliott 1986; Lee et al. 1995). Tests on several soils from Arkansas showed a reduction on the order of 50 percent due to freeze-thaw action (Elliott and Thornton 1988a). Lee et al. (1995) also found a 30-50% reduction in resilient modulus with one freeze-thaw cycle for soils sampled from in-service pavements.

1.3.9 Loading Waveform and Duration

The type of loading waveform and its duration and frequency are factors that affect the resilient response of materials. A haversine function is used in place of triangular or square loading waveform in the AASHTO testing method, because it better simulates a wheel load. As the duration of the load is reduced, the resilient modulus increases slightly (Elliot and Thornton 1986). The resilient modulus also increases with increased frequency of load applications (Elliot and Thornton 1986). It has been suggested that the 0.1 sec load required by the AASHTO T 307-99 procedure be increased to 0.2 seconds with a 0.8 sec hold (Andrei 1999). This longer loading period was suggested because loads are distributed over larger areas at greater depth. This means for a moving wheel load, the load at an upper layer in the pavement system will have a shorter duration than the loading at the top of the subgrade. Based on the above findings, this increase in loading time should decrease resilient modulus values.

1.4 Alternative Test Methods and Improvements to the M_R Test

The 1986 AASHTO Design Guide recommends that pavement design agencies obtain the equipment to measure resilient modulus or use another suitable method to estimate it. "In any case, a well planned experiment design is essential in order to obtain reliable correlations (AASHTO 1986)." In addition, the resilient modulus test is time

consuming, not always economically feasible, and a limited number of laboratories have the capabilities to perform the test. For this reason, there have been attempts by researchers to develop other methods. All of the methods fall into two categories, 1) modify the current procedure and 2) correlate the test with another method.

1.4.1 Modifications to the Resilient Modulus Test Procedure

Modifications to the test procedure were made to shorten the test or improve the results. Elliot and Thornton (1988b) believed that testing sophistication should be a function of required test accuracy and consequences of inaccurate results. Therefore, they suggested modifications to the AASHTO T274 procedure. These modifications included testing at a single confining pressure and deviator stress and reducing the number of load cycles. Claros et al. (1990) also suggested modifications to the T274 procedure from work on SHRP protocol P-46. The P-46 procedure eliminated the use of internal LVDT's, which is one that it attached directly to the sample. It was suggested that the use of internal LVDT's increases the variability of the results, since it is difficult to secure them in a manner where they would not slip and give an incorrect value of deformation. Another change was the use of a haversine stress pulse rather than a sinusoidal pulse, since the haversine better simulates the shape of a truckload on the pavement. Also, a closed-loop electrohydraulic system is to be used instead of other systems, since 0.1 sec load duration cannot be achieved with the pneumatic equipment. Air was suggested as a confining media. A change in the loading sequence was made to better represent the state of stress in the subgrade. All of these modifications were made to reduce the variability in the results.

Nazarian et al. (1996) suggested changes to the AASHTO T294 procedure for base materials. Grouting of specimens to the top and bottom platens was proposed to obtain more repeatable results along with measuring deformations over the middle one-third of the specimen. A new loading sequence to eliminate high deviator stresses at low confining pressures was suggested.

Andrei (1999) developed a harmonized protocol for the NCHRP Project 1-28A. The work involved modifying the NCHRP Project 1-28 "Laboratory Determination of Resilient Modulus for Flexible Pavement Design" by taking into account the stress paths of the loading. This was done to ensure that specimens did not fail early on in the test. A model was also developed that took into account deviator stress and confining pressure.

1.4.2 Correlations

Several correlations have been developed to obtain approximate values of resilient modulus for use in pavement design. One of the most well-known is the relationship developed by Heukelom and Forster (1960), which suggests that resilient modulus, in pounds per square inch, is 1500 times the CBR value. The Asphalt Institute (1982) has developed a similar method, which correlates R-value to resilient modulus. The AASHTO Guide also uses the group index and soil support value to estimate resilient modulus.

Drumm et al. (1990) developed two statistical models for eleven soils throughout Tennessee. The procedure uses soil index properties and a modulus obtained from unconfined-compression tests to estimate resilient modulus. The first model estimates a breakpoint resilient modulus at a deviator stress of 6 psi. The second model is a general

relationship for the stress-softening response of fine-grained soils as a function of deviator stress. Lee et al. (1995) conducted unconfined compression tests on five undisturbed cohesive soil specimens and developed a relationship between the stress at 1% axial strain and the resilient modulus at a deviator stress of 6 psi and a confining pressure of 3 psi. Thompson and Robnett (1979) also found a correlation between resilient modulus and unconfined-compression tests. A predictive model that takes into account the effects of the soil physical state, stress state, and type was developed by Li and Selig (1994). This method required conducting a resilient modulus test first at optimum moisture and density, but was then able to predict the modulus for the other states. Carmichael and Stuart (1985) developed two models for the USDA Forest Service to predict resilient modulus based on index properties and states of stress. Sweere and Galjaard (1988) developed a method of determining resilient modulus for a wide range of sands from simple repeated static loading triaxial tests.

A device was produced in Norway to measure resilient modulus in the field (Boyce et al. 1989; Boyce et al. 1990). The device is a portable variable impact test for pavement foundations, called ODIN, used to measure surface modulus. ODIN uses a swing arm arrangement to drop a weighted hammer and various diameter contact plates on the subgrade or subbase surface. Electronic equipment collects the signal from the accelerometer located inside the hammer at the moment of impact. The stresses produced by the device are similar to those under a wheel load, and the stiffness of clays and granular materials are not dependent on the rate of loading from the device. The unfiltered time-deceleration curve is collected and integrated twice to obtain a

displacement. For this to be possible, the initial velocity is assumed to be the $\sqrt{2gh}$. By assuming a Poisson's ratio of 0.5, the resilient modulus of the soil can then be calculated. Since soils are not linear elastic materials, the deceleration and displacements are not sinusoidal and so their peak values do not occur at the same point in time. The researchers hypothesized that this was due to inertia effects and the non-linear stress strain behavior of the material. Therefore, calculations based on the peak acceleration lead to modulus values which are too large. To avoid this problem, the researchers used the acceleration that occurred at the same time as the peak displacement.

An alternative test method (ATM), that is similar to the ODIN device, was developed at the University of Tennessee for determining lab values of resilient modulus (Li 1992). The details of the ATM are discussed later.

1.5 Resilient Modulus Models

In order to design pavements by a mechanistic approach, the state of stress in the pavement must be known. The state of stress and deformation will be a function of the resilient modulus of each of the pavement layers, and the moduli are a function of the stress state. A predictive equation will allow the designer to determine the resilient modulus of each layer (soil) as a function of the state of stress and in return determine the strain in the entire system.

1.5.1 Resilient Modulus Models

Several models have been proposed to characterize the resilient modulus properties of fine-grained subgrade soils. This section examines a few of the most popular and most recent.

Thompson and Robnett (1976, 1979) developed a bilinear model to analyze the stress softening resilient response of the soils:

$$M_R = k_2 + k_3(k_1 - \sigma_d) \quad \text{for } k_1 \geq \sigma_{di} \tag{1-2}$$

or

$$M_R = k_2 + k_4(\sigma_d - k_1) \quad \text{for } k_1 < \sigma_{di} \tag{1-3}$$

Where

σ_{di} = deviator stress at which the slope of M_R changes

k_1 through k_4 = material parameters

They used a "break point modulus" used to characterize the resilient properties of subgrade soils.

$$E_{ri} = k_1(\sigma_{di})^{k_2} \tag{1-4}$$

Where

E_{ri} = break point resilient modulus

k_1, k_2 = slopes of two linear equations

The relationship was found using a wide range of Illinois subgrade soils. The break point modulus was defined where there was a substantial change in the slope of the resilient modulus versus deviator stress plot. This point occurred at a deviator stress of 6 ksi. No confining stress was used in the tests.

One of the most popular models is the power model:

$$M_R = k_1(\sigma_d)^{k_2} \tag{1-5}$$

Where

M_R = resilient modulus

k_1, k_2 = material constants

σ_d = deviator stress = $\sigma_1 - \sigma_3$

σ_1 = major principal (vertical) stress

σ_3 = confining pressure

Moossazadeh and Witczak (1981) developed this nonlinear model, because up until that time most of the models treated pavement layer materials with parameters of constant magnitude. They realized that resilient modulus was stress dependent and developed the model accordingly.

In addition to the bilinear and power models, the semi-log model (Fredlund et al. 1977), the hyperbolic model (Drumm et al. 1990), and the octahedral shear stress model (Shackel 1973) have been proposed.

The model developed by Pezo (1993) includes confining pressure and deviator stress effects. The model has the form of:

$$M_R = k_1 \sigma_d^{K_2} \sigma_3^{k_3} \tag{1-8}$$

A regression model using both deviator stress and bulk stress was developed by Puppala and Mohammad (1997). The model has the basic form of:

$$M_R = k_1 p_a \left(\frac{\theta}{p_a}\right)^{k_2} \left(\frac{\sigma_d}{p_a}\right)^{k_3} \tag{1-6}$$

Where

k_1 through k_3 = material parameters

θ = bulk stress = $\sigma_1 + \sigma_2 + \sigma_3$

p_a = atmospheric pressure, which is used to make the material parameters dimensionless

Puppala and Muhammad (1977) chose this model, which they referred to as the triaxial stress state model, over the bulk stress and octahedral models because it offered the best predictions of resilient modulus on granular, cohesive, and mixed soil types.

Several researchers have proposed a model for all unbound fine-grained and coarse-grained materials (Witczak et al. 1995; Bonaquist and Witczak 1992; Uzan 1992; Witczak and Uzan 1988). This model is sometimes referred to as the "Witczak-Uzan universal model."

$$M_R = k_1 p_a \left(\frac{\theta}{p_a}\right)^{k_2} \left(\frac{\tau_{oct}}{p_a}\right)^{k_3} \tag{1-7}$$

Where

τ_{oct} = octahedral shear stress = $\frac{1}{3}\sqrt{(\sigma_1 - \sigma_2)^2 + (\sigma_1 - \sigma_3)^2 + (\sigma_2 - \sigma_3)^2}$

The model was found to produce excellent results, based on R-squared values, for the six different materials at different combinations of density and moisture content that were used in the study by Uzan (1992).

Hjelmstad and Taciroglu (2000) implemented resilient modulus models in finite element applications. Their work implemented the Uzan-Witczak constitutive model into a 3-D analysis where the resilient modulus, which is usually expressed as a term of stress invariants, was expressed in terms of strain invariants.

1.6 Recent University of Maryland Research

The resilient modulus of fine-grained soils is typically assumed to be a function of the confining pressure and deviator stress. Much research has been done on resilient modulus as a function of deviator stress (Seed et al. 1962; Fredlund and Wong 1977; Thompson and Robnett 1979; Thornton and Elliott 1986; Drumm et al. 1990) and a function of confining stress (Fredlund and Wong 1977; Thornton and Elliott 1986). As the confining stress increases, the resilient modulus increases. As the deviator stress increases, the resilient modulus decreases. For this reason the predictive equation chosen to model resilient modulus data needs to take both of these factors into account. This model also needs to be one, which can be implemented into a computer program (finite element code) for mechanistic analysis.

Researchers at the University of Maryland have investigated fourteen predictive nonlinear equations (Andrei 1999; Schwartz 2001). The research is a part of NCHRP Project 1-37A, which is developing the new 2002 Pavement Design Guide. Each of the fourteen equations was used to model results from 35 resilient modulus tests. The specimens were both base and subbase materials at varying moisture/density relationships. All of the models have the generalized form of Equation 1-8.

$$M_R = k_1 p_a \left(\frac{\theta - 3k_6}{p_a} \right)^{k_2} \left(\frac{\tau_{oct}}{p_a} + k_7 \right)^{k_3} \tag{1-8}$$

Where

M_R = resilient modulus

p_a = atmospheric pressure

θ = bulk stress = $\sigma_1 + \sigma_2 + \sigma_3$

τ_{oct} = octahedral shear stress = $\frac{1}{3}\sqrt{(\sigma_1 - \sigma_2)^2 + (\sigma_1 - \sigma_3)^2 + (\sigma_2 - \sigma_3)^2}$

k_1 through k_7 = material parameters

$k_1 > 0$

$k_2 \geq 0$

$k_3, k_6 \leq 0$

$k_7 \geq 1$

The bulk stress, θ, and octahedral shear stress, τ_{oct}, are invariants of the state of stress since they depend on the three principal stresses σ_1, σ_2, and σ_3. Derivation of the octahedral shear stress can be found in Nadai (1950), Desai (1984), or other continuum mechanics textbooks. Although the octahedral shear stress is smaller than the highest principal shear stress, it constitutes a single value, which is influenced by all three principal stresses (Juvinall 1967). Stress invariants are useful because they describe the state of stress without dealing with the orientation of the stresses.

The k_6 term in Equation 1-8 is used to account for pore water pressure or cohesion. It is also a measure of the ability of the material to resist tension. This also allows the modulus to be predicted in terms of effective stresses.

The 2002 Design Guide will use a simplified version of Equation 1-8 with $k_6 = 0$ and $k_7 = 1$ (Schwartz 2001). With the k_7 term equal to one, the irrationality of the model is eliminated. That is to say that when $\tau_{oct} = 0$, the term in the parenthesis is 1. This also ensures that the logarithm of the term raised to the k_3 power will always be positive. The model is as follows:

$$M_R = k_1 p_a \left(\frac{\theta}{p_a} \right)^{k_2} \left(\frac{\tau_{oct}}{p_a} + 1 \right)^{k_3} \tag{1-9}$$

Including the term for the atmospheric pressure assures that the calculated modulus has the same units of stress as the atmospheric pressure. In addition, the use of atmospheric pressure results in the k_1 through k_3 parameters being dimensionless. The k_1 parameter is a constant in the model equation. The equation takes into account the stiffening effect of the confining stress. This is why the k_2 parameter is constrained to be greater than or equal to zero, which indicates an increase the value of the resilient modulus as the confining pressure increases. The equation also takes into account the softening effect of the deviator stress. The τ_{oct} term in the equation is dependent only on the deviator stress, because the third term in the octahedral shear stress equation cancels out because of the fact that the confining pressure is constant in all directions. The k_3 component is constrained to be less than or equal to zero, which indicates that an increase in deviator stress will result in a reduction of the resilient modulus.

All three of the material parameters can be obtained through multiple linear regression analysis. Multiple linear regression is used when the relationship of the model depends on two or more predictive variables (Johnson and Bhattacharyya 1996). In this case, the input variables are confining pressure and deviator stress and the output variable is the resilient modulus. The linear regression is performed on the model with the form of:

$$\log\left(\frac{M_R}{p_a} \right) = a + k_2 * \log\left(\frac{\theta}{p_a} \right) + k_3 * \log\left(\frac{\tau_{oct}}{p_a} + 1 \right) \tag{1-10}$$

The regression constants of the model are log k_1, k_2, and k_3. The k_1 constant is obtained by taking the antilog of *a*. This model is often referred to as the "log-log" model.

Chapter 2 Resilient Modulus Testing

2.1 Materials

Repeated load triaxial tests, CBR, and ATM tests were conducted on four fine-grained soils from Tennessee. All of the soils were collected along highway embankments near the weather monitoring and data collection stations for the Tennessee Department of Transportation instrumented pavement sections (Rainwater et al. 1999). The sites chosen are located in four different physiographic regions of Tennessee: Blount County, I-140, Ridge and Valley; McNairy County, US-45, Southern Coastal Plain; Overton County, State Route 42, Eastern Highland Rim; and Sumner County, State Route 139, Central Basin (Wright 1998). Figure 2-1 shows the county locations.

The soils were returned to the lab and separated on a #4 sieve. All of the material retained on the #4 was discarded. Index tests were performed in general accordance with current ASTM and AASHTO specifications in the laboratory at the University of Tennessee. These tests include moisture-density, grain size analysis (sieve and hydrometer), and Atterberg limits. Table 2-1 shows the results of the tests. All of the soils are classified as low plasticity clays by the Unified Soil Classification System (USCS) and as clayey soils, ranging from A-6 to A-7-6, by the AASHTO Classification System. Results of material properties testing can also be found in Appendix A.

2.2 Repeated Load Triaxial Test

AASHTO T 307-99 "Determining the Resilient Modulus of Soils and Aggregate Materials" was the procedure used to perform the repeated load triaxial tests for the four site soils. Materials Testing Systems 810 (MTS) equipment was used to test the samples.

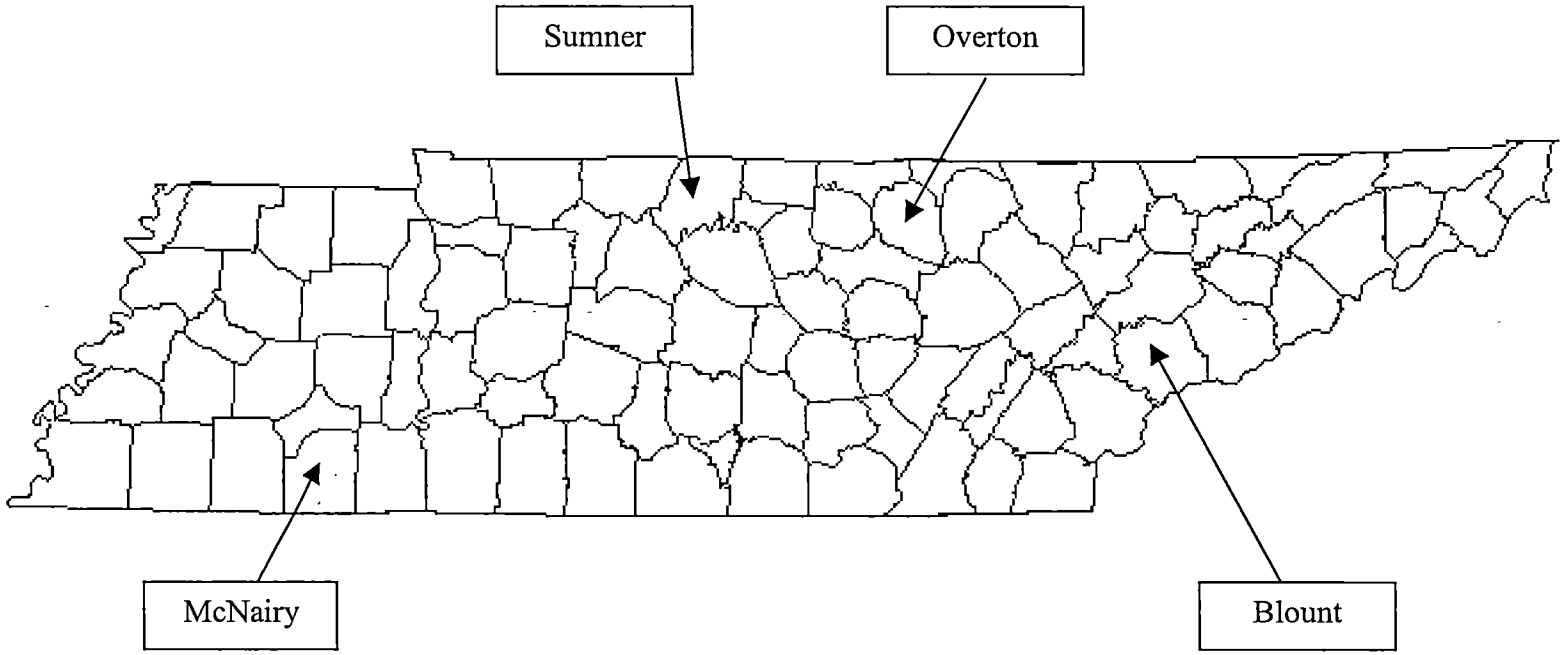

Figure 2-1 Locations of Soils for Testing

Table 2-1 Soil Properties

Location	Optimum Water Content (%)	Maximum Dry Density (pcf)	Atterberg Limits			Percent Passing #200 Sieve (%)	Soil Classification		
			LL	PL	PI		USCS	AASHTO	Group Index
Blount	21.0	102.0	43	22	21	85.1	CL	A-7-6	18
McNairy	13.5	115.0	30	16	14	57.7	CL	A-6	5
Overton	16.0	109.0	29	17	12	78.6	CL	A-6	8
Sumner	17.5	103.5	32	21	11	80.8	CL	A-6	8

The MTS equipment is a closed loop, top-loading, electro-hydraulic system. The system has two internally mounted spring-loaded linear variable differential transformers (LVDT's) to measure displacement. In previous editions of the AASHTO testing procedure, internal LVDT's meant ones that were attached directly to the specimen. An external LVDT was one that was mounted outside of the triaxial chamber. The use of the word internal for this setup is one that means that the LVDT is mounted inside of the triaxial chamber and attached to the top and bottom loading platens, not the sample itself. This is a deviation from the AASHTO testing procedure. The procedure calls for the LVDT's to be mounted outside of the triaxial cell. The system is set up for internal mounting, which has been found to be more reliable because it does not measure the slop in the frame or piston. The MTS uses air as a confining media and an internal load cell mounted underneath the bottom platen to measure stresses. The procedure calls for a load cell to be mounted between the chamber piston and actuator. The current setup is a more accurate method. The internal load cell is not affected by confining pressure as long as the system is in force control. If the system is in displacement control, then changes in confining stress will result in changes in load. For this reason it is important to apply confining pressures after the system switches from displacement to force control. The software used for control and data acquisition is MTS TestStar V4.0.

Figure 2-2 shows the testing sequences for subgrade and base / subbase materials. The sequence for subgrade materials was used for the experiment because it is for Type II soils, which are fine-grained. As can be seen from Figure 2-2, the loading consists of a conditioning phase and a testing sequence that includes 15 stress levels (five deviator

TABLE 1 - Testing Sequence for Subgrade Soil

Sequence No.	Confining Pressure, σ_3		Max. Axial Stress, σ_{max}		Cyclic Stress, σ_{cyclic}		Constant Stress, $0.1\sigma_{max}$		No. of Load Applications
	kPa	psi	kPa	psi	kPa	psi	kPa	psi	
0	41.4	6.0	27.6	4.0	24.8	3.6	2.8	0.4	500-1000
1	41.4	6.0	13.8	2.0	12.4	1.8	1.4	0.2	100
2	41.4	6.0	27.6	4.0	24.8	3.6	2.8	0.4	100
3	41.4	6.0	41.4	6.0	37.3	5.4	4.1	0.6	100
4	41.4	6.0	55.2	8.0	49.7	7.2	5.5	0.8	100
5	41.4	6.0	68.9	10.0	62.0	9.0	6.9	1.0	100
6	27.6	4.0	13.8	2.0	12.4	1.8	1.4	0.2	100
7	27.6	4.0	27.6	4.0	24.8	3.6	2.8	0.4	100
8	27.6	4.0	41.4	6.0	37.3	5.4	4.1	0.6	100
9	27.6	4.0	55.2	8.0	49.7	7.2	5.5	0.8	100
10	27.6	4.0	68.9	10.0	62.0	9.0	6.9	1.0	100
11	13.8	2.0	13.8	2.0	12.4	1.8	1.4	0.2	100
12	13.8	2.0	27.6	4.0	24.8	3.6	2.8	0.4	100
13	13.8	2.0	41.4	6.0	37.3	5.4	4.1	0.6	100
14	13.8	2.0	55.2	8.0	49.7	7.2	5.5	0.8	100
15	13.8	2.0	68.9	10.0	62.0	9.0	6.9	1.0	100

Note: Load sequences 14 and 15 are not to be used for materials designated as Type 1.

TABLE 2 - Testing Sequences for Base/Subbase Materials

Sequence No.	Confining Pressure, σ_3		Max. Axial Stress, σ_{max}		Cyclic Stress, σ_{cyclic}		Constant Stress, $0.1\sigma_{max}$		No. of Load Applications
	kPa	psi	kPa	psi	kPa	psi	kPa	psi	
0	103.4	15.0	103.4	15.0	93.1	13.5	10.3	1.5	500-1000
1	20.7	3.0	20.7	3.0	18.6	2.7	2.1	0.3	100
2	20.7	3.0	41.4	6.0	37.3	5.4	4.1	0.6	100
3	20.7	3.0	62.1	9.0	55.9	8.1	6.2	0.9	100
4	34.5	5.0	34.5	5.0	31.0	4.5	3.5	0.5	100
5	34.5	5.0	68.9	10.0	62.0	9.0	6.9	1.0	100
6	34.5	5.0	103.4	15.0	93.1	13.5	10.3	1.5	100
7	68.9	10.0	68.9	10.0	62.0	9.0	6.9	1.0	100
8	68.9	10.0	137.9	20.0	124.1	18.0	13.8	2.0	100
9	68.9	10.0	206.8	30.0	186.1	27.0	20.7	3.0	100
10	103.4	15.0	68.9	10.0	62.0	9.0	6.9	1.0	100
11	103.4	15.0	103.4	15.0	93.1	13.5	10.3	1.5	100
12	103.4	15.0	206.8	30.0	186.1	27.0	20.7	3.0	100
13	137.9	20.0	103.4	15.0	93.1	13.5	10.3	1.5	100
14	137.9	20.0	137.9	20.0	124.1	18.0	13.8	2.0	100
15	137.9	20.0	275.8	40.0	248.2	36.0	27.6	4.0	100

Figure 2-2 AASHTO T307-99 Testing Sequences

stresses at three confining pressures). The conditioning phase serves two purposes. The first is to minimize bedding effects (irregularities between the specimen surface and loading platens). The second is to simulate the stress history of the material (construction activities). The load is applied by a 1.0 sec pulse hold function as shown in Figure 2-3. There is a 0.1 sec haversine load followed by a 0.9 sec hold. A haversine function is used to simulate traffic loading. In Figure 2-2, the cyclic stress is the deviator stress applied to the specimen. The sum of the confining pressure plus the maximum axial stress is the major principal stress. When setting up the test template, there was no need to adjust the loads to account for a net upward or downward resultant due to confining stress. As was stated above, the MTS system is not affected by confining pressure if it is in force control. For this reason, the load applied corresponds to the deviator stress.

2.3 Sample Preparation

All of the samples were prepared using static compaction. The method is slightly different from the T 307-99 procedure, which is modification of the "double plunger method." The samples were remolded manually using the MTS load frame while in displacement control. The samples were all prepared in five equal lifts at optimum moisture and density. Five metal spacers, of varying heights, were constructed to compact the soil into equal lifts of 4.06 cm (1.6 inches). AASHTO recommends a mold size with a minimum diameter of five times the maximum particle size and a length of at least twice the diameter. For fine-grained soils, which pass a #4 sieve, the maximum nominal particle size is 0.47 cm (0.187 inches). Therefore, a sample with a 5.08 cm (2 in.) diameter and 10.16 cm (4 in.) height would be adequate to test. However, it was

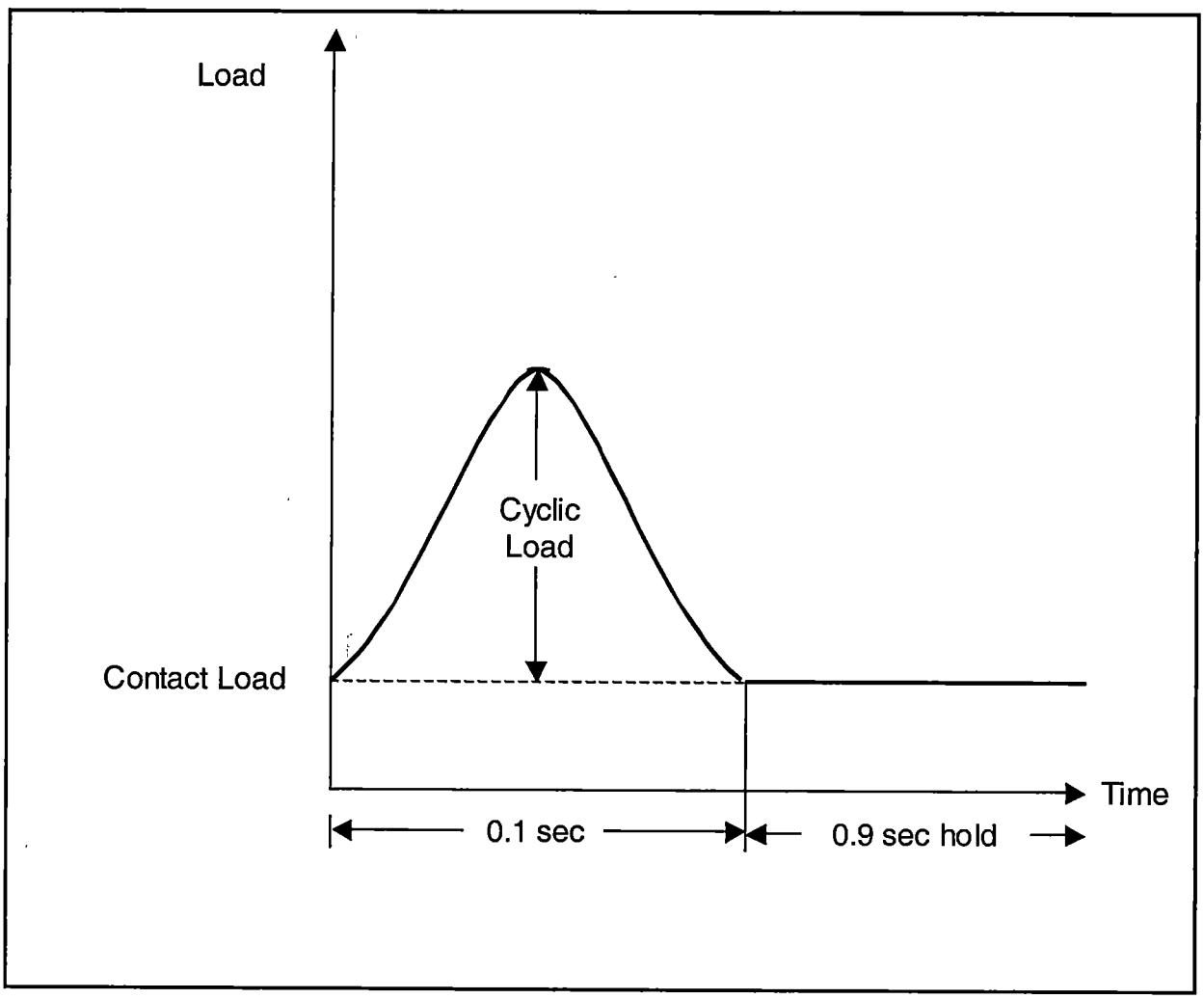

Figure 2-3 Haversine Loading Function

decided to use a 10.16 cm (4 in.) diameter specimen that was 20.32 cm (8 in.) in height. This was a convenient sample size for several reasons. First of all, the top and bottom loading platens have a 20.32 cm (4 in.) inside diameter. A split mold to prepare the specimen with a 20.32 cm (4 in.) diameter is readily available through most soil testing equipment distributors. A sample of this size is also easily handled. Material that passes a 1.91 cm (¾ in.) sieve can be tested in the future with no change in the sample preparation procedure or equipment. Finally, the 10.16 cm (4 in.) diameter is a common size and has been used by other researchers (Ping et al 2000; Andrei 1999; Sweere and Galjaard 1988).

To prepare the sample, a predetermined amount of soil for the desired moisture and density is weighed out and placed in the split mold. The appropriate spacer is then attached to the MTS loading piston. The spacers are fabricated in a manner so that when the spacer is pressed into the mold and the top is flush with the top of the mold, the lift will be 4.06 cm (1.6 in.) or 1/5 of the sample height. The spacer should remain in contact with the specimen for at least one minute before removing. This is done to reduce the amount of sample rebound. Between each lift, the top of the sample is scarified to help ensure a good bond between lifts.

There is another deviation to the test procedure outlined in T 307-99, related to data collection. AASHTO requires that a minimum of 200 data points per load cycle be recorded for each LVDT. This would result in a large amount of unnecessary data to filter though to obtain information needed for the last 5 cycles of each of the 15 loading sequences. Instead, the deformation is recorded at the maximum and minimum loading

for each cycle. A typical pulse hold signal is shown in Figure 2-4, with compression force as negative. The maximum displacement is assumed to occur when the sample is subjected to the greatest or most negative load. The minimum displacement is then assumed to correspond to the smallest load or least negative load following the maximum displacement. The difference between the two displacements is taken to be the recoverable displacement and used in the calculation of resilient modulus. The difference between the actual minimum and maximum load divided by the cross sectional area of the specimen is the deviator stress. There is a slight difference in the force signal and force command. The spectrum amplitude control (SAC) function was input into the test template to remedy this discrepancy between signal and command. The SAC function is an algorithm that monitors the command signal and feedback signal end levels in a table. The difference is monitored by the system and it continuously adjusts the over-programming to make the two coincide (MTS 1998). However, noise in the signal due to confining pressure did not allow this optimization function to be used. The system was having to "work" too hard to filter out the noise, and would often go offline. Sequences 4, 9, and 14 experienced the most difficulty. MTS technical support was made aware of this issue, but as of this date it has not been resolved.

2.4 Repeated Load Triaxial Test Results

Resilient modulus tests were performed for each of the four site subgrade soils. Twelve tests were performed on the Blount County soil, seven on the McNairy County soil, eight on the Overton County soil, and eight on the Sumner County soil. All of the results can be found in Appendix B. Figure 2-5 shows typical results of resilient

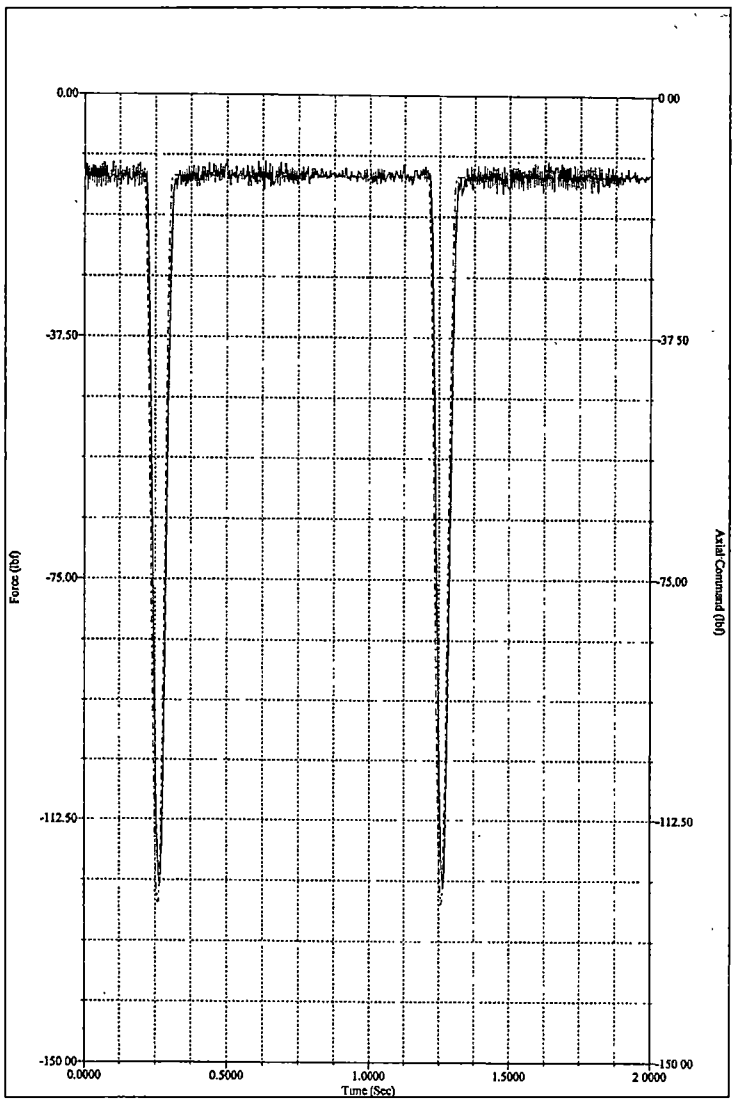

Figure 2-4 Typical Pulse Hold Signal

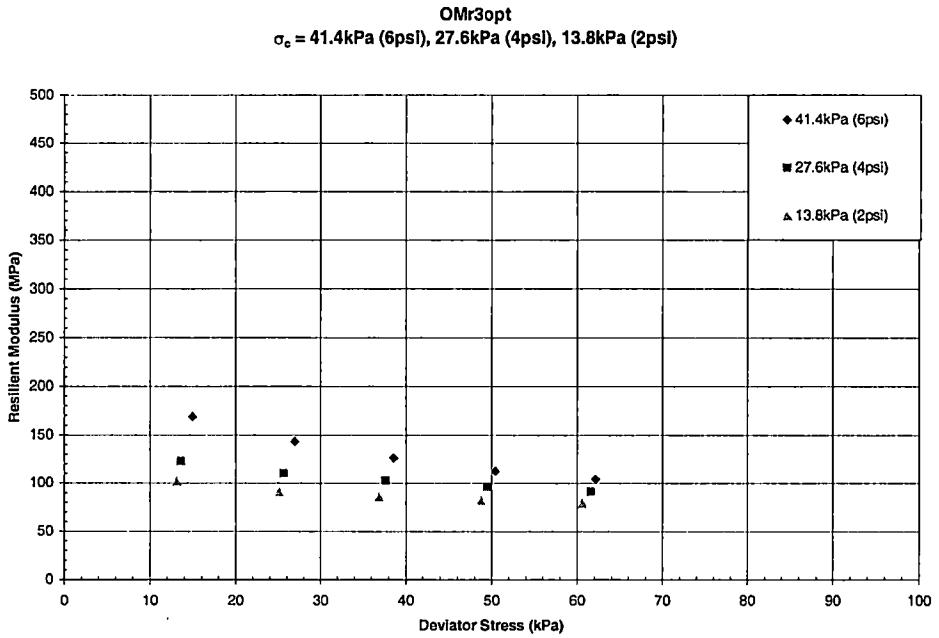

Figure 2-5 Typical Repeated Load Triaxial Test Results

modulus versus deviator stress for three different confining stresses (41.4 kPa, 27.6 kPa, and 13.8 kPa). There are 5 data points for each confining stress for a total of 15 data points. There are two factors that affect the results. First is the confining pressure. As the confining pressure increases, there is an increase in resilient modulus. Second, as the deviator stress increases, there is a decrease in resilient modulus. This is a typical response for fine-grained material (Jones and Wiczak 1977; Elliot and Thornton 1988a; Hudson 1992; Drumm et al. 1997; Andrei 1999; Kim and Kweon 2000). Also, it can be seen at higher deviator stresses, the effect of the confining pressure is reduced. If the deviator stress is increased high enough, it appears that the value of resilient modulus calculated would be the same for all three confining pressures.

Each test was modeled using Equation 2-1 proposed by NCHRP Project 1-37A.

$$M_R = k_1 p_a \left(\frac{\theta}{p_a} \right)^{k_2} \left(\frac{\tau_{oct}}{p_a} \right)^{k_3} \tag{2-1}$$

The k parameters were found by multiple linear regression. The three parameters were averaged for each test and used to create one model for each individual site. Basic statistical parameters were also performed to verify ability of the model to match the data. The results of the material parameter analysis are summarized in tables located in Appendix B. The average correlation coefficient, R^2 value, is 0.96 for Blount County and 0.97 for the remaining three counties. These high R^2 values indicate that the model fits the measured data very well.

The general equations for each site are as follows.

Blount County:

$$M_{R\ \text{Blount}} = 2070 p_a \left(\frac{\theta}{p_a}\right)^{0.476} \left(\frac{\tau_{oct}}{p_a}\right)^{-2.24} \quad (2\text{-}2)$$

McNairy County:

$$M_{R\ \text{McNairy}} = 2070 p_a \left(\frac{\theta}{p_a}\right)^{0.662} \left(\frac{\tau_{oct}}{p_a}\right)^{-3.06} \quad (2\text{-}3)$$

Overton County:

$$M_{R\ \text{Overton}} = 1750 p_a \left(\frac{\theta}{p_a}\right)^{0.643} \left(\frac{\tau_{oct}}{p_a}\right)^{-3.35} \quad (2\text{-}4)$$

Sumner County:

$$M_{R\ \text{Sumner}} = 1530 p_a \left(\frac{\theta}{p_a}\right)^{0.589} \left(\frac{\tau_{oct}}{p_a}\right)^{-3.27} \quad (2\text{-}5)$$

The effect of confining pressure and deviator stress are correctly accounted for in the model equations. The k_2 parameters are all positive, which indicates an increase in modulus with increasing confining stress. The k_3 parameters are all negative, which indicates a decrease in modulus with increasing deviator stress. Graphs showing the models fit to the test data are located in the Appendix B.

2.5 Differences in Results

"Are the results for the four soils different" is the next question that arises. Figures 2-6 to 2-9 show the models plotted for each site at the three values of confining stress. In all of the figures, the values of resilient modulus are the highest for Blount County, followed by McNairy, Overton, and Sumner. A trend in the lines can be observed. For the confining pressure of 41.4 kPa (6 psi), the model has a slight

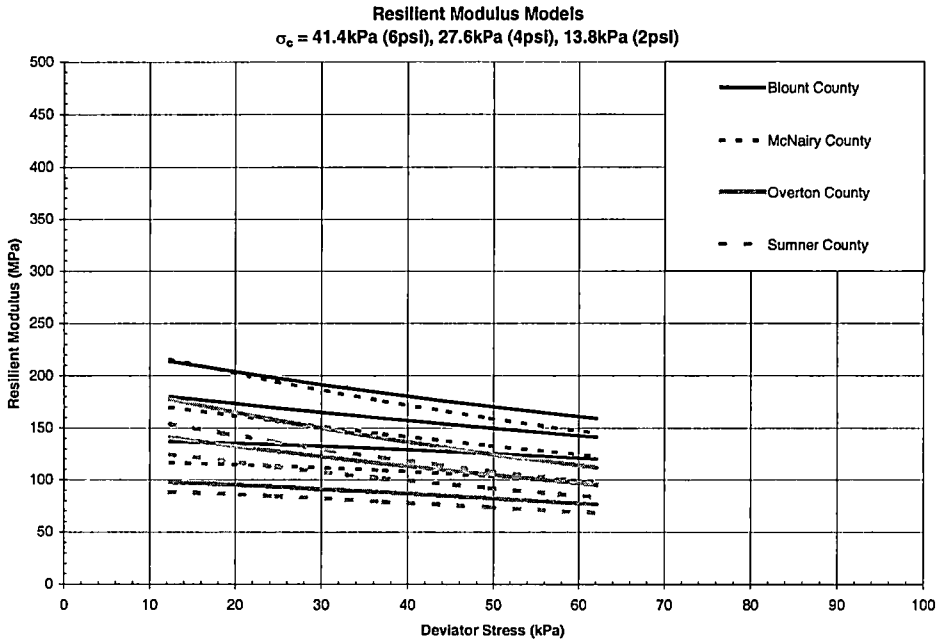

Figure 2-6 Resilient Modulus Models

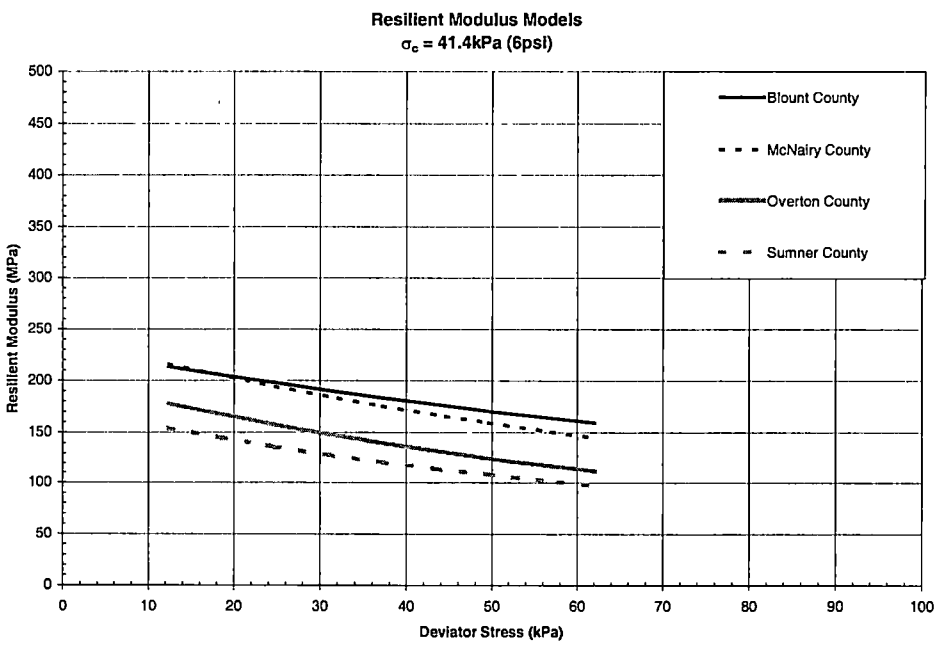

Figure 2-7 Resilient Modulus Models for 41.4kPa (6psi) Confining Stress

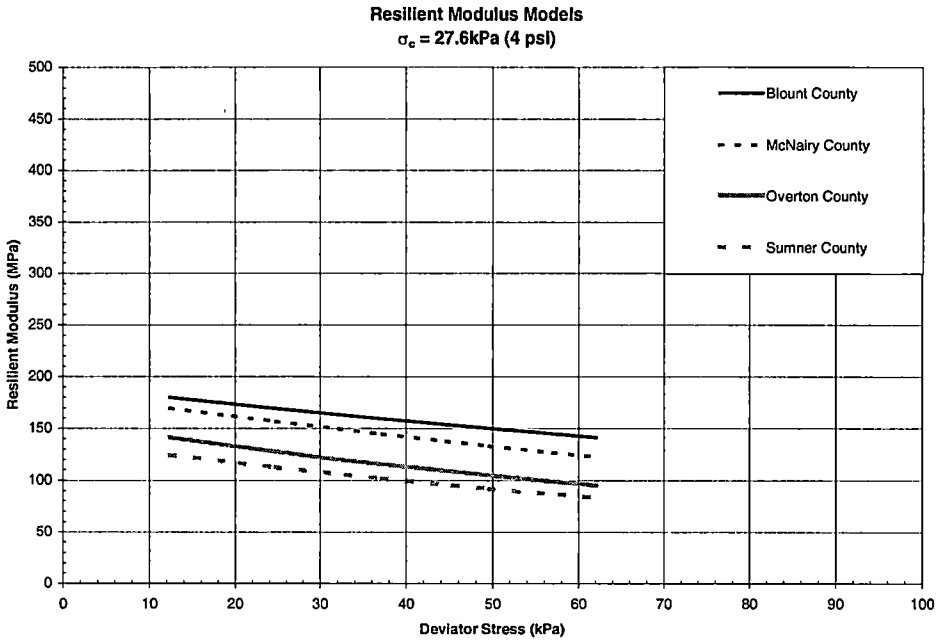

Figure 2-8 Resilient Modulus Models for 27.6kPa (4psi) Confining Stress

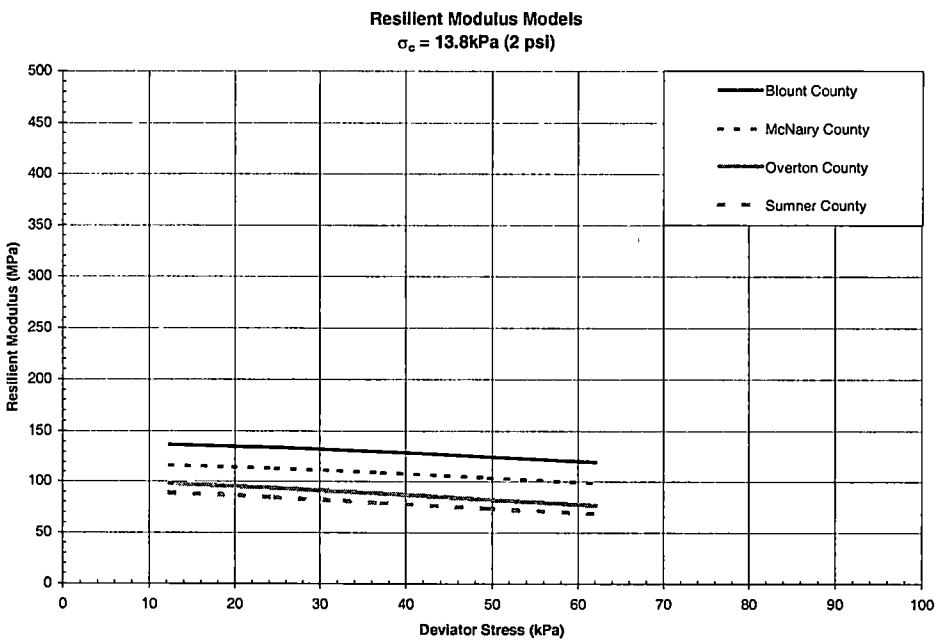

Figure 2-9 Resilient Modulus Models for 13.8kPa (2psi) Confining Stress

curvature. As the confining pressure is reduced to 13.8 kPa (2psi), the model is nearly linear.

There is a measurable difference in the results as has been shown. Is this difference great enough to be considered in engineering applications? To answer this question, resilient modulus calculations were made for a typical 25.40 cm (10 in.) pavement section consisting of a 15.24 cm (6 in.) asphalt concrete layer and a 10.16 cm (4 in.) stone base. Li (1992) analyzed this section using the finite element method. A standard single axle load of 80 kN (18kips), which was assumed to produce a circular surface load of 551.5 kPa (80 psi) with a radius of 15.24 cm (6 in.), was used to find the stresses at the top of the subgrade layer. The vertical stress at the top of the subgrade was found to be 92.4 kPa (13.4 psi) and the horizontal stress 20.3 kPa (2.95 psi) for a medium stiffness subgrade. Li (1992) varied the subgrade modulus based on the bilinear model of Thompson and Robnett (1979) and their definition of subgrade stiffness. Li calculated resilient modulus values that ranged from 85.5 MPa (12.4 ksi) to 33 MPa (4.8 ksi) for a medium stiffness subgrade. Based on this computed stress state at the top of the subgrade, the resilient modulus was determined for each or the site soils using the models. The vertical stress is assumed to be the major principal stress and the horizontal stress is assumed to be the confining pressure. The calculated resilient modulus results are as follows:

1. Blount County: 125 MPa
2. McNairy County: 104 MPa
3. Overton County: 80 MPa

4. Sumner County: 71 MPa

The modulus for Blount County is 43 percent greater than that of Sumner County.

Li (1992) analyzed a second pavement system that was 40.64 cm (16 in.) thick with a 25.40 cm (10 in.) asphalt layer and a 15.24 cm (6 in.) base layer. The vertical and horizontal stresses were found to be 23.9 kPa (3.47 psi) and 8.2 kPa (1.19 psi), respectively. Even though there is a reduction in the stresses at the top of the subgrade due to increased layer thickness, the computed modulus values for the four site soils are still significantly different as shown below.

1. Blount County: 116 MPa
2. McNairy County: 92 MPa
3. Overton County: 77 MPa
4. Sumner County: 72 MPa

The modulus for Blount County is 38 percent greater than Sumner County.

To determine if the resilient modulus values for the soils are significantly different for engineering applications, the values for Blount and Sumner County for the 40.64 cm (16 in.) pavement cross-section were used to design a pavement system. The asphalt concrete layer for a system with a 15.24 (6in.) untreated granular base and the assumed modulus value for each site was determined using the Asphalt Institute's (AI) Thickness Design Manual (1981). The AI method is based on a multi-layered elastic system that uses a modulus of elasticity and a Poisson's ratio to characterize the materials in each layer. Traffic is expressed in terms of the number of 80 kN (18,000 lb) single-axle load applications (EAL). Critical thickness values are determined for the horizontal

tensile strain, ε_t, at the bottom of the asphalt layer and the vertical compressive strain, ε_c, at the surface of the subgrade layer (Asphalt Institute 1981).

The required thickness of asphalt concrete was found to be 180 mm (7.1 in.) for Blount County and 205 mm (8.1 in.) for Sumner County, assuming a 3 million EAL. The difference of 25 mm (1.0 in.) between the two designs is significant. This suggests that the soils are indeed different and the difference in resilient modulus values has a significant impact on pavement design. It should be noted that this analysis neglects the fact that resilient modulus varies with stress state, and the finite element analysis of Li (1992) used an assumed bilinear relationship for subgrade modulus. A more accurate approach would be to use an iterative procedure that assumes an initial value of resilient modulus and chooses a pavement thickness. The stresses and strains would then be calculated with the finite element model, using an appropriate subgrade relationship, and the new modulus value from the finite element analysis would be used for the pavement design. This procedure would continue until the modulus used for the design is approximately equal to that in the finite element analysis, and the asphalt concrete and subgrade strains are acceptable.

2.6 Stress Ratio

The AASHTO T 307-99 testing procedure follows the common practice of maintaining a constant confining pressure while cycling through the deviator stress (see Figure 2-2). For this type of loading, the state of stress increments follow a stress path towards a failure state of stress as shown in Figure 2-10. In order to avoid failure, the harmonized protocol (Andrei 1999) based on the NCHRP Project 1-28A suggests that a

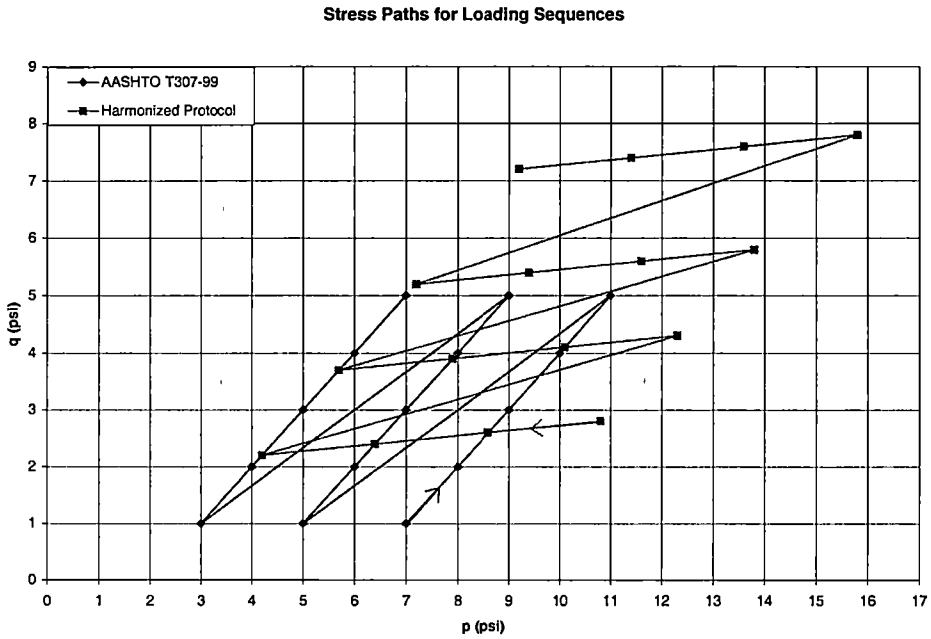

Figure 2-10 Stress Path for Loading Sequences (adopted from Andrei 1999)

Table 2-2 Testing Sequences for Triaxial Testing

Sequence	Confining Pressure σ_3 (psi)	Contact Stress (psi)	Cyclic Stress (psi)	Principal Stress Ratio (σ_1/σ_3)	Maximum Stress (psi)	σ_1 (psi)	Number of Load Applications
AASHTO T307-99 - Test Sequence for Type II Materials (Fine-Grained Subgrades)							
Conditioning	6.0	0.4	3.6	1.7	4.0	10.0	500-1000
1	6.0	0.2	1.8	1.3	2.0	8.0	100
2	6.0	0.4	3.6	1.7	4.0	10.0	100
3	6.0	0.6	5.4	2.0	6.0	12.0	100
4	6.0	0.8	7.2	2.3	8.0	14.0	100
5	6.0	1.0	9.0	2.7	10.0	16.0	100
6	4.0	0.2	1.8	1.5	2.0	6.0	100
7	4.0	0.4	3.6	2.0	4.0	8.0	100
8	4.0	0.6	5.4	2.5	6.0	10.0	100
9	4.0	0.8	7.2	3.0	8.0	12.0	100
10	4.0	1.0	9.0	3.5	10.0	14.0	100
11	2.0	0.2	1.8	2.0	2.0	4.0	100
12	2.0	0.4	3.6	3.0	4.0	6.0	100
13	2.0	0.6	5.4	4.0	6.0	8.0	100
14	2.0	0.8	7.2	5.0	8.0	10.0	100
15	2.0	1.0	9.0	6.0	10.0	12.0	100
Harmonized Protocol II - Test Sequence for Fine-Grained Subgrades							
Conditioning	4.0	0.8	7.0	3.0	7.8	11.8	1000
1	8.0	1.6	4.0	1.7	5.6	13.6	100
2	6.0	1.2	4.0	1.9	5.2	11.2	100
3	4.0	0.8	4.0	2.2	4.8	8.8	100
4	2.0	0.4	4.0	3.2	4.4	6.4	100
5	8.0	1.6	7.0	2.1	8.6	16.6	100
6	6.0	1.2	7.0	2.4	8.2	14.2	100
7	4.0	0.8	7.0	3.0	7.8	11.8	100
8	2.0	0.4	7.0	4.7	7.4	9.4	100
9	8.0	1.6	10.0	2.5	11.6	19.6	100
10	6.0	1.2	10.0	2.9	11.2	17.2	100
11	4.0	0.8	10.0	3.7	10.8	14.8	100
12	2.0	0.4	10.0	6.2	10.4	12.4	100
13	8.0	1.6	14.0	3.0	15.6	23.6	100
14	6.0	1.2	14.0	3.5	15.2	21.2	100
15	4.0	0.8	14.0	4.7	14.8	18.8	100
16	2.0	0.4	14.0	8.2	14.4	16.4	100

maximum value of the principal stress ratio (σ_1/σ_3) should be specified as a limiting value. Once the limiting value is reached, the deviator stress is decreased and a similar sequence is performed at a higher confining pressure. Table 2-2 shows the proposed testing sequences. This would mean that the stress paths would proceed from 1 to 2 to 3 and so forth.

Figure 2-10 shows the stress path for the current AASHTO T307-99 procedure along with the proposed harmonized protocol. Figure 2-10 is a plot of the stress sequences in p-q space where:

$$p = \frac{\sigma_v + \sigma_h}{2} = \frac{\sigma_1 + \sigma_3}{2} \tag{2-1}$$

$$q = \frac{\sigma_v - \sigma_h}{2} = \frac{\sigma_1 - \sigma_3}{2} \tag{2-2}$$

Where

p = center of Mohr's circle or mean stress

$$\text{q} = \text{shear stress} = \frac{1}{2}\sigma_d$$

The p-q diagram is a series of stress points, which are connected by a line or curve called a stress path. The stress path represents a change of stress. As can be seen from the figure, the material is alternating between stress states that bring it close to failure, which would be represented as the K_f line in the p-q stress space, and stress states of minimum damage for the AASHTO method. If a material is weak, it may fail early during the test. For a strong material, the stress state may never approach failure and information for higher stress ratios will not be gathered. The harmonized protocol suggests starting off

with stress ratios that are not likely to fail the specimen and then proceeding to higher ratios. The tests performed in this study did not use the harmonized protocol, but there was no evidence of sample yielding in any of the tests.

Chapter 3 CBR Testing

The California Bearing Ratio (CBR) is a standardized test used to measure the strength of base, subbase, and subgrade materials. ASTM D 1883-94, the Standard Test Method for CBR (California Bearing Ratio) of Laboratory-Compacted Soils, is the testing method used for remolded soils. In the test, a standardized piston having an area of 3.0 in.^{2} (1.95 in. diameter) is used to penetrate the soil, that has been soaked for 96 hours, at a loading rate of 0.05 in./min. The piston is driven 0.5 in. into the soil and the stress is recorded at 0.025 in. increments. The CBR value is the ratio of the strength of the soil to that of high-quality crushed rock. The values for high quality crushed rock are given in Table 3-1. Equation 3-1 is used to calculate the bearing ratio.

$$\text{CBR} = \frac{\text{penetration stress (psi)}}{\text{standard penetration stress (psi)}} * 100 \qquad (3\text{-}1)$$

Usually the CBR value decreases as the penetration increases (Huang 1993). For this reason the value at 0.1 in. is used as the CBR. However for some soils, the value at 0.2 in. is greater. If this is the case, the test should be rerun. If the test produces a similar result, the value at the 0.2 in. penetration should be used as the CBR. Figure 3-1 (Liu and Evett 2000) shows some general ratings of soils that are to be used as base, subbase, and subgrade materials for roads and airport runways.

The CBR is often used to estimate the resilient modulus of a soil and is used in the AASHTO Guide (1986, 1993). Heukelom and Foster (1960) developed the following correlation between CBR and resilient modulus.

$$M_R(psi) = 1500(CBR) \qquad (3\text{-}2a)$$

Table 3-1 Standard Values for High Quality Crushed Rock (ASTM D 1883)

Penetration	Pressure
0.100 in. (2.54 mm)	1000 psi (6.9 MPa)
0.200 in. (5.08 mm)	1500 psi (10.3 MPa)
0.300 in. (7.62 mm)	1900 psi (13.1 MPa)
0.400 in. (10.16 mm)	2300 psi (15.9 MPa)
0.500 in. (12.70 mm)	2600 psi (17.9 MPa)

Table 23–1 Soil Ratings for Roads and Runways [2, 3]

CBR No.	*General Rating*	*Uses*	*Classification System*	
			Unified	*AASHTO*
0–3	Very poor	Subgrade	OH, CH, MH, OL	A5, A6, A7
3–7	Poor to fair	Subgrade	OH, CH, MH, OL	A4, A5, A6, A7
7–20	Fair	Subbase	OL, CL, ML, SC, SM, SP	A2, A4, A6, A7
20–50	Good	Base, subbase	GM, GC, SW, SM, SP, GP	A1*b*, A2–5, A3, A2–6
>50	Excellent	Base	GW, GM	A1*a*, A2–4, A3

Figure 3-1 Soil Ratings for Road and Runways (after Liu and Evett 2000)

$$M_R(kg/cm^2) = 100(CBR) \quad (3\text{-}2b)$$

$$M_R(MPa) = 10(CBR) \quad (3\text{-}2c)$$

Most researchers reference the paper by Heukelom and Klomp (1962) for this correlation.

The use of Equation 3-2 to estimate resilient modulus has several flaws. First the test is really a measure of the shear or punching shear strength of the soil and not a dynamic measurement or measurement of stiffness. The soaking condition corresponds to submerged subgrades with shallow water table, and may not be adequate for other conditions of a deep water table (Uzan 1998). The correlation with resilient modulus was developed using field, not laboratory, measurements of CBR. Heukelom and Klomp (1962) state that the correlation between the two is rough because the multiplier on CBR (1500 psi, 100 kg/cm^2, 10 MPa) actually varies within a factor of two from 750 to 3000 psi, 200 to 50 kg/cm^2, and 5 to 20 MPa.

Drumm et al. (1993) found that the correlation was not applicable to eight subgrade soils in Tennessee (Figure 3-2). Figure 3-2 also indicates the range that is to be expected using the assumed M_R = 1500CBR relationship.

For the current research, CBR tests were conducted on the four site soils. The specimens were remolded in 15.24 cm (6 in.) diameter molds in accordance with ASTM D 698-91. The samples were compacted to optimum moisture and density conditions in order to compare with the repeated load triaxial test specimens. The samples were soaked for 96 hours in accordance with ASTM procedures and to model the worst-case scenario. Table 3-2 shows the results for the testing. All of the soils have a very poor to poor to fair general rating based on Figure 3-1. Figures 3-3 through 3-6 show the CBR

Relationship Between Resilient Modulus and CBR

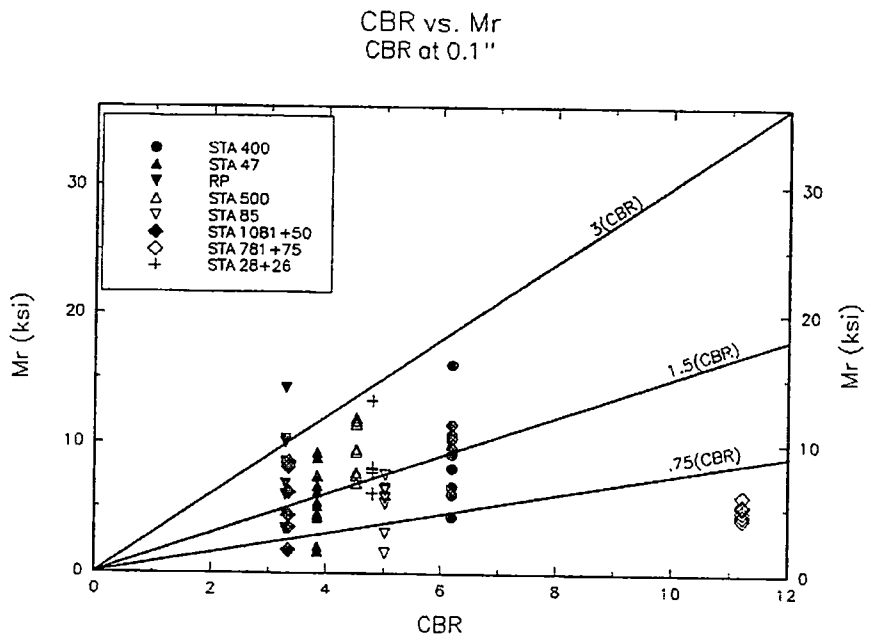

Figure 2. Relationship between M_r and CBR at 0.1".

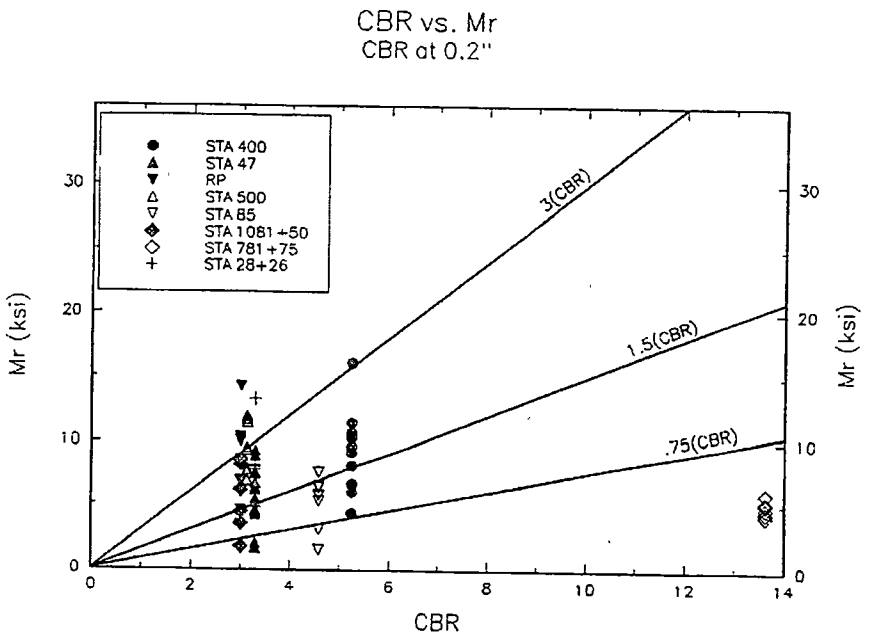

Figure 3. Relationship between M_r and CBR at 0.2".

Figure 3-2 Relationships between M_R and CBR for Tennessee Soils (Drumm et al. 1993)

Table 3-2 CBR Test Results

Site	Penetration at 0.1"	Penetration at 0.2"
Blount County	4.8	4.7
McNairy County	4.2	4.4
Overton County	5.4	5.3
Sumner County	2.5	2.6

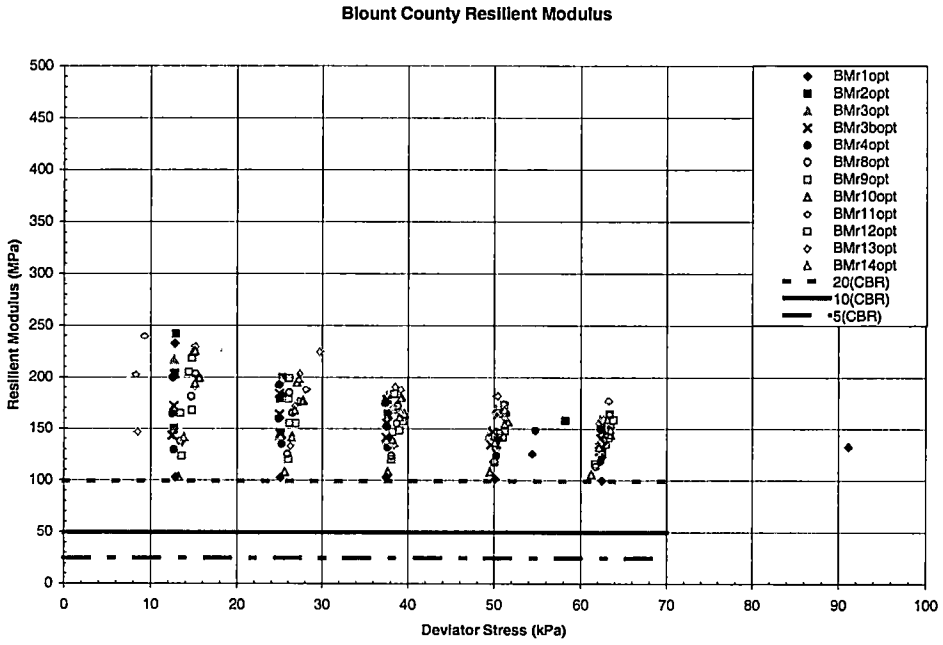

Figure 3-3 CBR Correlation with Blount County

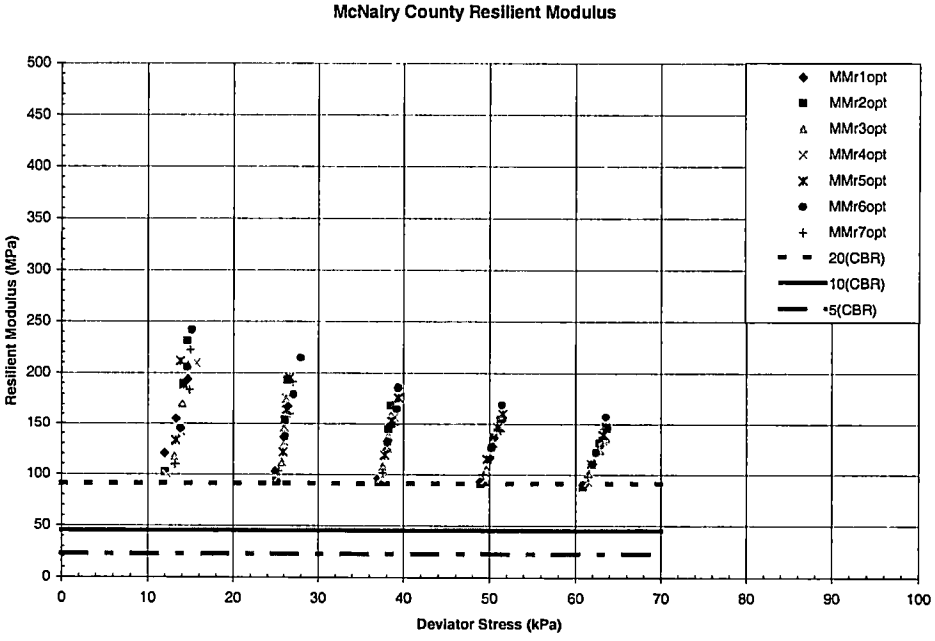

Figure 3-4 CBR Correlation with McNairy County

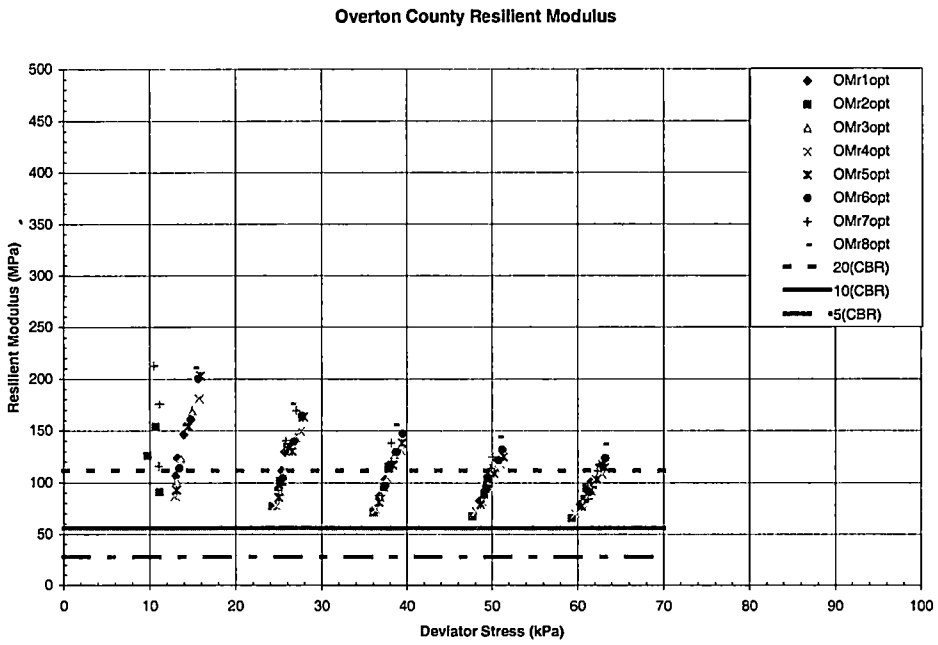

Figure 3-5 CBR Correlation with Overton County

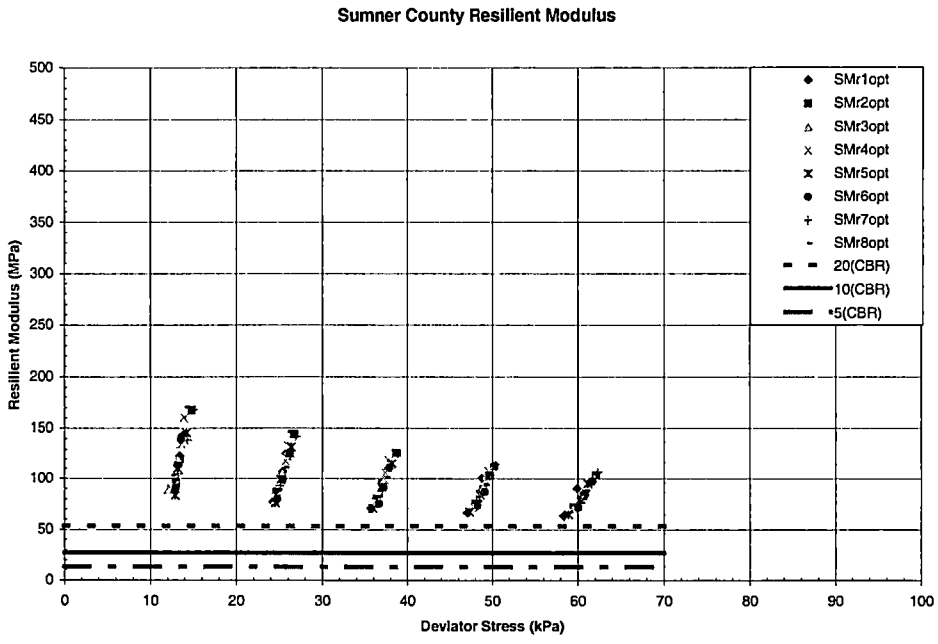

Figure 3-6 CBR Correlation with Sumner County

correlation with resilient modulus plotted against the actual repeated load triaxial data. Also shown on the plots are the upper and lower limits to the original equation. As can be seen from the figures, the resilient modulus values estimated from Equation 3-2c are not representative of actual values. The values are much lower than actual, producing an overly conservative estimate of resilient modulus. Therefore, the CBR correlation should not be used to determine resilient modulus values for fine-grained soils in Tennessee, because pavement thickness would be increased to compensate for the lower modulus values.

Chapter 4 Alternative Test Method

4.1 Previous ATM Research

An alternative test method (ATM) to the standard resilient modulus test was developed (Li 1992; Drumm et al. 1997) and tested by Madgett (1994) and Reeves (1995) at the University of Tennessee. Li (1992) developed a theoretical model based on a single degree of freedom, lumped mass spring system to calculate resilient modulus and deviator stress. The equations were developed for a weighted hammer falling onto a mass of soil confined in a Proctor mold. Because of the lateral confinement, the test actually measures the constrained modulus. Using the peak acceleration, mass of the hammer, drop height, and an assumed value of Poisson's ratio, the constrained modulus can be converted to resilient modulus and the deviator stress can be found from the following equations:

$$M_R = \frac{(1+\nu)(1-2\nu)}{1-\nu} * D = \frac{(1+\nu)(1-2\nu)}{1-\nu} * \frac{(m_o + F_m m_1)^2 A_p^{\,2}}{2ghm_o} * \frac{L}{A_{sec}} \tag{4-1}$$

$$\sigma_d = \frac{1-2\nu}{1-\nu} * \frac{A_p m_o}{A_{sec}} \tag{4-2}$$

Where:

M_R = resilient modulus

D = constrained modulus

ν = Poisson's ratio

$m = m_o + F_m m_1$

m_o = mass of hammer

m_1 = mass of soil specimen

F_m = mass participation factor = 0.5

L = length of specimen

A_p = peak deceleration

h = drop height of the hammer

g = acceleration of gravity

A_{sec} = cross sectional area of the specimen

σ_d = deviator stress

A second method was proposed to calculate the resilient modulus of the soil based on the area under the acceleration curve. The area underneath the time-acceleration curve from time zero to peak acceleration can be measured. This area represents the velocity of the hammer. In this way, the velocity is not calculated but actually measured using the ATM, presumably reducing the amount of error in underlying assumptions. The area measurement replaces the velocity term in Equation 4-1. The equation is as follows:

$$M_R = \frac{(1+\nu)(1-2\nu)}{1-\nu} * D = \frac{(1+\nu)(1-2\nu)}{1-\nu} * \frac{(m_o + F_m m_1)^2 A_p^{\ 2}}{Area^2 m_o} * \frac{L}{A_{sec}} \qquad (4\text{-}3)$$

Madgett (1994) and Revees (1995) concluded that the area method did not work well; however, they estimated the area assuming a sinusoidal time-acceleration history.

The derivation of the equations and underlying assumptions can be found in Appendix E or the thesis of Li (1992). One of the major assumptions that requires emphasis is the choice of 0.5 for the mass participation factor. The mass participation

factor represents the portion of the soil mass assumed to be accelerated by the falling hammer. It is assumed that the displacement, velocity, and acceleration in the soil sample are distributed linearly along the height of the sample, from maximum at the top to zero at the bottom.

The ATM is a fairly simple device that does not require much space (Figure 4-1). The ATM consists of a 10.16 cm (4 in.) diameter proctor mold where a soil specimen can be prepared. The specimen can easily be compacted at any density on the Proctor curve by selecting the appropriate water content. The mold is placed on the base of the device and secured by two wing nuts. A hammer with weights is attached at a set distance above the specimen. An adjustable arm controls the drop height. An accelerometer measures the time-acceleration history of the hammer as it impacts the soil. The signal is sent to a computer, which displays the signal and records it to a signal file. This is done by means of a digital oscilloscope card.

4.2 Previous ATM Results

The ATM procedure has been described by Li (1992) and Madgett (1994). Li (1992) found that the resilient modulus determined by the ATM for three subgrade soils in Tennessee was similar to that obtained by the standardized repeated load test at the time. The ATM values were slightly higher than the triaxial values. The ATM values also tended to increase with an increase in deviator stress, which is opposite of the normal trend for fine-grained materials. In the ATM test, the confining pressure increases with increasing deviator stress. In the triaxial test, the confining pressure is held constant as the deviator stress is changed. For nonlinear materials, Poisson's ratio changes with

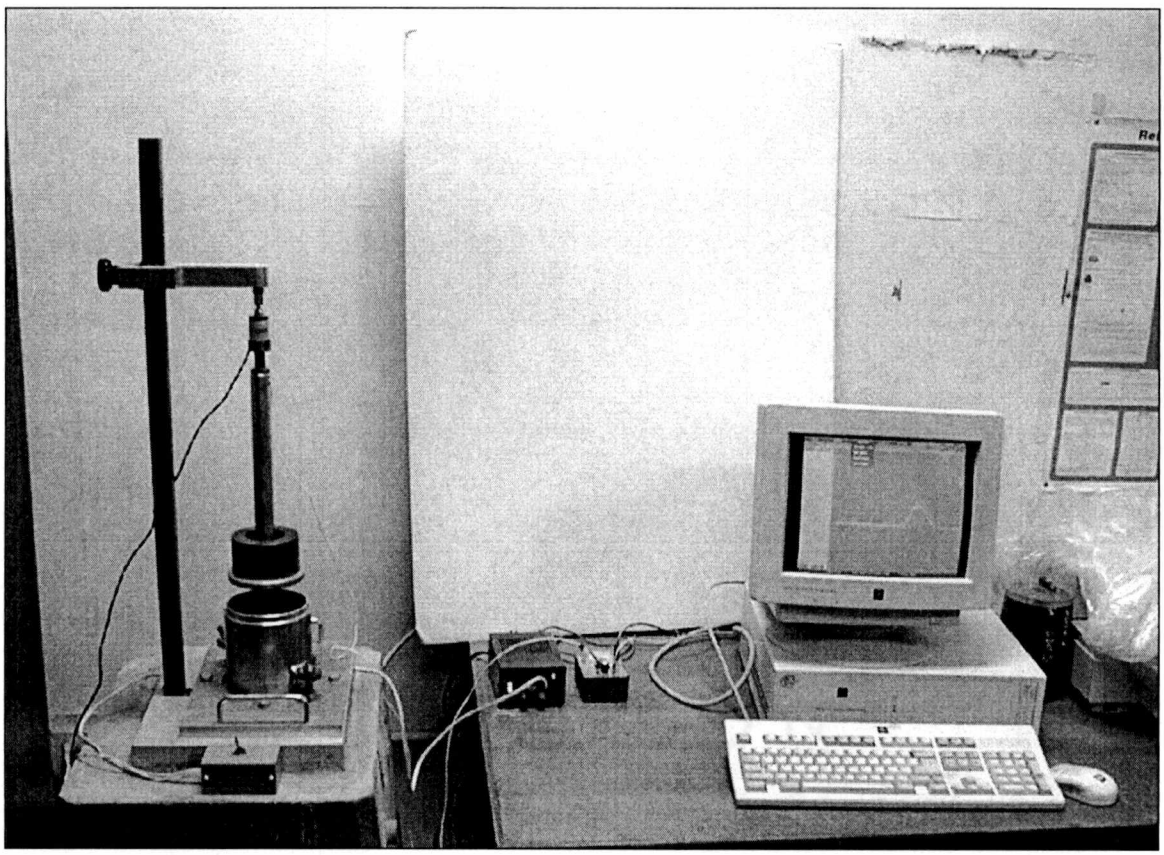

Figure 4-1 ATM Setup

deviator stress and stress path or different loading conditions. Therefore, the value of Poisson's ratio should change under different loadings. Li found that a decrease in Poisson's ratio leads to a slight increase in modulus and a significant increase in deviator stress. This probably explains why there is an increase in the modulus with increased deviator stress.

Madgett (1994) continued the work started by Li. A digital oscilloscope was integrated into the system so that the time-acceleration history could be gathered. This meant that it was no longer necessary to assume a history that was sinusoidal, since the curve could be captured in a digital format. At the time of the research, the development of the area method was still not complete.

For six subgrade soils from Tennessee, referred to as Phase II materials, samples compacted at optimum moisture and density produced the same trend of increasing modulus with increasing deviator stress (Madgett 1994). During the constrained test, the confining stress increases as the vertical stress increases because no horizontal strains are allowed. In general, it was found that the values obtained by the ATM were lower than values obtained by cyclic triaxial testing. Madgett also observed that the ATM was capable of measuring differences in stiffness between soft and firm soils.

Three of the soils used in the study above were saturated after being compacted to optimum moisture and density conditions. It was found that the ATM device could measure a decrease in modulus when the degree of saturation was greatly increased. However at lower degrees of saturation above optimum, the ATM showed an increase in modulus. This increase was described as being a result of skin friction due to swelling,

since the specimen could not swell in a radial direction (Madgett 1994).

Reeves (1995) continued work on the ATM device. A computer program was developed to read peak deceleration values from the oscilloscope and perform ATM calculations. The procedure is described by Reeves (1995).

Reeves (1995) conducted ATM tests at optimum moisture and density on the same eight subgrade soils, described as Phase I materials, that Hudson (1992) used in triaxial testing. Again, an increase in resilient modulus was observed with an increase in deviator stress. To convert the constrained modulus measured by the ATM to resilient modulus, Poisson's ratio must be assumed. The relationship between resilient modulus and Poisson's ratio can be seen in Equations 4-1 and 4-3. Li (1992), Madgett (1994), and Reeves (1995) all used a value of 0.45 for Poisson's ratio since it is consistent with common pavement design practices and since it has a small effect on pavement responses (Huang 1993). The range of Poisson's ratio is 0.30-0.50 for fine-grained soils and 0.40-0.50 for saturated soft clays (Huang 1993). Again, if smaller values of Poisson's ratio are chosen, the calculated resilient modulus and deviator stress both become larger. Madgett compared interpolated values of resilient modulus at a confining pressure of 41.4 kPa (6psi) and a deviator stress of 27.6 kPa (4psi) since SHRP Protocol P46 suggested reporting values for this stress state. Of 8 site soils tested and the 6 soils tested by Madgett (1994), all but three values of the ATM calculated modulus values fell within 25% of the triaxial test data, which was considered to be sufficient for pavement design. It was speculated that the values outside this range were due to variations in compaction moisture content.

Poisson's ratio is, however, not a constant value, but varies with states of stress also. In working with granular materials, Boyce (1980) developed relationships for resilient Poisson's ratio, which is dependent on the stress ratio (σ_1/σ_3). As can be seen from Equation 4-3, if the value of Poisson's ratio increases, there should be a decrease in resilient modulus. If the variation in Poisson's ratio with variable stress ratio could be determined, the ATM values should correspond better with the repeated load triaxial results.

All of the previous triaxial tests conducted by Hudson (1992), Madgett (1994), and Reeves (1995) followed SHRP Protocol P46 with a few minor exceptions described by Hudson (1992).

4.3 Improvements to the ATM

Since the last research with the ATM device, a few improvements have been made to the device itself and to the data processing. First of all a new release mechanism was added. A magnetic release was installed to insure more consistent hammer drops. The old "quick connect" pressure fitting did not allow the hammer to drop consistently and perpendicular to the soil. The fitting made the hammer susceptible to starting off its fall to one side. This was caused by one of the three ball bearings, inside of the fitting, being released after the first two. The cylindrical track was removed to keep the hammer from making contact during free fall. The track was meant as a guide, but the hammer would often make contact, disrupting the signal. During earlier stages of testing, the old oscilloscope card failed and was replaced with a new card. To further reduce noise and insure more consistent drops, the ATM base was grouted to a concrete block and the

adjustment arm was shimmed at the base to make it perpendicular. To aid in the data processing, a Visual Basic program was developed (Zuo 2000) to calculate resilient modulus. The program made modulus calculations for the peak and area methods. The program was later modified to calculate modulus based on double integration technique of the time-acceleration history (Choi 2001).

4.4 Visual Basic Program for ATM

Based on the work done by Boyce et al. (1989, 1990), the ATM program was modified to find the maximum displacement by integrating the time-acceleration curve twice. A typical ATM signal file is shown in Figure 4-2. To calculate the maximum displacement the signal is converted from voltage to acceleration. As can be seen in Figure 4-2, there is a considerable amount of noise in the signal. If this noise is integrated, large errors occur in the calculation of displacement. To eliminate the noise in the signal, a couple of steps were added to the program. The first step was to establish a threshold value of 0.05 volts. The noise at the beginning and end of the signal is 0.039 volts, which is less than the threshold value. All of the data points below the threshold value are counted. The total amount of noise, or sum of the accelerations, is divided by the total number of data points. This value is taken as the average amount of noise in the signal. The average noise is then subtracted from each data point in the actual impact portion of the curve. The second step modifies the signal when it crosses the threshold. The program sets all values before that point to zero acceleration. After the signal reaches its peak value and returns to zero, it will then cross the threshold value again and all the data points collected from that point on are set to zero also. A high pass filter is

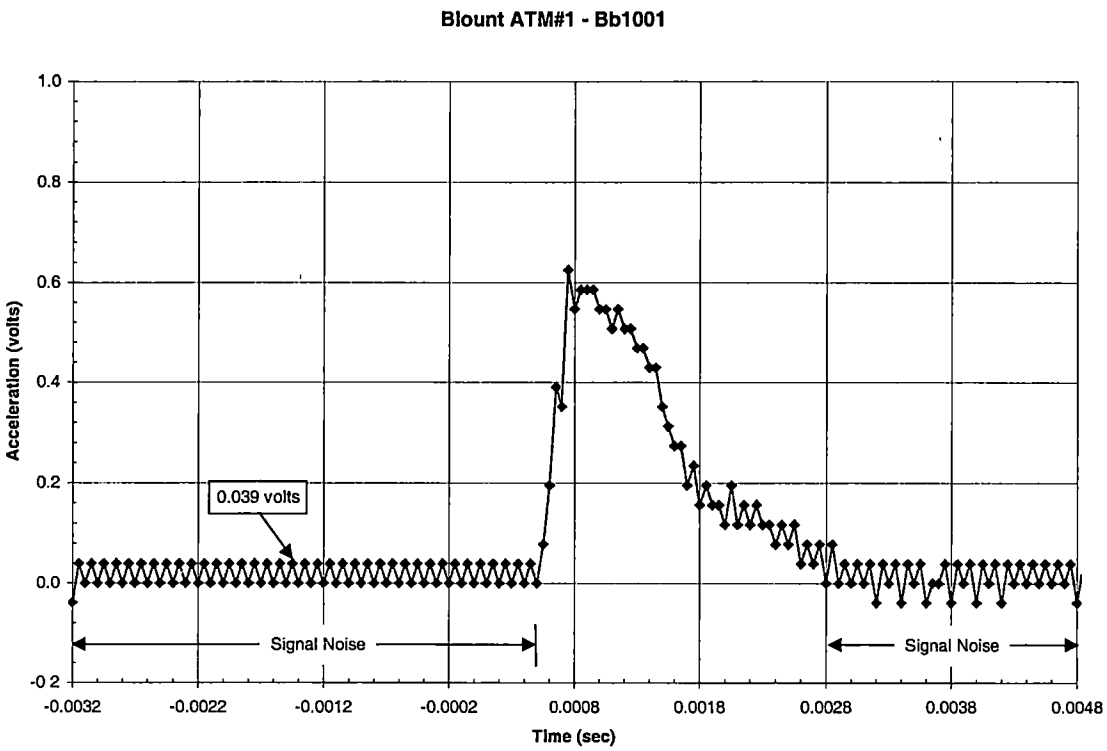

Figure 4-2 Typical ATM Signal

the function used to fit the line between data points. Figure 4-3 shows the original ATM signal and filtered signal. The area underneath the curve is found by using the Trapezoid Rule. The base of the trapezoid is broken up into 0.00005 sec increments. This is the sampling rate from the oscilloscope. The Trapezoid Rule is a much more accurate approximation of the area than the left or right endpoint rules (Stewart 1991). For future work, the Midpoint Rule may be considered since it has been found to be the most accurate of the four methods (Stewart 1991). However, the difference between the Midpoint Rule and Trapezoid rule is negligible, since both have errors with the same order of magnitude. For the double integration technique to work, an assumption of the initial velocity must be made. Boyce (Boyce et al 1990) assumed the initial velocity to be equal to $\sqrt{2gh}$. The initial velocity for the ATM is calculated by finding the area under the impact portion of the time-acceleration curve.

The double integration of the time-acceleration history is a more accurate way of determining the maximum displacement than the area method used in past research with the ATM. Figure 4-2 shows that there is a rapid rise to peak deceleration and then the signal returns more slowly. With the old area method, the material was assumed to be elastic. The deceleration and displacements were then assumed to be sinusoidal. Therefore, only half the area underneath the time-acceleration curve was used and then doubled since the curve was considered symmetric. The new method also has the advantage of an improved filter for the data. Removing the noise in a consistent manner reduces the error associated with it, thus producing more accurate results.

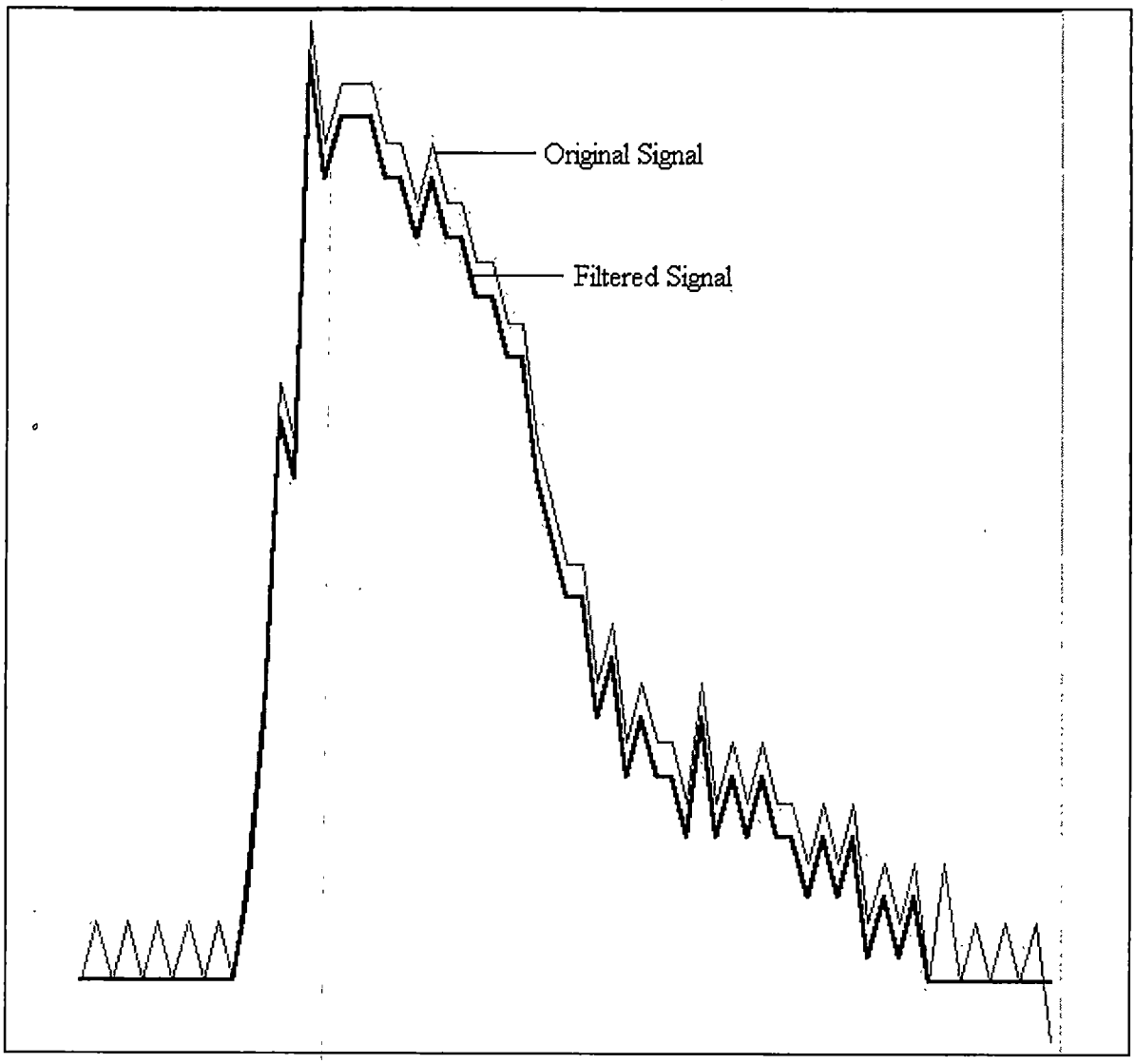

Figure 4-3 ATM Signal with Filtering

4.5 Resilient Modulus Calculations from ATM

The resilient modulus calculations are made in the following way. Equation 4-2 calculates the deviator stress from the peak acceleration of the time-acceleration curve from the ATM. The constrained modulus is calculated by the following equation.

$$D = \frac{\sigma_1}{\varepsilon_r} = \frac{\left(Am_o / A_{\text{sec}}\right)}{\left(\delta_{\max} / F_m L\right)} \cdot R_f \qquad (4\text{-}4)$$

Where

D = constrained modulus

ε_r = recoverable strain

σ_1 = major principal stress = vertical stress

A = acceleration

m_o = mass of hammer

A_{sec} = cross sectional area of the specimen

δ_{max} = maximum displacement

F_m = mass participation factor

L = length of specimen

R_f = reduction factor

It is the assumption of this equation that all of the displacement experienced by the soil is completely recoverable. This is a safe assumption as long as the deviator stress applied to the soil is much less than the strength of the soil. The constrained modulus is then converted to resilient modulus by the relationship shown in Equation 4-1, assuming a Poisson's ratio of 0.45.

The mass participation factor needs to reflect the portion of the soil that actually contributes to the strain. In the previous research, the factor was chosen to be 0.5. This same assumption is still made. A reduction factor, R_f, is added to the equation as a way in which to make the data fit to the actual measured values from the repeated load triaxial test. Currently the reduction factor is set to 1.0.

4.6 ATM Results for Site Soils

Two Proctor specimens were prepared at optimum moisture content and density for each of the four site soils. Ninety signal files were collected on each specimen. The small weight (1.159kg) was used first. Ten drops at heights of 10mm, 20mm, and 30mm were recorded. The same was done for the large weight (1.575kg) and a combination of both weights (2.087kg). The eight specimens were analyzed using the new double integration method. Specimen properties and results of testing are located in Appendix C.

For comparison with the previous methods, the old ATM program with the peak and area methods was used for the first specimen from Blount County. Figure 4-4 shows the result using the peak method with the old ATM program. Figure 4-5 is the result using the area method. As was observed in previous work, the results from the peak method fall below actual measured values of modulus. The same trend of increasing modulus with increasing deviator stress also continues. Again, since the ATM is a

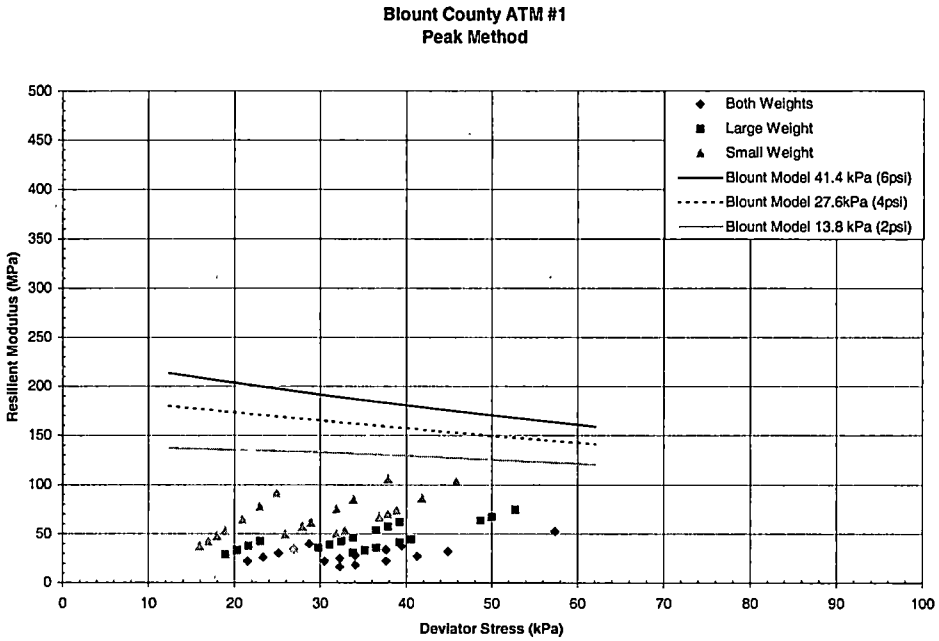

Figure 4-4 Typical ATM Result for Peak Method

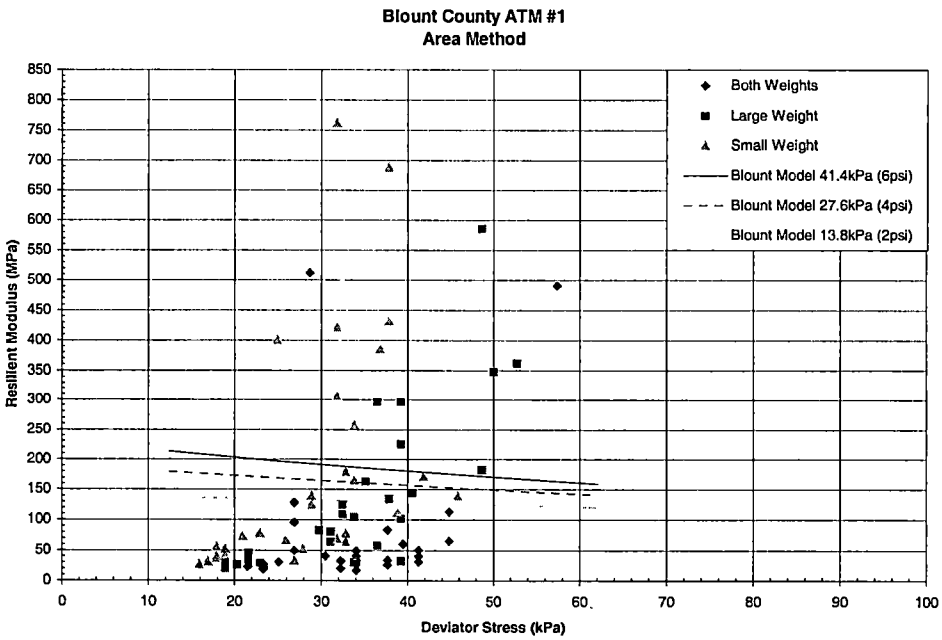

Figure 4-5 Typical ATM Result for Area Method

constrained test, the confining stress increases as the vertical stress increases, because only vertical strains are allowed. As was described in Chapter 2, modulus will increase with increasing confining stress. The results of the area method are inconclusive, since no pattern can be established. The results are typical for all four of the site soils.

Figure 4-6 is a typical result for the new double integration technique. Larger hammer weights result in higher values of resilient modulus. Also, the larger the hammer weight, the greater the overall deviator stress. The deviator stress is also a function of drop height. Typically, the higher the drop height, the larger the deviator stress. However, drop height does not appear to have an effect on resilient modulus for a given weight. This is counterintuitive, since one would expect the modulus to decrease with a greater deviator stress. The deviator stress should increase because there is more energy being input into the soil with greater drop heights. This should in turn increase the peak acceleration. Peak acceleration is used in both the calculation of modulus and deviator stress. There may be a couple of explanations for why there is not a decrease in modulus with increasing deviator stress. First, the test is a confined compression test. As the vertical stress is increased, there is an increase in radial stress or confining stress. As was shown in Chapter 2, modulus increases with increasing confining stress. Another explanation could be that the change in recoverable strain in the sample is in proportion to the change in peak acceleration. With acceleration in the numerator of Equation 4-4 and strain in the denominator, the change would cancel each other out.

The values of resilient modulus calculated from the ATM for each site are very close. This is to be expected since the results from the standard test were also close.

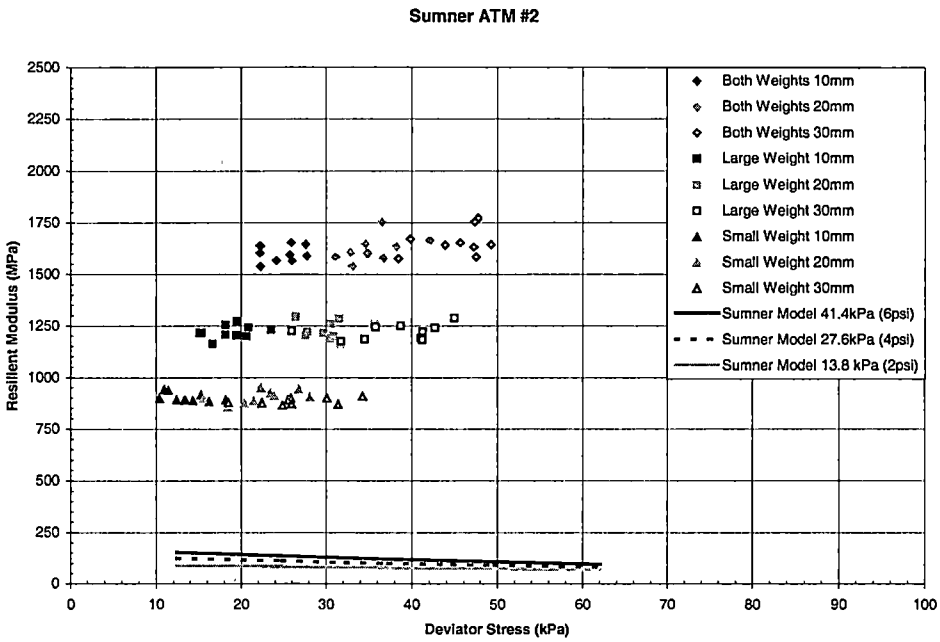

Figure 4-6 Typical ATM Result Using Double Integration Technique

4.7 Loading Rate Effects

As was shown previously, the calculated values of resilient modulus for the ATM were considerably larger than the actual measured values of the repeated load triaxial test for the same range of deviator stress. Part of this error may be due to loading rate effects. The ATM is a one-dimensional compression test where there is zero radial strain. This type of test is commonly referred to in soil mechanics as a consolidometer, oedometer, or one-dimensional compression device. The test boundary conditions are most accurately described from a continuum mechanics viewpoint by the term "uniaxial strain" (Jackson et al. 1980).

It has been recognized that uniaxial strain response of soils under rapid loading differs from the response of soils loaded under quasi-static loading rates (Farr 1990). Most of the research in this area has come from an interest of a single transient load as with nuclear weapons and blast effects. Loading rate effects of dynamic loads affect a materials mechanical response. This includes the stress, strain, and strength of the material (Farr 1990). Researchers have found that loading rate has an effect on the constrained modulus of soils. Farr (1990) found that there is an increase in modulus with increasing loading rate. This effect tended to level off when the time to peak load approaches the submillisecond range. He observed that the dynamic to static loading of the constrained modulus test was near a factor of two. Farr (1990) sites that other research has show differences in modulus up to ten times for some partially saturated granular soils under undrained conditions. Jackson (Jackson et al. 1980) found that the stiffness of sands increased dramatically when loading times drop below a millisecond.

For times greater than a millisecond, it was found that the loading rate effects could be ignored.

Farr (1990) explains the general mechanisms of loading rate effects by: "Schindler (1968) theorized that loading-rate effects existed because, 'grains can be arranged differently during densification; pore fluids under pressure can flow and transfer additional load to a structural skeleton; interaction amongst the three phases that comprise the soil mass can take several forms; the amount of pore fluid that can be dissolved in the pore is time sensitive; etc.' Of these reasons, particle rearrangement seems to be the major contributor to a loading-rate effect, especially for dry or minimally saturated granular materials. The initial response of a soil sample during a uniaxial strain test is dictated by elastic deformations at the contact points. The particles then rearrange due to slippage at the contact points at higher stress levels. If the soil particles cannot rearrange into a denser configuration because the load is being applied too rapidly, the load will be absorbed by deformation of the soil particle instead of producing permanent compaction. This would result in a stiffening of the soil."

Another aspect of the loading rate effect is the size of the specimen. Both Jackson (Jackson et al 1980) and Schindler (1967) used specimens that had large diameters relative to the thickness. Schindler used a 10.16 cm (4.0 in.) diameter specimen that was 2.54 cm (1.0 in.) in height, which is a height to diameter ratio of 1:4. Jackson used specimens with a ration of 1:7.6. The large height to diameter ratios were used to prevent sidewall friction from influencing center deflections and to minimize the transit time of propagating stress waves.

The repeated load triaxial test is not a uniaxial test. The confining stress is regulated. However, it is believed that the loading rate effects still play a role. In the test, a load of 0.1 sec duration is applied. The time to peak is 0.05 sec. From the information presented earlier, it would be expected that the loading rate would have no effect on the results for the standard test. During the ATM test, the time to peak is much faster. By looking at the loading rate, the time to peak acceleration can be calculated. The time to peak can also be seen by plotting the time-acceleration signal produced by the ATM. From this analysis, it was found that the time to peak is generally on the order of 10^{-4} sec. Since the time to peak is below one millisecond, loading rate effects are the probable cause for the increased modulus values.

In addition, the height of the ATM specimens is 1.34 cm (4.465 in.) and the diameter is 10.16 (4.0 in.). Therefore the height to diameter ratio is 1:0.90. This means there may be an increase in the stiffness due to sidewall friction. Cooking spray is used along the walls of the proctor mold to help reduce this error, however the samples still have a tendency to adhere to the walls.

Nondestructive deflection testing (NDT) methods, such as the falling weight deflectometer (FWD), can be used to estimate roadbed soil resilient modulus. The AASHTO Pavement Design Guide recommends using a reduction factor of no more than 0.33 when using a NDT method (AASHTO 1993). This factor is used because it has been found that backcalculated resilient modulus values exceed laboratory resilient modulus values by a factor of three or more for both observed data and finite element

analysis (AASHTO 1993). It is likely that this difference in field and laboratory methods is due to loading rate effects.

4.8 Corrected Acceleration

Greater modulus values from the ATM can be attributed to loading rate effects. However this may not be the entire cause. The choice of acceleration value may lead to elevated values. As describe by Boyce (Boyce et al.1990), a calculation based on the peak acceleration leads to a modulus value that is too large. For the reasons described in Chapter 1, they used the acceleration that corresponded to the peak displacement. All of the ATM tests were reanalyzed using this approach. The results can be found in Appendix C. A typical result is shown in Figure 4-7, which is the same data that was presented in Figure 4-6. Figure 4-7 is a comparison of the ATM resilient modulus values for both the peak acceleration and acceleration occurring at maximum displacement. While the new calculation did not significantly reduce the scatter in the data, the modulus values were slightly reduced. However, the ATM values are at least six times greater than the actual measured values.

4.9 Confining Pressure

As has been stated several times before, confining pressure effects the resilient modulus values. To determine the effect, the confining pressure for each test was calculated. The confining pressure ranged anywhere from 40kPa (5.8 psi) to 220kPa (31.9 psi). The confining pressures in the traditional test are 41.4kPa (6 psi), 27.6kPa (4 psi), and 13.8kPa (2psi). The confining pressures for the ATM are generally much higher than the traditional test. This is another explanation of why the modulus values

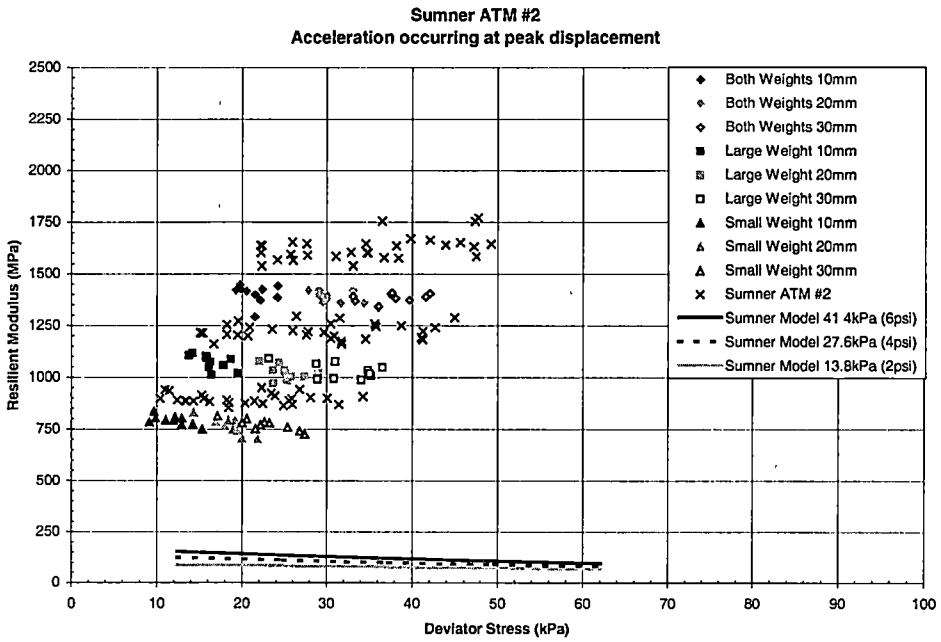

Figure 4-7 Typical ATM Result Using Double Integration Technique with Corrected Acceleration

calculated from the ATM are larger. Table 4-1 is a summary of the average confining pressures for each combination of drop height and weight for Sumner ATM #2. The small weight at a drop height of 10 mm has a confining stress that is closest to the confining stresses in the standard test. As can be seen in Figure 4-7, this combination has modulus values closest to those measured by the standard test method. Based on this information, the confining pressure for the small drop weight and 10 mm drop height for the other site soils were calculated. The values are shown in Table 4-2. As with Sumner ATM #2, the values for these other tests were slightly larger than the maximum confining stress in the standard test.

4.10 Polyurethane

It has been proposed that the use of synthetic samples (polyurethane) to calibrate resilient modulus equipment may be an excellent choice (Claros et al. 1990; Stokoe et al. 1990). Polyurethane specimens have the advantages over other materials, such as sand, because they can be fabricated with consistent material properties like stiffness. Some of the other advantages of synthetic samples are (Claros, et al. 1990; Stokoe, et al. 1990):

1. They are easy to construct in the appropriate sizes for resilient modulus equipment.
2. They have physical characteristics that remain constant with time.
3. They have stiffness properties that can be determined by independent tests.
4. They can be repeatedly tested as desired by different personnel and laboratories or both.

Table 4-1 Confining Pressures for Sumner ATM #2

Test	Hammer Weight	Drop Height (mm)	$\sigma_{c\ average}$ (kPa)
Sumner ATM #2	Both	10	96.9
Sumner ATM #2	Both	20	136.9
Sumner ATM #2	Both	30	168.9
Sumner ATM #2	Large	10	74.0
Sumner ATM #2	Large	20	113.2
Sumner ATM #2	Large	30	143.4
Sumner ATM #2	Small	10	53.6
Sumner ATM #2	Small	20	84.2
Sumner ATM #2	Small	30	102.1

Table 4-2 Confining Pressures for Small Weight and 10 mm Drop Height

Test	Hammer Weight	Drop Height (mm)	$\sigma_{c\ average}$ (kPa)
Blount ATM #1	Small	10	68.3
Blount ATM #2	Small	10	56.9
McNairy ATM #1	Small	10	70.4
McNairy ATM #2	Small	10	67.1
Overton ATM #1	Small	10	53.2
Overton ATM #2	Small	10	58.1
Sumner ATM #1	Small	10	61.0
Sumner ATM #2	Small	10	53.6

5. Specimens with any reasonable subgrade stiffness (from about 2,500 to 10,000psi, Young's modulus) can be manufactured.
6. The properties are essentially independent of stress and strain so that the flaws or limitations or both in the measurement systems can be evaluated.

To verify that the ATM is measuring the stiffness of the soil, a polyurethane sample was tested. A 2.54 cm (1.0 in.) thick gum rubber sample with a durometer hardness of shore 40A, which is about the stiffness of a rubber band, was tested. The stiffness of polyurethane is measured on a durometer hardness scale, which is an international standard for the measurement of rubber, sponge rubber, plastic, and other nonmetallic materials. Polyurethane is measured on a "Shore A" scale. The sample was noticeably much less stiff than the soils used. Constrained modulus tests were performed on a sample of McNairy soil and on the polyurethane. The constrained modulus for an average of three tests on the soil was 65 MPa (9.43 ksi) and 15 MPa (2.18ksi) for the polyurethane. The constrained modulus indicated that the soil was a little over four times the stiffness of the polyurethane. From the results in Figures 4-8 and 4-9, it can be seen that the ATM measures modulus values for the polyurethane that are at least three times less than that of the soil specimens. The polyurethane behaves in a manner that is intuitive. The deviator stress is increased with increased drop height and increased weight. The polyurethane is not a frictional material, therefore the confining pressure has little effect on the behavior.

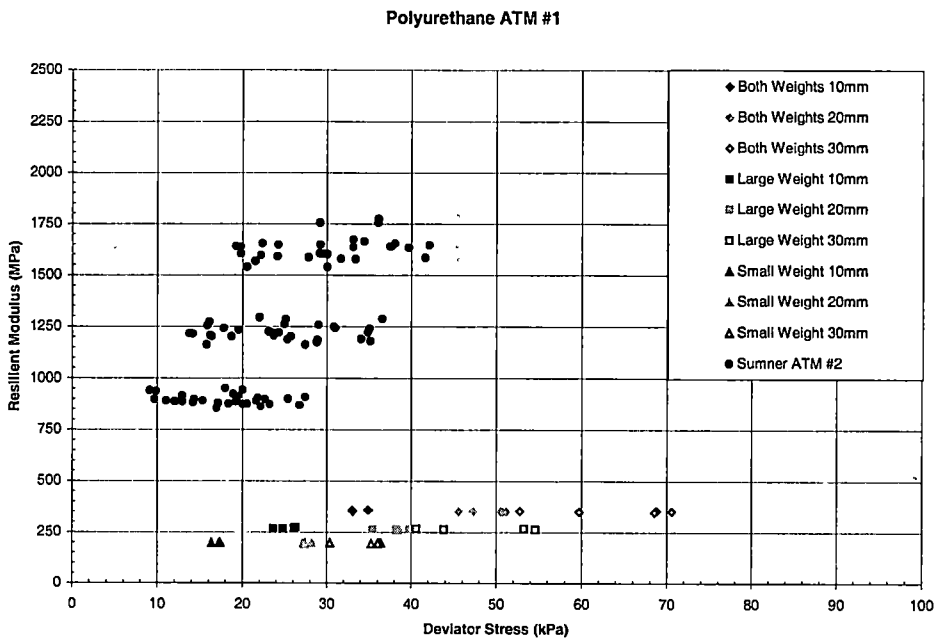

Figure 4-8 ATM Result Using Polyurethane with Peak Acceleration

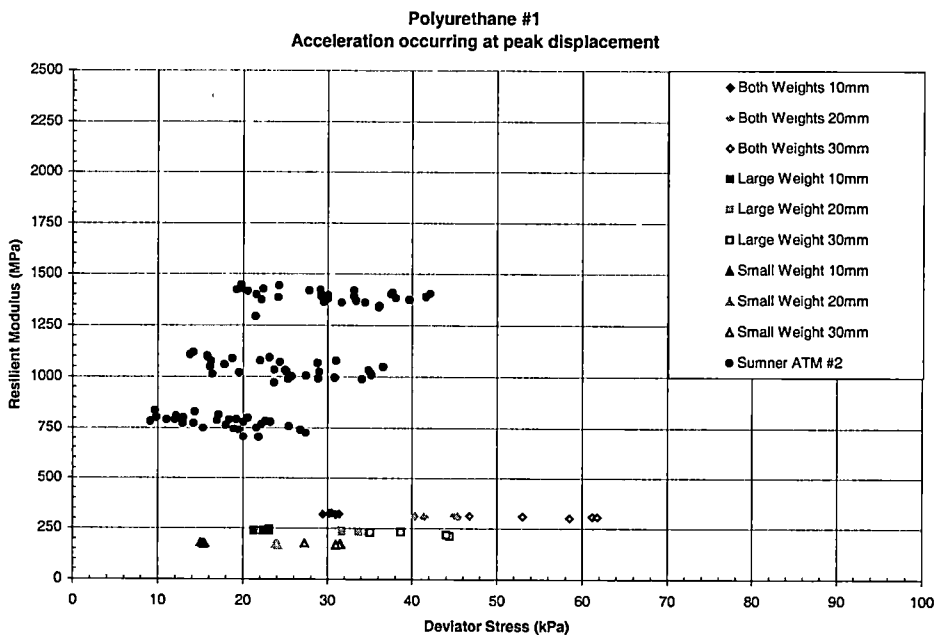

Figure 4-9 ATM Result Using Polyurethane and Acceleration Occurring at Peak Displacement

4.11 Stress Paths

In Section 2.6, the stress path for the repeated load triaxial test was investigated. The stress path for the AASHTO T 307-99 procedure and harmonized protocol were discussed and compared. In this section the stress path for the ATM will be compared to the repeated load triaxial test to see if the stress paths are consistent. Figures 4-9 and 4-10 show the stress paths for two separate ATM samples for various assumed values of Poisson's ratio. The stress path for the T 307-99 procedure is included in the figures. Stress path plots for the other tests can be found in Appendix C.

Figures 4-10 and 4-11 show that the stress path in the ATM is dependent on Poisson's ratio or the K_o, loading condition. The reason for this is because the confining pressure is calculated by multiplying the major principal stress by the K_o term, which is a function of Poisson's ratio for confined compression.

$$\sigma_3 = K_o \sigma_1 = \frac{\nu}{1-\nu} \sigma_1 \tag{4-5}$$

Since the stress path for the ATM is independent of the material type, both of the samples follow the same stress path. Poisson's ratio is assumed to be 0.45 for all of the ATM testing. Looking at the stress path for Poisson's ratio of 0.45 shows that the ATM falls within the same range of shear stresses as the standard procedure. However, the mean stress for the ATM is generally higher.

4.12 Reduction Factor

As has been previously shown, the new double integration technique has greatly reduced the scatter in the data. However, the resilient modulus values are much greater than actual resilient modulus values. This can be attributed to loading rate effects,

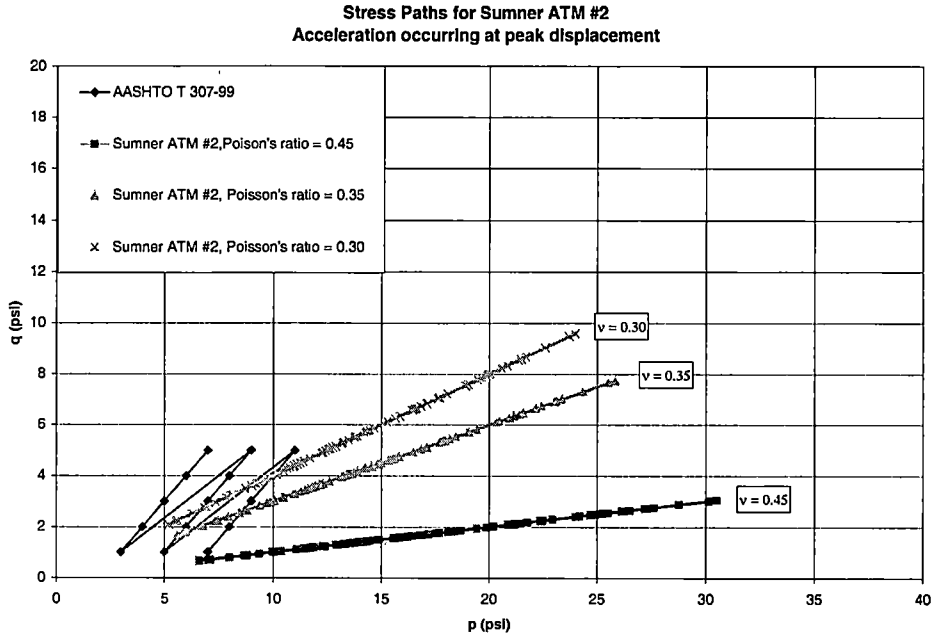

Figure 4-10 Stress Paths for Sumner ATM #2

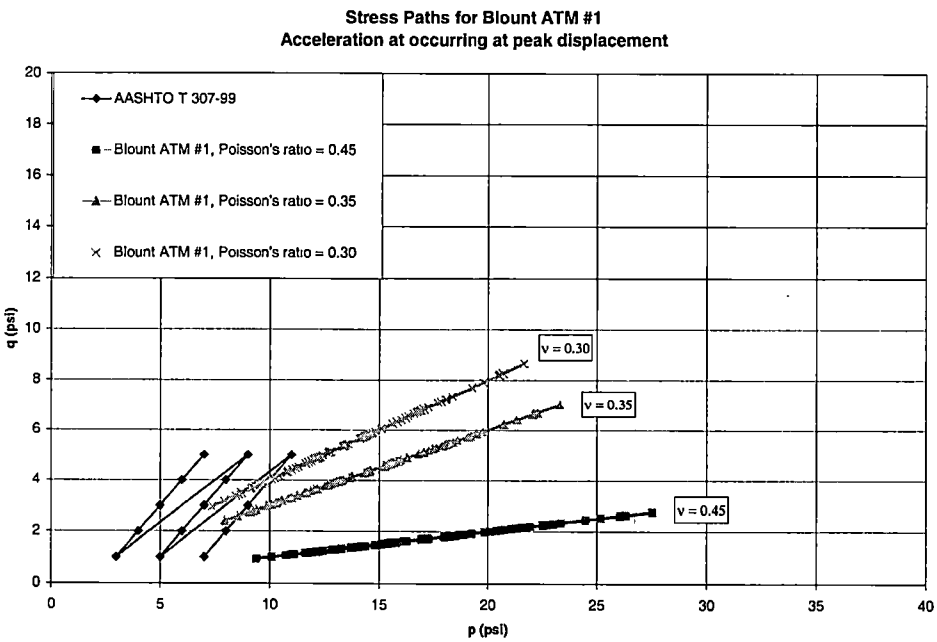

Figure 4-11 Stress Paths for Blount ATM #1

confining pressure, and length of the sample. The ATM data presented earlier did not incorporate a reduction factor. This section looks at the development of single reduction factor that can be applied to all four of the fine-grained soils.

To determine a reduction factor, values of resilient modulus representing the triaxial testing were plotted versus values from the ATM testing. The values on the ordinate, referred to as "Lab Resilient Modulus," were determined by inputting the major and minor principal stresses calculated from each ATM test into the model equation for each site (Equations 2-2 through 2-5). Figures 4-12 through 4-15 show the results with reduction factors plotted as straight lines. The 1 to 1 relationship in the figures corresponds to a reduction factor of 1.0. Reduction factors ranging from 0.20 to 0.35 are also shown.

Based on the data presented in Figures 4-12 through 4-15, a reduction factor of 0.30 is chosen. This factor was chosen because it was the approximate average of the reduction factors that fit the data for the large weight. The large weight was found to behave best during testing. This factor is also consistent with the 0.33 value recommended by AASHTO for correcting nondestructive test methods such as the falling weight deflectometer. Figure 4-16 shows the factor applied to the data from the second ATM test for Sumner County. The reduced ATM data still does not appear to fit the modeled resilient modulus very well; however, the correction factor was based on principal stresses in the ATM tests. The deviator stresses from the ATM fall within the range of deviator stress from the triaxial test; however, the major and minor principal

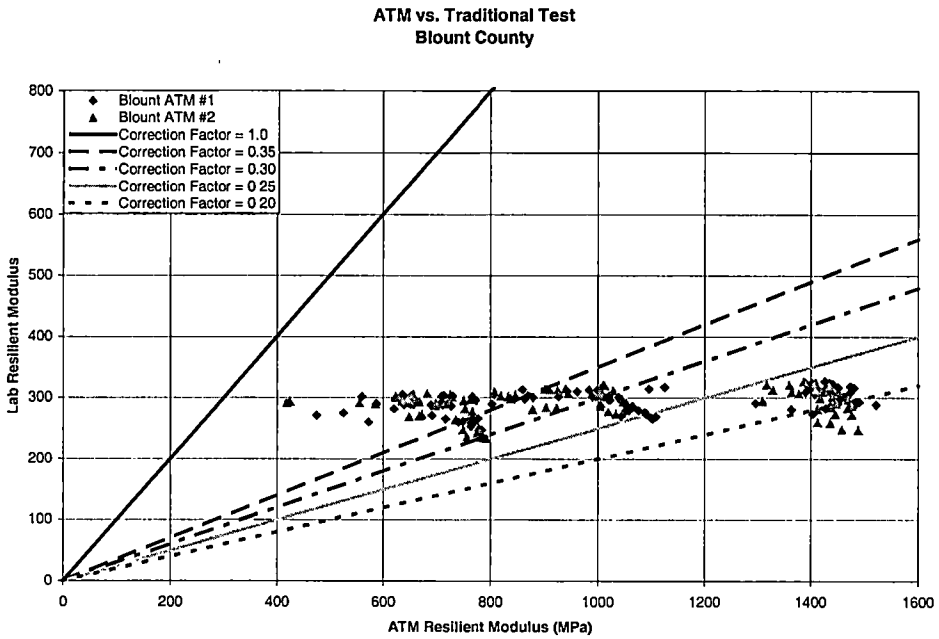

Figure 4-12 ATM Versus Traditional Test for Blount County

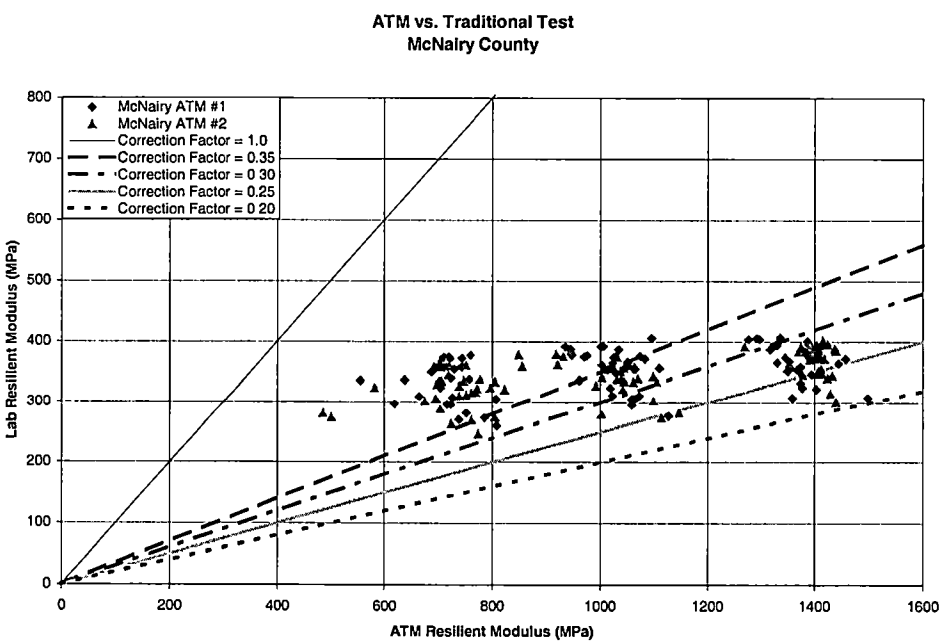

Figure 4-13 ATM Versus Traditional Test for McNairy County

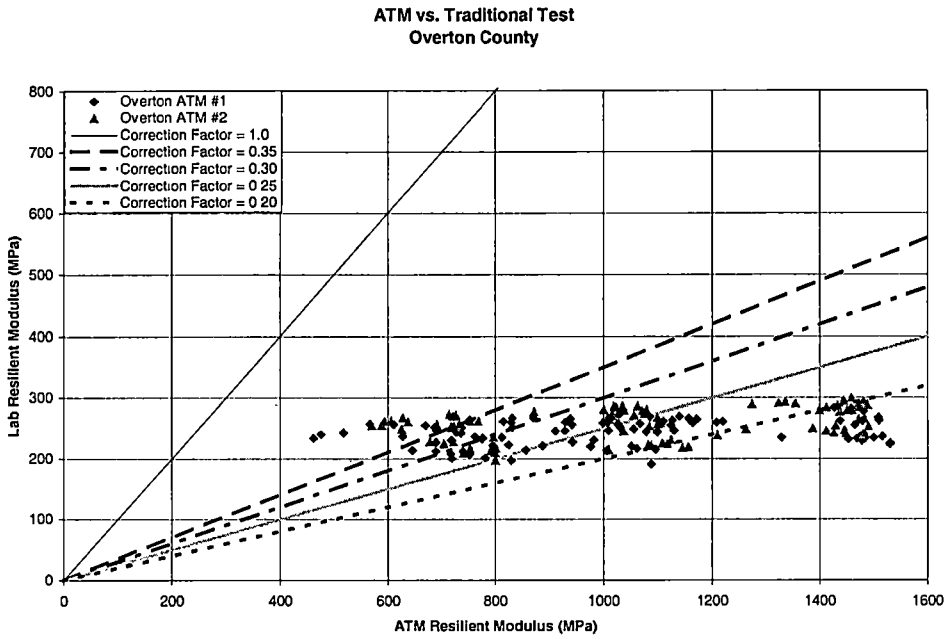

Figure 4-14 ATM Versus Traditional Test for Overton County

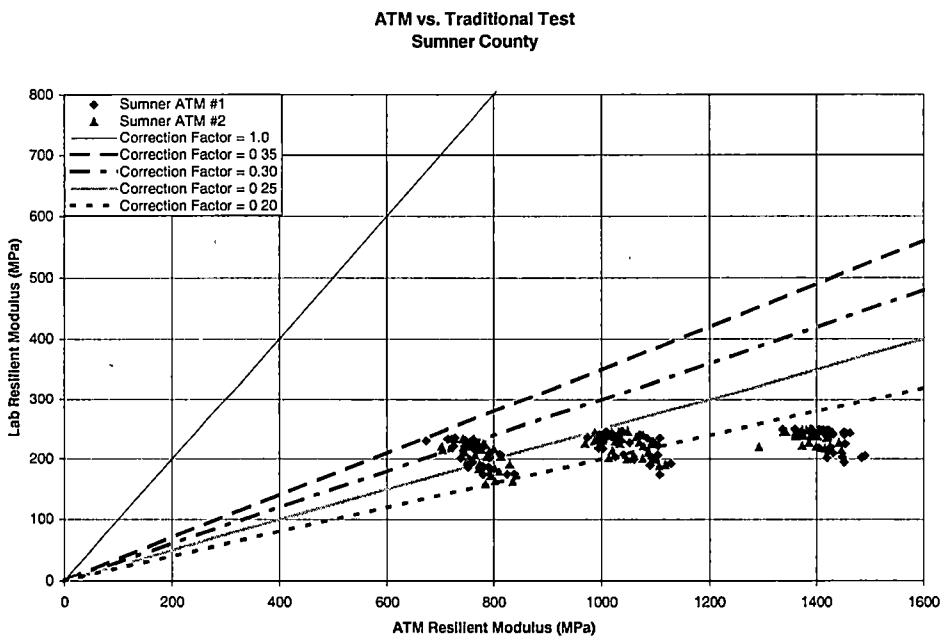

Figure 4-15 ATM Versus Traditional Test for Sumner County

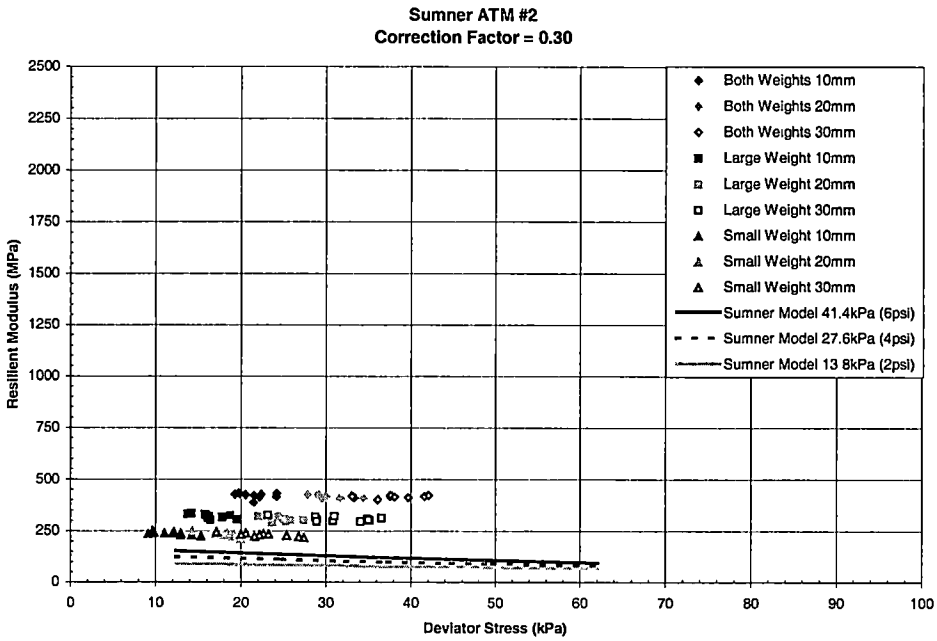

Figure 4-16 Sumner ATM #2 with Correction Factor = 0.30

stresses are greater in the ATM. The larger confining pressures developed in the ATM test are the most likely cause for the greater modulus values.

4.13 Limitations of the ATM

The stress path for the ATM is a limitation along with the assumption of Poisson's ratio and should be investigated. Poisson's ratio not only affects the slope of the stress path and magnitude of the confining pressure, but it is also used in converting constrained modulus to resilient modulus. For fine-grained soil, typical values of Poisson's ratio range from 0.35 to 0.45. As can be seen from Equation 4-1, the Poisson's ratio term is constant, C. The equation could be written as:

$$M_R = C * D \tag{4-6}$$

For Poisson's ratio of 0.35 the constant is equal to 0.62, and for a Poisson's ratio of 0.45 the constant is 0.26. Using a Poisson's ratio of 0.45 results in a conservative resilient value from the ATM. One potential way to eliminate many of these assumptions would be to test samples outside of the proctor mold. In this way, there is no confining stress and the deviator stress may be more accurately calculated.

One of the major limitations of the new ATM double integration technique is the sample length. The modulus calculations are highly dependent on the length of the sample and the assumed mass participation factor of 0.5. For example, if the length of the polyurethane were changed from 2.54 cm (1.0 in.) to the length of the soil samples, the resilient modulus values would almost be the same because the measured displacements are of the same magnitude. The ATM should not be as sensitive to this factor. The change in accelerations from sample to sample should be the major factor. A

change in sample length would also increase the height to diameter ratio and reduce the effects of sidewall friction if tested in the proctor mold. More work should be conducted to determine an appropriate sample length to reduce its influence. The contribution of the soil length to the actual strain should also be investigated.

Chapter 5 Conclusions and Recommendations

5.1 Conclusions

The University of Tennessee Soils Laboratory now has the ability to perform repeated load triaxial testing. The 35 tests performed on four site soils throughout the state of Tennessee show that the MTS setup is consistent in measuring the resilient modulus of fine-grained soils. The research has shown that the proposed model for the new 2002 Guide fits the resilient modulus values very well as indicated by the high R^2 values. In addition, the use of the CBR correlation to resilient modulus was shown not to apply to fine-grained soils.

The consistency of the alternative test method has been improved by using the double integration technique. Using the acceleration occurring at the peak displacement as opposed to the maximum acceleration was shown to improve the results even further. However, the time-integration scheme used to integrate the acceleration-time history has been found to be unstable, yielding different results as the time interval was changed. In fact, the comparisons shown in Chapter 4 are incorrect due to this time-integration problem, and the suggested correction factors are not valid. New correction factors remain to be determined. The ATM was shown to be able to detect changes in stiffness between different materials, but additional work is necessary if the ATM is to be used in practice. Appendix F explores the integration process in detail, using for comparison a sinusoidal acceleration-time history that can be integrated exactly.

The ATM method was developed to be a more cost effective and faster method than the traditional test. The ATM may still prove to be a more cost effective method, but the

issue of a faster and better method is now in question. Once the test specimens were remolded, it was possible to perform eight repeated load triaxial tests in one eight hour day, along with the calculations. This number of tests is very reasonable for use of the test on a production basis in view of the fact that other standardized soil tests, such as the moisture-density test and especially the commonly used CBR test, have the same time constraints.

Since the 2002 AASHTO Pavement Design Guide is moving toward a purely mechanistic design procedure, it will be necessary to develop models for the relationship of resilient modulus that take into account the effect of deviator stress and confining pressure. At this time, there is no such equation developed for the ATM. The ATM is only good for determining a modulus value at a single value of deviator stress that is dependent on an assumed value of Poisson's ratio or K_o. Even though it is easy to find resilient modulus values for different stress states by using different combinations of drop heights and weights, the model developed for the standard test is still preferable and more compatible with pavement design methods. With the speed and accuracy of today's data collection and testing equipment, the standardized test method should be used in place of any current alternative method unless accurate mechanistic models can be produced.

5.2 Recommendations

Additional research should be done to investigate the time-integration scheme and the effect of loading rate on the ATM specimens. This should yield a correction factor, R_f, in Equation 4-4 that should bring the values from the ATM and triaxial test in better agreement. For now, it is recommended that resilient modulus calculations be made

using the large weight at a drop height of 10 mm or 20mm, because these combinations perform best in the laboratory testing. The effect of ATM specimens with a smaller length and testing outside of the proctor mold should also be investigated. A quality control program using polyurethane specimens should also be implemented.

Soil samples at different moisture contents and densities along with varying degrees of saturation should be tested and compared with repeated load triaxial results. At the same time, the proposed model for the 2002 AASHTO Pavement Design Guide could be analyzed for goodness of fit for the varying soil conditions, since it is not likely that soil subgrades would remain at ideal conditions, but will become saturated during wet seasons and dry out during summer months. Testing samples of the same size with the MTS and ATM equipment, may lead to better correlations between the two machines. There would also be reference values to score proficiency tests of new users. The influence of modifications to the equipment or changes in procedure could easily be quantified if samples with consistent and unchanging material properties are available.

References

AASHO. (1962). "Special report 6E – the AASHO road test, report 5: pavement research." Highway Research Board, National Research Council, Washington, D.C.

American Association of State Highway and Transportation Officials. (1986). "AASHTO guide for the design of pavement structures." AASHTO, Washington, D.C.

American Association of State Highway and Transportation Officials. (1993). "AASHTO guide for the design of pavement structures." AASHTO, Washington, D.C.

Andrei, D. (1999). "Development of a harmonized test protocol for the resilient modulus of unbound materials used in pavement design," Thesis presented in partial fulfillment of the requirements for the Master of Science Degree, University of Maryland, College Park, MD.

Asphalt Institute. (1981). "Thickness design manual." Asphalt Pavements for Highways and Streets, Manual Series No. 1 (MS-1).

Asphalt Institute. (1982). "Research and development of the asphalt institute's thickness design manual, ninth edition." Research Report No. 82-2.

Bonaquist, R., and Witczak, M.W. (1992). "Assessing the nonlinear behavior of subgrade and granular bases from surface deflection basins." *Proceedings, 7th International Conference on Asphalt Pavements, Nottingham, England.*

Boyce, H.R. (1980). "A non-linear model for the elastic behaviour of granular materials under repeated loading." *International Symposium on Soils Under Cyclic and Transient Loading*, Swansea, January 7-11, 285-294.

Boyce, J.R., Cobbe, M.I., and Fleming, P.R. (1989) "Development of a prototype variable impact testing apparatus." *Proceedings, 3rd International Symposium on Unbound Aggregates in Roads*, University of Nottingham, 397-407.

Boyce, J.R., Fleming, P.R., King, G., Rodgers, C.D.F., and Cobbe, M.I. (1990). "A new variable impact test for pavement and foundations." *Proceedings, 3rd International Conference on Bearing Capacity of Roads and Airfields*, Trondheim, Norway, July 3-9, 1990, 185-194.

Carmichael III, R.F., and Stuart, E. (1985). "Predicting resilient modulus: a study to determine the mechanical properties of subgrade soils." *Transportation Research Record 1043*, Transportation Research Board, Washington, D.C., 145-148.

Claros, G., Hudson, W.R., and Stokoe II, K.H. (1990). "Modifications to resilient modulus testing procedure and use of synthetic samples for equipment

calibration." *Transportation Research Record 1278*, Transportation Research Board, Washington, D.C., 51-62.

Choi, T.H. (2001). Personal conversation.

Desai, C.S. (1984). "*Constitutive laws for engineering materials, with emphasis on geologic materials.*" Prentice-Hall, Inc., Englewood Cliffs, New Jersey.

Drumm, E.C., Boateng-Poku, Y., and Pierce, T.J. (1990). "Estimation of subgrade resilient modulus from standard tests." *Journal of Geotechnical Engineering*, ASCE, Vol 116, No. 5, 774-789.

Drumm, E.C., Hudson, J., Li, Z., Madgett, M., and Baker, D. (1993). "*Resilient response of Tennessee subgrades volume 2:handbook of resilient modulus and index properties.*" Department of Civil and Environmental Engineering, The University of Tennessee, Knoxville, TN.

Drumm, E.C., Li., Z., Reeves, J.S., and Madgett, M.R. (1996). "Alternative test method for resilient modulus of fine-grained subgrades." *Geotechnical Testing Journal*, ASTM, Vol 19, No. 2, 141-154.

Drumm, E.C., Reeves, J.S., Madgett, M.R., and Trolinger, W.D. (1997). "Subgrade resilient modulus correction for saturation effects." *Journal of Geotechnical and Geoenvironmental Engineering*, ASCE, Vol 123, No. 7, 663-670.

Elliot, R.P., and Thornton, S.I. (1988a) "Resilient modulus and AASHTO pavement design." *Transportation Research Record 1196*, Transportation Research Board, Washington, D.C., 116-124.

Elliot, R.P., and Thornton, S.I. (1988b) "Simplification of subgrade resilient modulus." *Transportation Research Record 1192*, Transportation Research Board, Washington, D.C., 1-7.

Farr, J.V. (1990). "One-dimensional loading-rate effects." *Journal of Geotechnical Engineering*, ASCE, Vol 116, No. 1, 119-135.

Federal Highway Administration (FHWA). (1994). "AASHTO design procedures for new pavements: participant's manual." *U.S. Department of Transportation, Federal Highway Administration, National Highway Institute: Publication No. FHWA-HI-94-023*, Washington, D.C.

Federal Highway Administration (FHWA). (2000). "LTPP and the new 2002 pavement design guide." *U.S. Department of Transportation, Federal Highway Administration: Publication No. FHWA-RD-00-129*, Washington, D.C.

Fredlund, D.G., Bergan, A.T., and Wong, P.K. (1977). "Relation between resilient modulus and stress conditions for cohesive subgrade soils." *Transportation Research Record 642*, Transportation Research Board, Washington, D.C., 73-81.

Harichandran, R.S., Buch, N., and Baladi, G.Y. (2001) "Flexible pavement design in Michigan: transition from empirical to mechanistic methods." *Proceedings, 80th Annual Meeting of the Transportation Research Board*, Washington, D.C., January 7-11, Paper No. 01-2817.

Heukelom, W., and Foster, C.R., (1960). "Dynamic testing of pavements." *Proceeding of the American Society of Civil Engineers*, Journal of the Soil Mechanics and Foundations Division, 86(SM1), 1-28.

Heukelom, W., and Klomp, J.G., (1962). "Dynamic testing as a means of controlling pavements during and after construction." *Proceedings, International Conference on the Structural Design of Asphalt Pavements*, University of Michigan, Ann Arbor, Michigan, August 20-24, 667-679.

Hjelmstad, K.D., and Taciroglu, E. (2000) "Analysis and implementation of resilient modulus models for granular solids." *Journal of Engineering Mechanics*, ASCE, Vol 126, No. 8, 821-830.

Hveem, F.N. (1955) "Pavement deflections and fatigue failures." *Proceedings, Highway Research Board, Bulletin 114*, Washington, D.C., January 11-14, 43-73.

Huang, Y.H. (1993). "*Pavement analysis and design.*" Prentice Hall, Inc., Englewood Cliffs, New Jersey.

Hudson, J.M. (1992). "The resilient response of fine-grained Tennessee subgrade soils." Thesis presented in partial fulfillment of the requirements for the Master of Science Degree, Department of Civil Engineering, University of Tennessee, Knoxville, TN.

Jackson, J.G., Ehrgott, J.Q., and Rohani, B., (1980). "Loading rate effects of compressibility of sand." *Journal of the Geotechnical Engineering Division*, ASCE, Vol 106, No. GT8, 839-852.

Jones, M.P., and Witczak, M.W. (1977). "Subgrade modulus of the San Diego test road." *Transportation Research Record 641*, Transportation Research Board, Washington, D.C., 1-6.

Juvinall, R.C. (1967). "*Engineering considerations of stress, strain, and strength.*" McGraw-Hill Book Company, Inc., New York.

Johnson, R.A., and Bhattacharyya, G.K. (1996). "*Statistics: principles and methods, 3rd edition.*" John Wiley and Sons, Inc., New York.

Kim, D.S., and Kweon, G.C. (2000) "Deformational characteristics of subgrade soils in Korea." *Proceedings, 79th Annual Meeting of the Transportation Research Board*, Washington, D.C., January, 9-13, Paper No. 00-1431.

Lamb, T.W., and Whitman, R.V. (1969). "*Soil Mechanics.*" John Wiley and Sons, New York.

Lee, W., Bohra, N.C., Altschaeffl, A.G., and White, T.D. (1995) "Resilient modulus of cohesive soils and the effect of freeze-thaw." *Canadian Geotechnical Journal*, Vol 32, No. 4, 559-568.

Lee, W., Bohra, N.C., Altschaeffl, A.G., and White, T.D. (1997) "Resilient modulus of cohesive soils." *Journal of Geotechnical and Geoenvironmental Engineering*, Vol 123, No. 2, 131-135.

Li, Z. (1992). "An alternative test method for resilient modulus of fine grained subgrades," Thesis presented in partial fulfillment of the requirements for the Master of Science Degree, Department of Civil Engineering, University of Tennessee, Knoxville, TN.

Li, D., and Selig, E.T. (1994) "Resilient modulus for fine-grained subgrade soils." *Journal of Geotechnical Engineering*, ASCE, Vol 120, No. 6, 939-957.

Liu, C., and Evett, J.B., (2000). "*Soil properties: testing measurement, and evaluation, 4th edition.*" Prentice Hall, Inc., Upper Saddle River, New Jersey.

Madgett, M.R. (1994). "Verification testing and alternative test methods for the resilient modulus of fine grained soils," Thesis presented in partial fulfillment of the requirements for the Master of Science Degree, Department of Civil Engineering, University of Tennessee, Knoxville, TN.

Monosmith, C.L., Seed, H.B., Mitry, F.G., and Chan, C.K. (1967). "Prediction of pavement deflections from laboratory tests." *Proceeding, 2nd International Conference on the Structural Design of Asphalt Pavements*, University of Michigan, Ann Arbor, Michigan, August 7-11, 109-140.

Monosmith, C.L. (1992). "Analytically based asphalt pavement design and rehabilitation: theory to practice, 1962-1992." *Transportation Research Record 1354*, Transportation Research Board, Washington, D.C., 5-26.

Moossazadeh, J., and Witczak, M.W. (1981). "Prediction of subgrade moduli for soil that exhibits nonlinear behavior." *Transportation Research Record 810*, Transportation Research Board, Washington, D.C., 9-17.

MTS. (1998). "TestStar II: testware-sx application manual." MTS Systems Corporation.

Nadai, A. (1950). "*Theory of flow and fracture of solids, 2nd edition.*" McGraw Hill Book Company, Inc., New York.

Nazarian, S., Pezo, R., Melarkode, S., and Picornell, M. (1996). "Testing methodology for resilient modulus of base materials." *Transportation Research Record 1547*, Transportation Research Board, Washington D.C., 46-52.

Pezo, R.F., Kim, D.S., Stokoe II, K.H., and Hudson, W.R. (1991). "A reliable resilient modulus testing system." *Transportation Research Record 1307*, Transportation Research Board, Washington, D.C., 90-98.

Pezo, R.F. (1993) "A general method of reporting resilient modulus tests of soils – a pavement engineer's point of view." *Proceeeding, 72nd Annual Meeting of the Transportation Research Board, Washington, D.C.*

Ping, W.V., Yang, Z., and Liu, J. (2000). "Effect of specimen size on resilient modulus of Florida base materials." *Proceedings, 79th Annual Meeting of the Transportation Research Board*, Washington, D.C., January, 9-13, Paper No. 00-0679.

Puppala, A.J., and Mohammad, L.N. (1997). "A regression model for better characterization of resilient properties of subgrade soils." *Proceedings, Eighth International Conference on Asphalt Pavements*, Seattle, Washington, August 10-14, 859-866.

Rainwater, N. R., Yoder, R.E., Drumm, E.C., and Wilson, G.V. (1999) "Comprehensive Monitoring Systems for Measuring Subgrade Moisture Conditions," *Journal of Transportation Engineering*, ASCE, Vol. 125, No. 5, pp 439-448.

Reeves, J.S. (1995). "Saturation effects on the resilient response of fine-grained soil," Thesis presented in partial fulfillment of the requirements for the Master of Science Degree, Department of Civil Engineering, University of Tennessee, Knoxville, TN.

Schindler, L., (1967). "An improved facility for testing soils in one-dimensional compression." *Proceedings, International Symposium on Wave Propagation and Dynamic Properties of Earth Materials*, Albuquerque, New Mexico, 847-859.

Schwartz, C.W. (2001). "Implementation of a nonlinear resilient modulus constitutive model for unbound pavement material." *Proceedings of the tenth international conference on computer methods and advances in geomechanis*, Tucson, Arizona, January 7-12, 1385-1390.

Shackel, B. (1973). "The derivation of complex stress-strain relations." *Proceedings, 8th International Conference on Soil Mechanics and Foundations Engineering*, Moscow, 353-359.

Seed, H.B., Chan, C.K., and Lee, C.E. (1962) "Resilience characteristics of subgrade soils and their relation to fatigue failures in asphalt pavements." *Proceedings, International Conference on the Structural Design of Asphalt Pavements*, University of Michigan, Ann Arbor, Michigan, August 20-24, 611-636.

Stewart, J. (1991). "*Calculus, 2nd edition.*" Brooks/Cole Publishing Company, Pacific Grove, California.

Stokoe II, K.H., Kim, D.S., and Andrus, R.D. (1990) "Development of synthetic specimens for calibration and evaluation of M_R equipment." *Transportation Research Record 1278*, Transportation Research Board, Washington, D.C., 63-71.

Sweere, G.T.H., and Galjaard, P.J. (1988). "Repeated static loading triaxial tests for determination of resilient properties of sands." *Transportation Research Record 1278*, Transportation Research Board, Washington, D.C., 51-62.

Thompson, M.R., and Robnett, Q.L. (1976). "Final report, resilient properties of subgrade soils." *Civil Engineering Studies, Transportation Engineering Series No. 14*, Illinois Cooperative Highway and Transportation Series No. 160.

Thompson, M.R., and Robnett, Q.L. (1979). "Resilient properties of subgrade soils." *Transportation Engineering Journal*, ASCE, Vol 105, No. TE1, 71-89.

Thornton, S.I., and Elliot, R.P. (1986) "Resilient modulus – what is it?" *Proceedings of the 37th Annual Highway Geology Symposium*, Helena, Montana, August 20-22, 267-282.

Uzan, J. (1992) "Resilient characterization of pavement materials." *International Journal for Numerical and Analytical Methods in Geomechanics*, Vol 16, 453-459

Uzan, J. (1998). "Characterization of clayey subgrade materials for mechanistic design of flexible pavements." *Transportation Research Record 1629*, Transportation Research Board, Washington, D.C., 189-196.

Witczak, M.W., and Uzan, J. (1988) "The universal airport pavement design system, report I of IV: granular material characterization." Department of Civil Engineering, University of Maryland, College Park, MD.

Witczak, M.W., Qi, X., and Muhammad, Mirza, M.W. (1995) "Use of nonlinear subgrade modulus in AASHTO design procedure." *Journal of Transportation Engineering*, ASCE, Vol 121, No. 3, 273-282.

Wright, W.C. (1998). "In situ water content measurement of compacted highway subgrades using time domain reflectometry," Thesis presented in partial fulfillment of the requirements for the Master of Science Degree, Department of Civil Engineering, University of Tennessee, Knoxville, TN.

Zuo, G. (2000). Personal conversation.

Appendices

Appendix A Soil Information

Blount County

Soil Classification	
AASHTO	USCS
A-7-6 (18)	CL

$\gamma_{d\ opt}$ (pcf)	w_{opt} (%)	LL	PL	PI	Percent Passing #200 Sieve	CBR
102.0	21.0	43	22	21	64.2	4.8

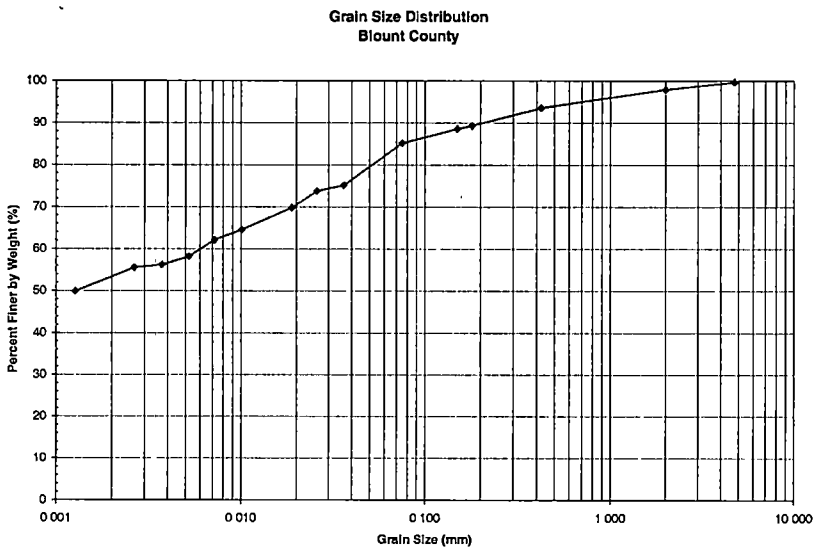

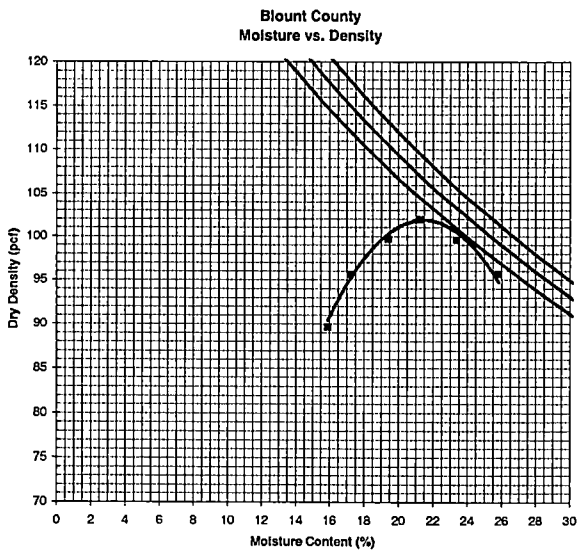

McNairy County

Soil Classification	
AASHTO	USCS
A-6 (5)	CL

$\gamma_{d\ opt}$ (pcf)	w_{opt} (%)	LL	PL	PI	Percent Passing #200 Sieve	CBR
115.0	13.5	30	16	14	57.7	4.4

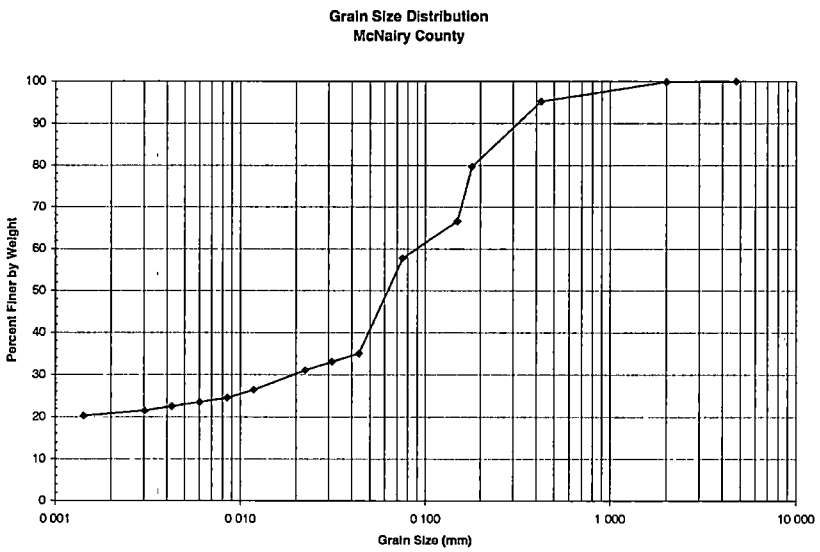

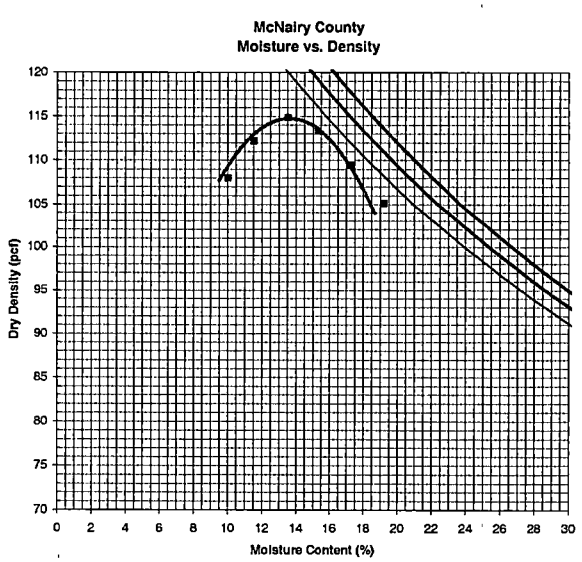

Overton County

Soil Classification	
AASHTO	USCS
A-6 (8)	CL

$\gamma_{d\ opt}$ (pcf)	w_{opt} (%)	LL	PL	PI	Percent Passing #200 Sieve	CBR
109.0	16.0	29	17	12	78.6	5.4

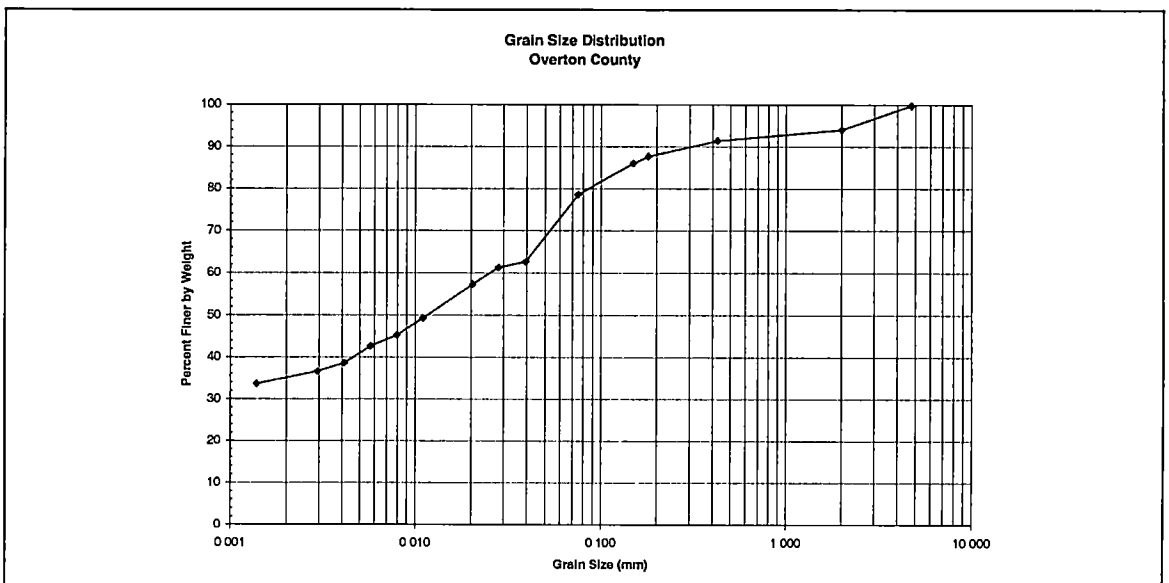

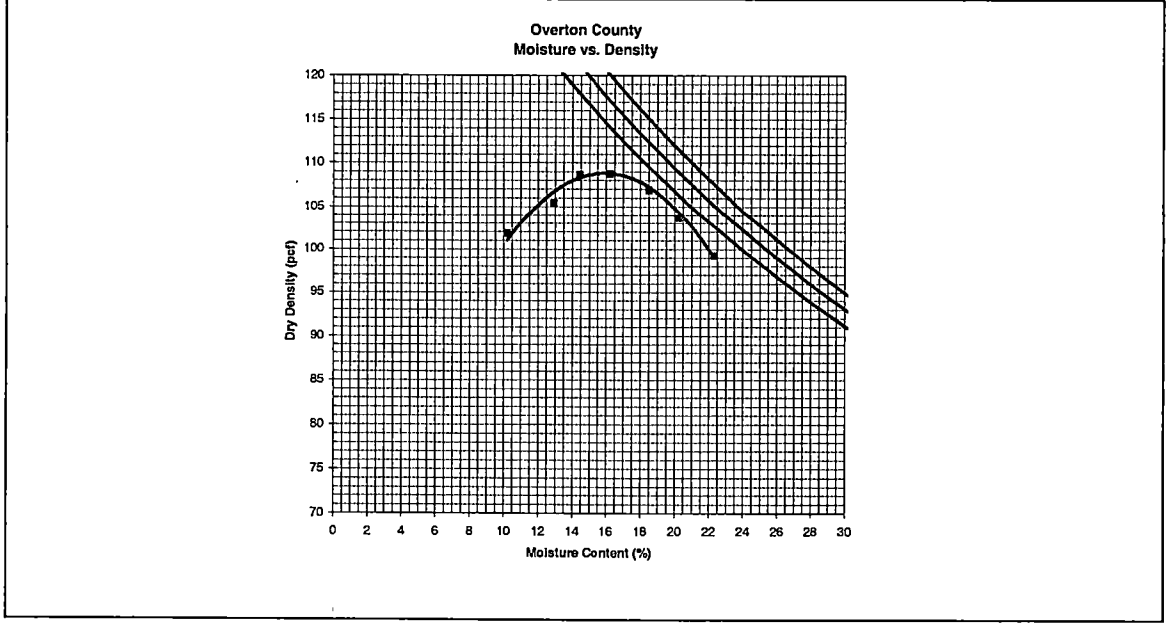

Sumner County

Soil Classification	
AASHTO	USCS
A-6 (8)	CL

$\gamma_{d\ opt}$ (pcf)	w_{opt} (%)	LL	PL	PI	Percent Passing #200 Sieve	CBR
103.5	17.5	32	21	11	80.8	2.6

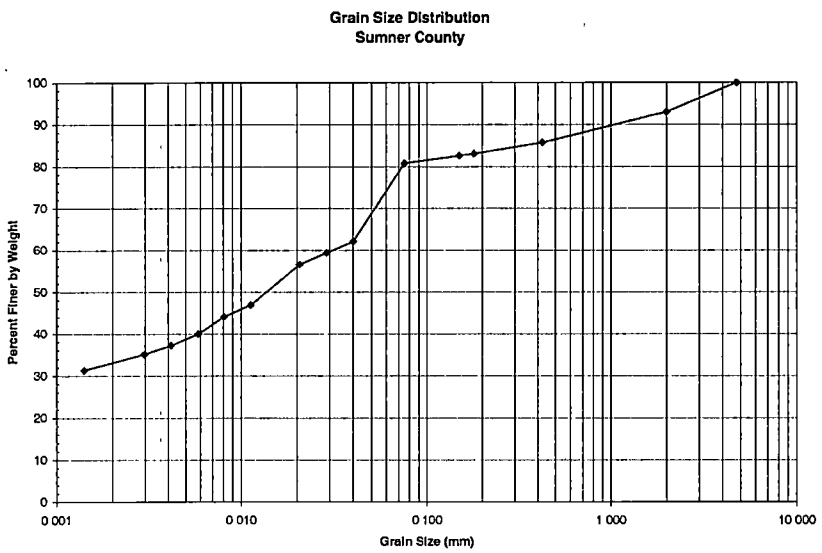

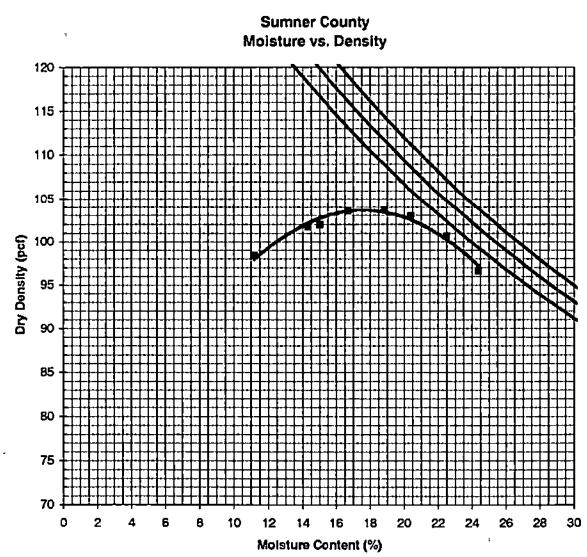

Appendix B Repeated Load Triaxial Test Data

Blount County

List B - 1 Blount County Resilient Modulus Sample Properties

Specimen Number	Dry Density (pcf)	Water Content (%)	Log - log model			
			K1	K2	K3	R^2
BMr1opt	102.3	20.4	1862	0.71797	-2.70751	0.95
BMr2opt	102.2	20.6	2291	0.40823	-2.51488	0.96
BMr3opt	101.9	20.9	2005	0.37991	-1.85126	0.94
BMr3bopt	101.9	20.9	1949	0.32684	-1.73740	0.98
BMr4opt	102.3	20.5	1940	0.41348	-2.07196	0.97
BMr8opt	102.5	20.2	2049	0.48415	-2.38440	0.98
BMr9opt	102.6	20.2	1880	0.45147	-2.12435	0.96
BMr10opt	102.4	20.3	2139	0.78052	-2.92241	0.93
BMr11opt	102.6	20.1	2150	0.51083	-2.21771	0.98
BMr12opt	102.4	20.4	2194	0.31171	-1.91305	0.96
BMr13opt	102.1	20.7	2265	0.50897	-2.25323	0.97
BMr14opt	101.9	21.0	2139	0.42062	-2.12797	0.96
Ave.	102.3	20.5	2072	0.47623	-2.23551	0.96
Standard Deviation	0.3	0.3	146	0.14279	0.34979	

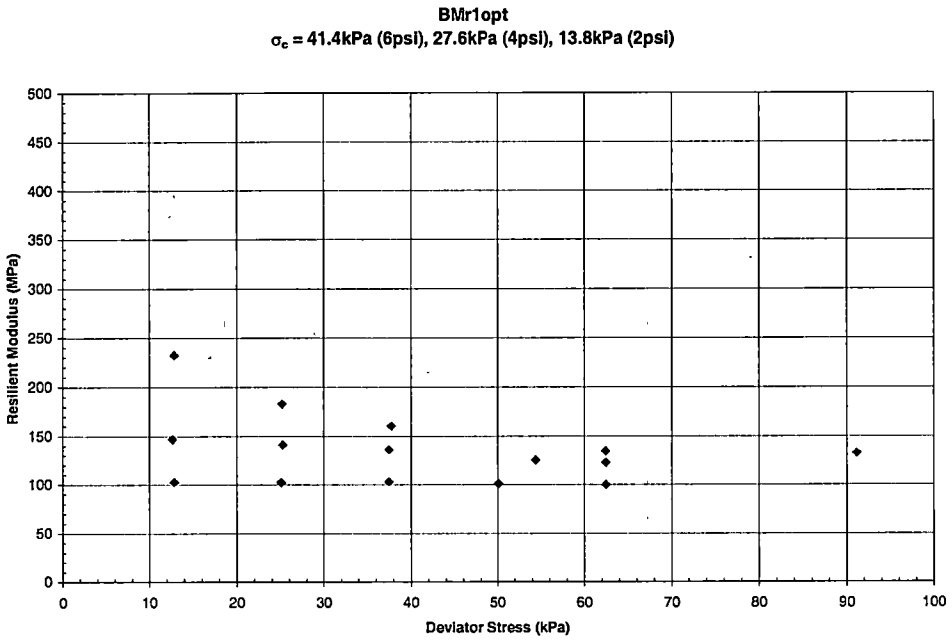

Graph B - 1 Resilient Modulus vs. Deviator Stress for Blount County - BMr1opt

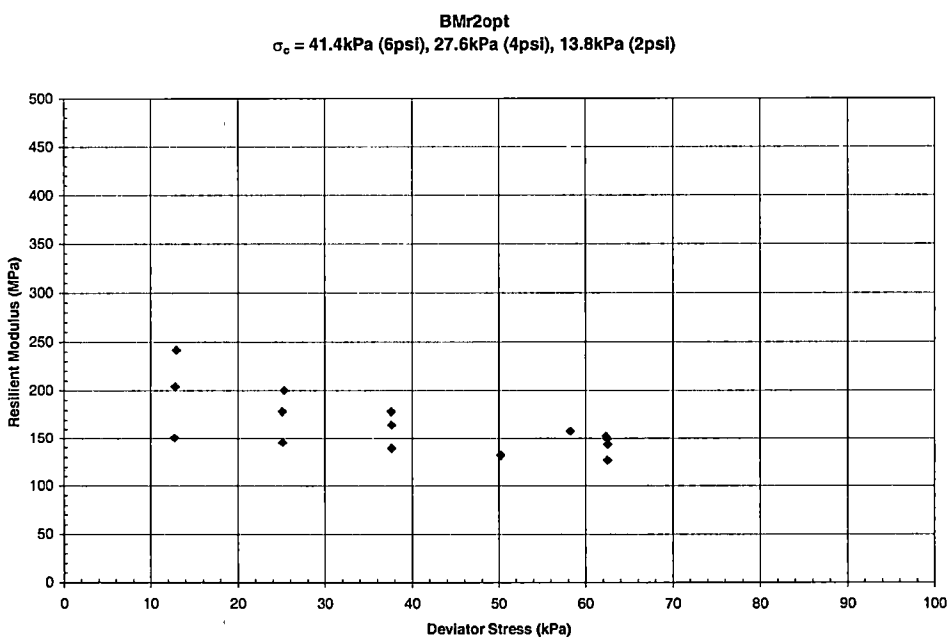

Graph B - 2 Resilient Modulus vs. Deviator Stress for Blount County – BMr2opt

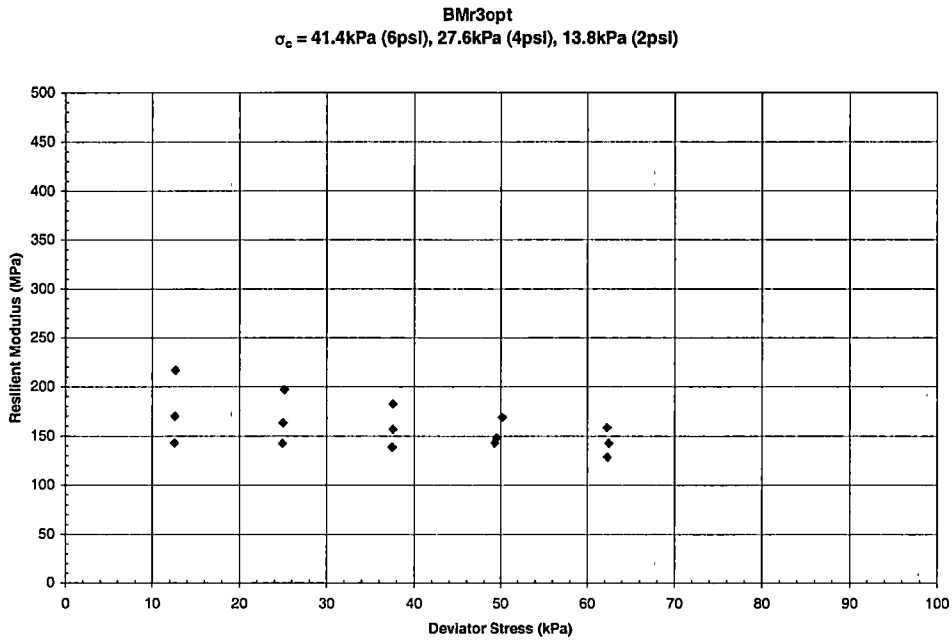

Graph B - 3 Resilient Modulus vs. Deviator Stress for Blount County – BMr3opt

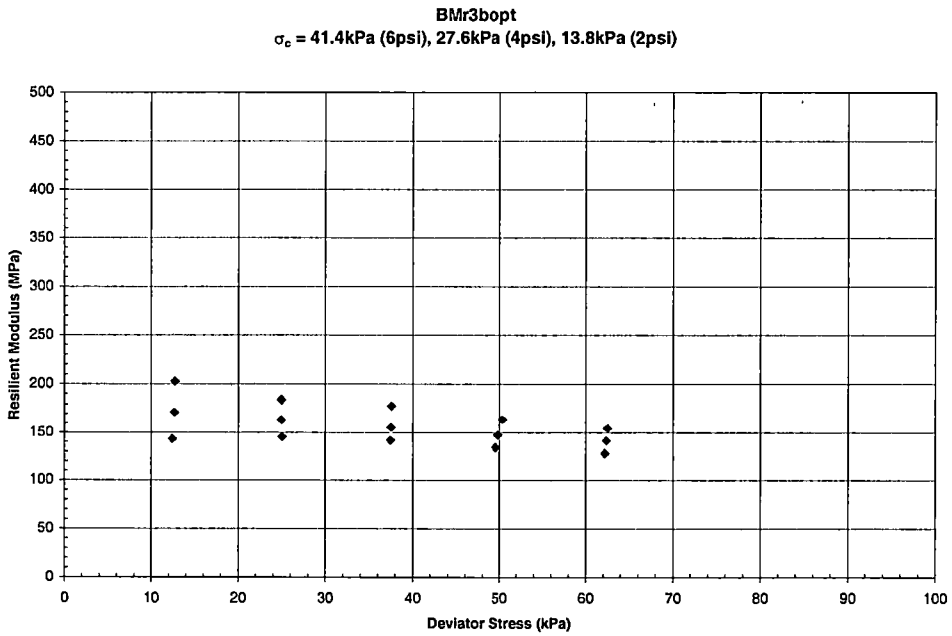

Graph B - 4 Resilient Modulus vs. Deviator Stress for Blount County – BMr3bopt

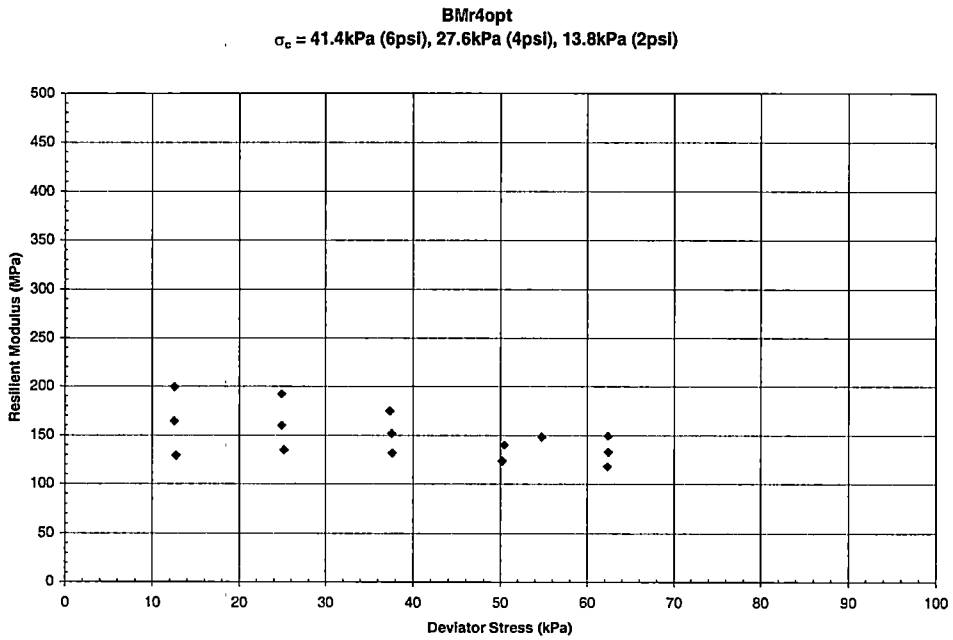

Graph B - 5 Resilient Modulus vs. Deviator Stress for Blount County – BMr4opt

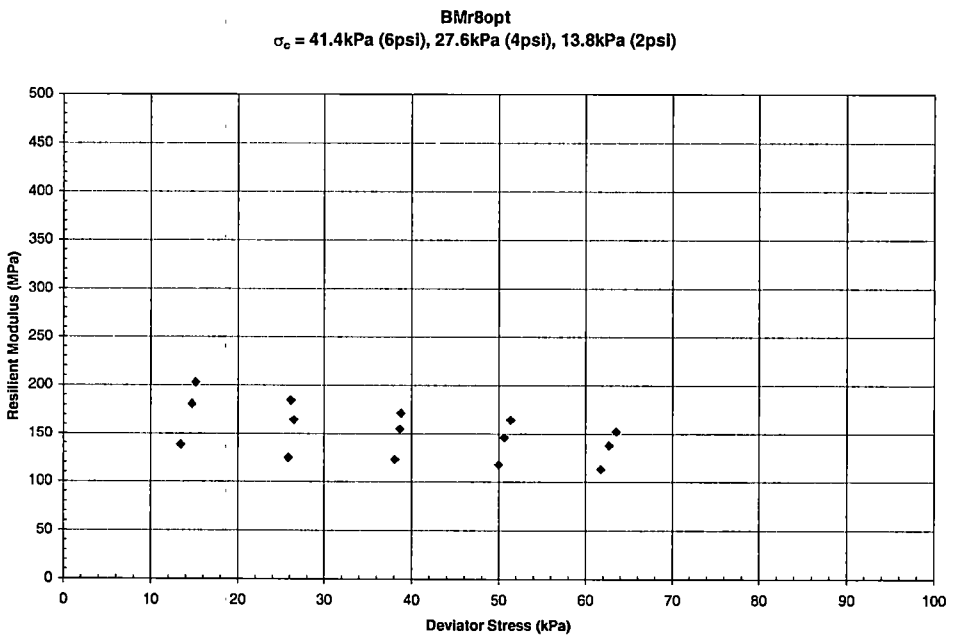

Graph B - 6 Resilient Modulus vs. Deviator Stress for Blount County – BMr8opt

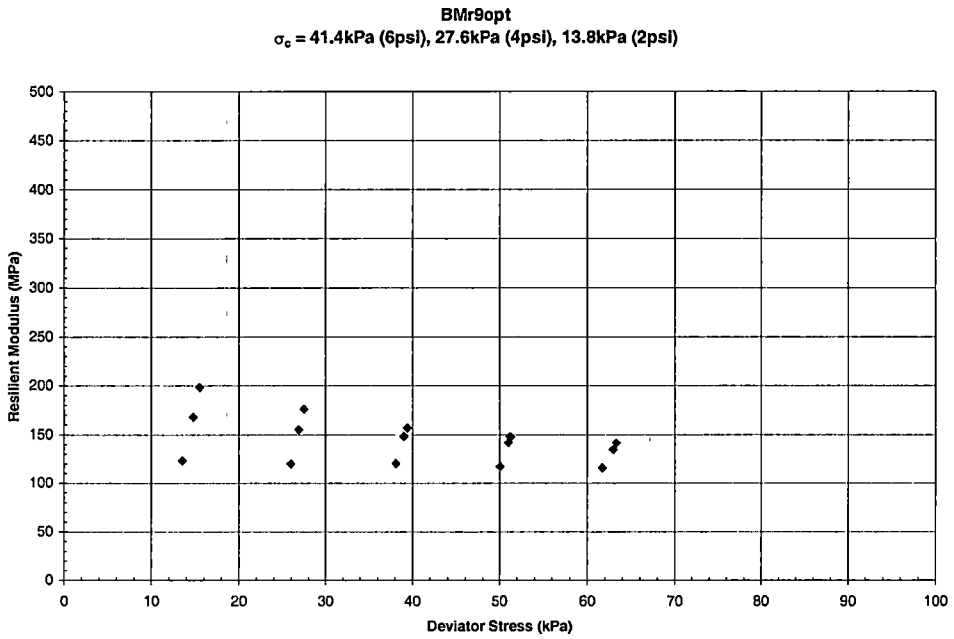

Graph B - 7 Resilient Modulus vs. Deviator Stress for Blount County – BMr9opt

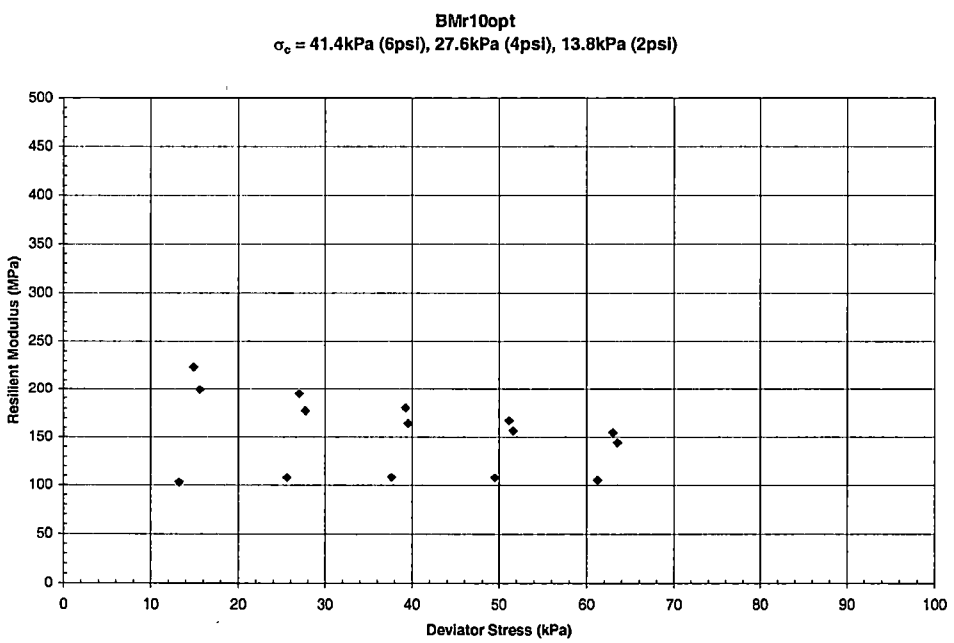

Graph B - 8 Resilient Modulus vs. Deviator Stress for Blount County - BMr10opt

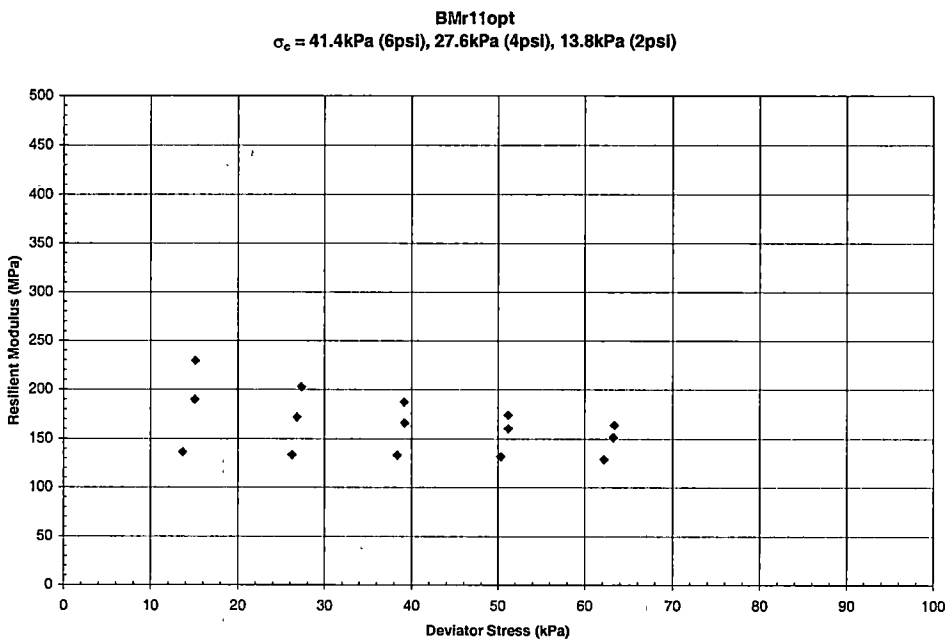

Graph B - 9 Resilient Modulus vs. Deviator Stress for Blount County - BMr11opt

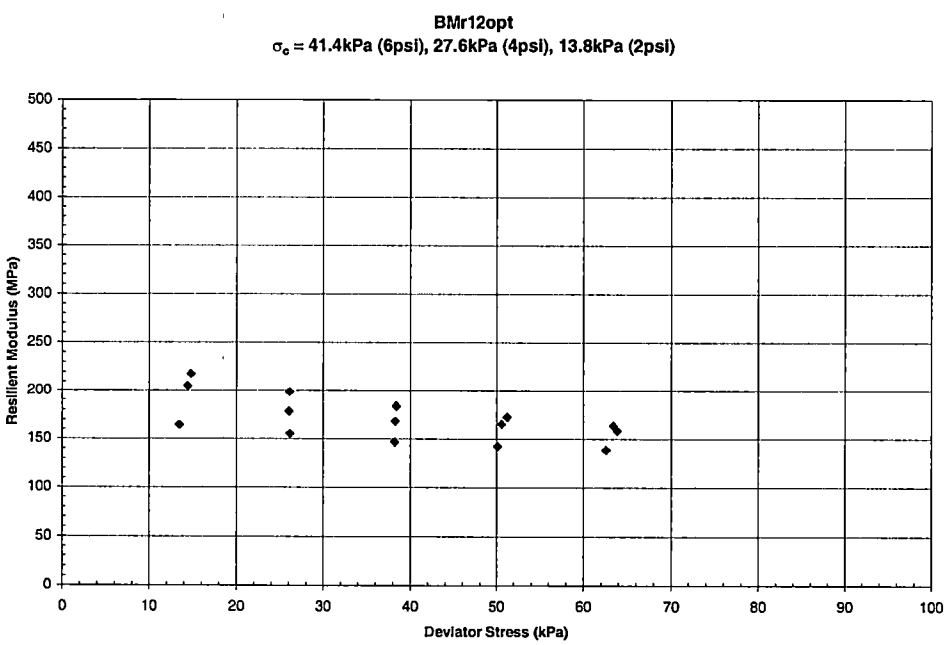

Graph B - 10 Resilient Modulus vs. Deviator Stress for Blount County - BMr12opt

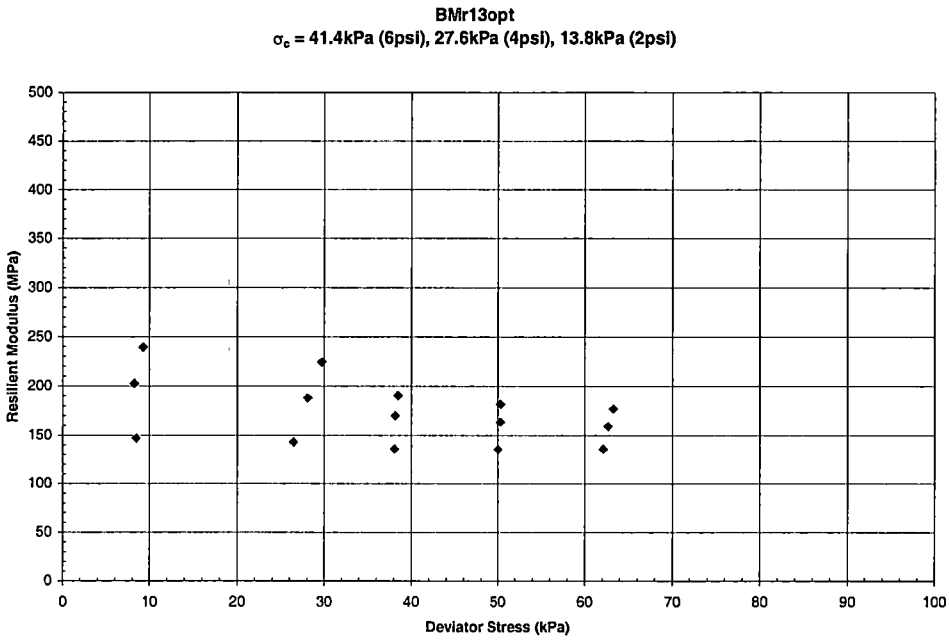

Graph B - 11 Resilient Modulus vs. Deviator Stress for Blount County - BMr13opt

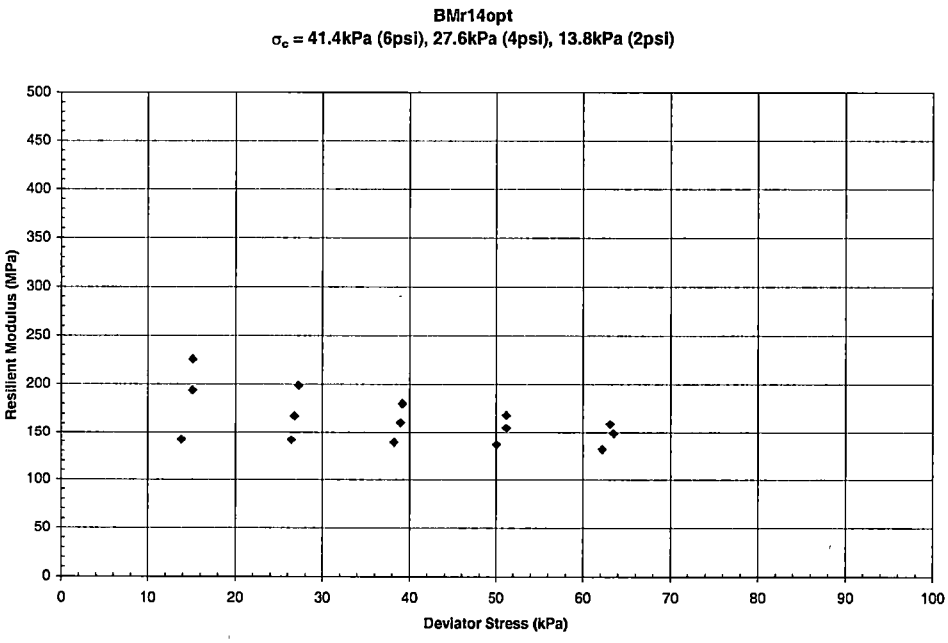

Graph B - 12 Resilient Modulus vs. Deviator Stress for Blount County - BMr14opt

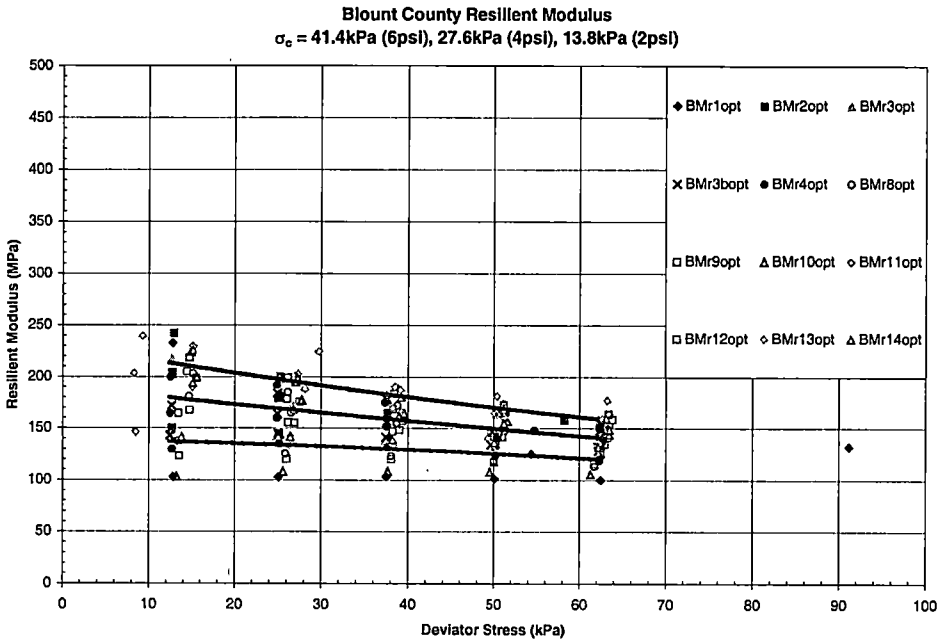

Graph B - 13 Resilient Modulus vs. Deviator Stress for Blount County with Models

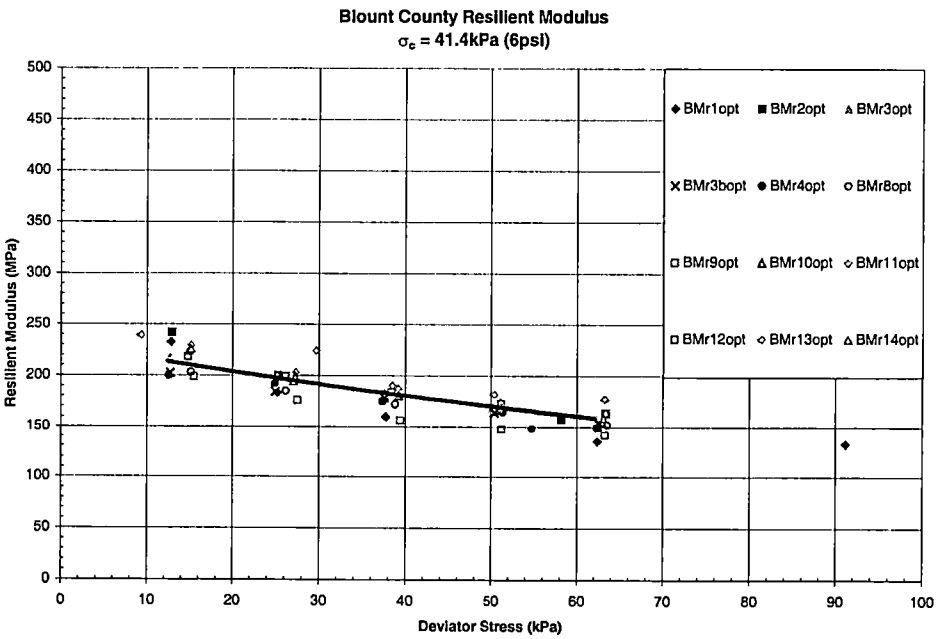

Graph B - 14 Resilient Modulus vs. Deviator Stress for Blount County with Model, Confining Pressure = 41.4kPa (6psi)

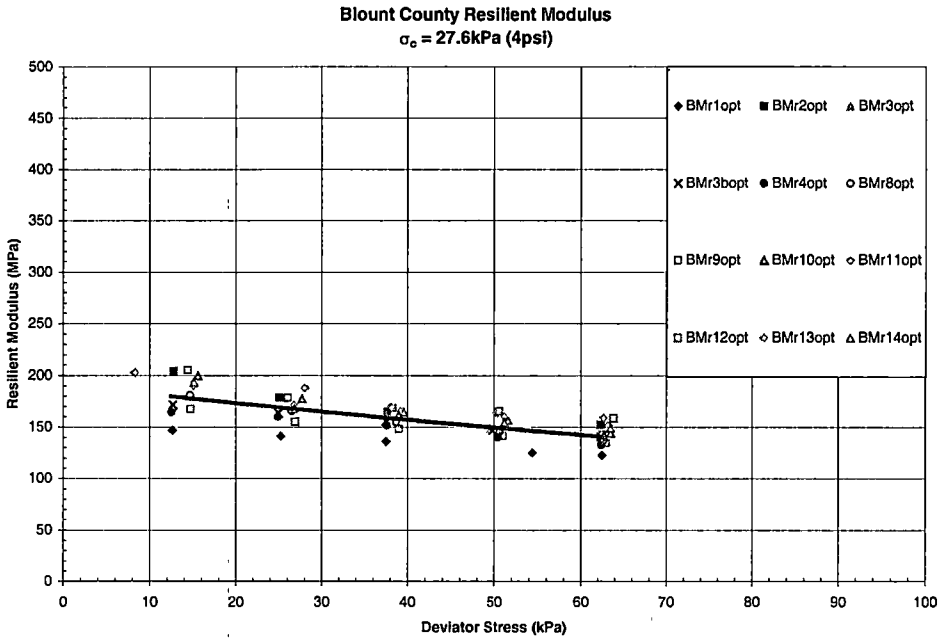

Graph B - 15 Resilient Modulus vs. Deviator Stress for Blount County with Model, Confining Pressure = 27.6kPa (4psi)

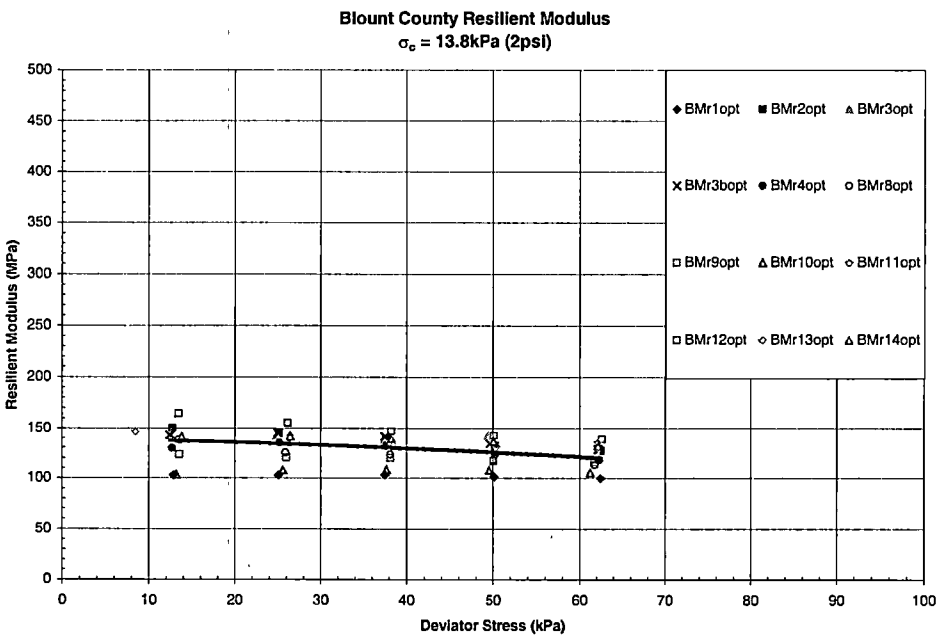

Graph B - 16 Resilient Modulus vs. Deviator Stress for Blount County with Model, Confining Pressure = 13.8kPa (2psi)

McNairy County

List B - 2 McNairy County Resilient Modulus Sample Properties

Specimen Number	Dry Density (pcf)	Water Content (%)	Log - log model			
			K1	K2	K3	R^2
MMr1opt	115.2	13.1	1909	0.58583	-3.16674	0.98
MMr2opt	115.3	13	2175	0.90236	-3.70995	0.96
MMr3opt	115.5	12.8	1966	0.57009	-2.82214	0.98
MMr4opt	115.5	12.9	1811	0.72329	-2.91429	0.97
MMr5opt	115.6	12.8	2131	0.55030	-2.68795	0.98
MMr6opt	115.2	13.1	2398	0.53362	-2.86620	0.98
MMr7opt	115.5	12.8	2126	0.76952	-3.21946	0.97
Ave.	115.4	12.9	2074	0.66214	-3.05525	0.97
Standard Deviation	0.2	0.1	195	0.13922	0.34469	

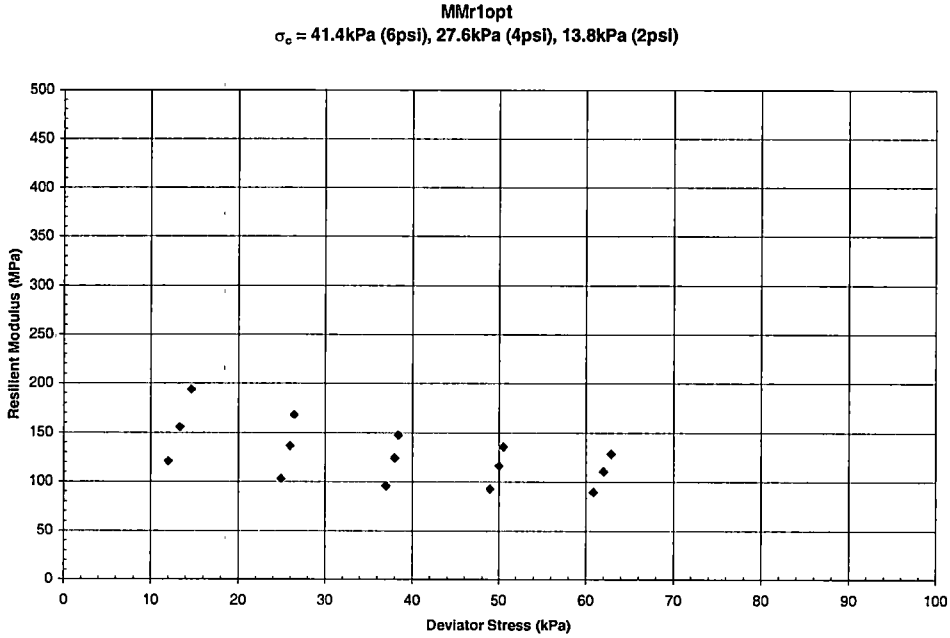

Graph B - 17 Resilient Modulus vs. Deviator Stress for McNairy County - MMr1opt

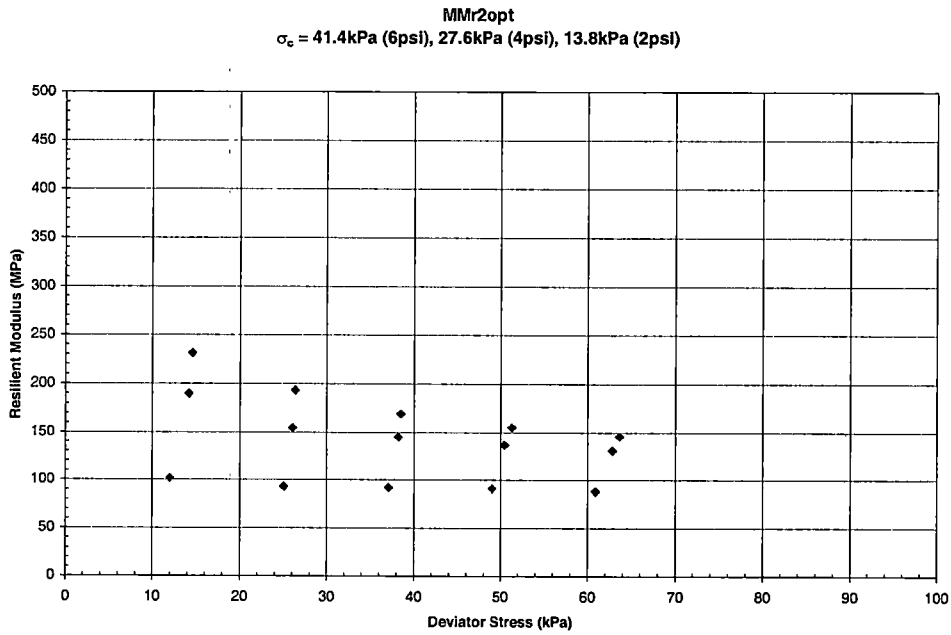

Graph B - 18 Resilient Modulus vs. Deviator Stress for McNairy County – MMr2opt

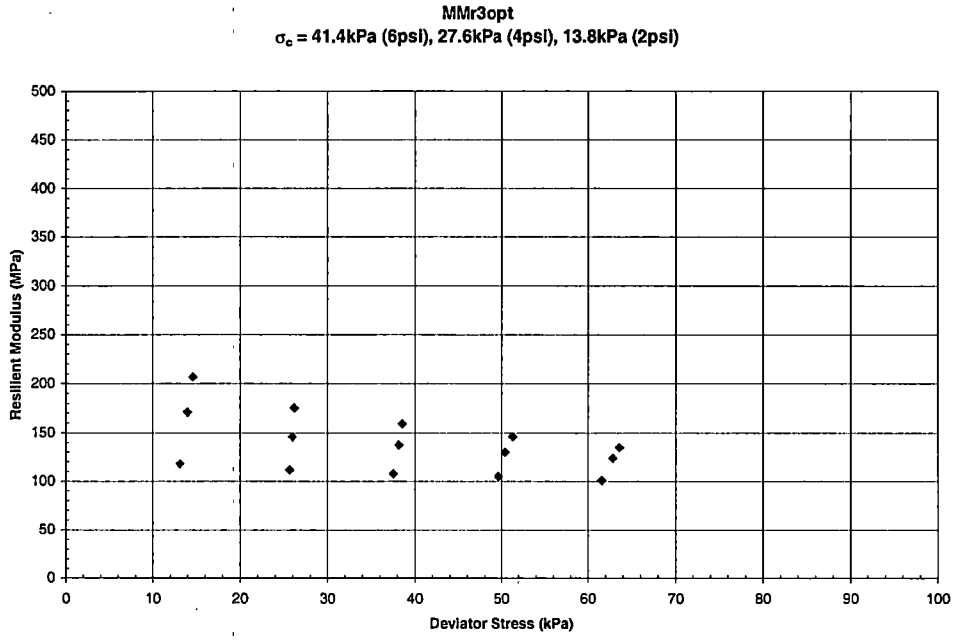

Graph B - 19 Resilient Modulus vs. Deviator Stress for McNairy County – MMr3opt

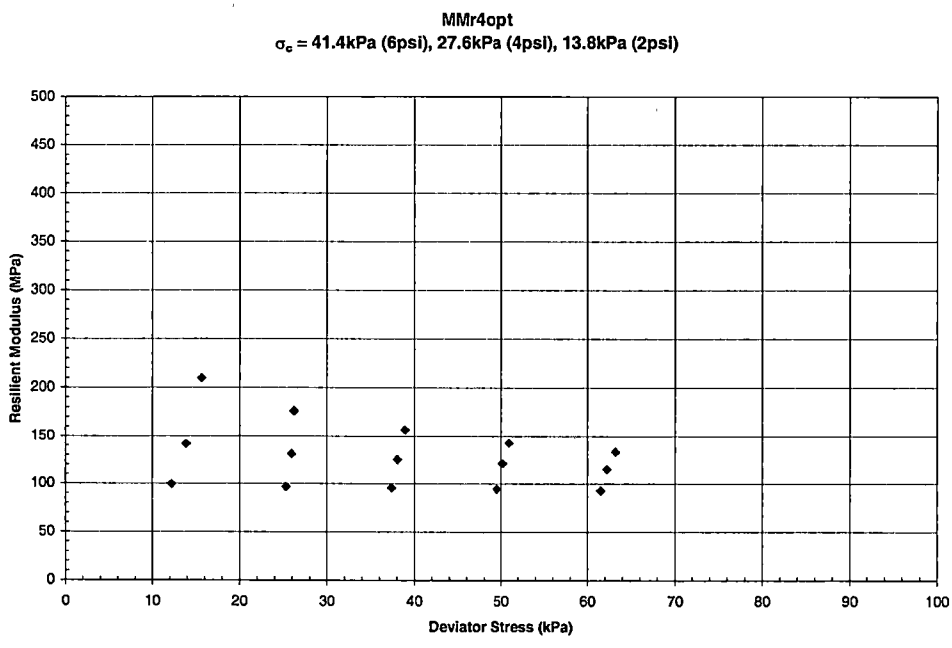

Graph B - 20 Resilient Modulus vs. Deviator Stress for McNairy County – MMr4opt

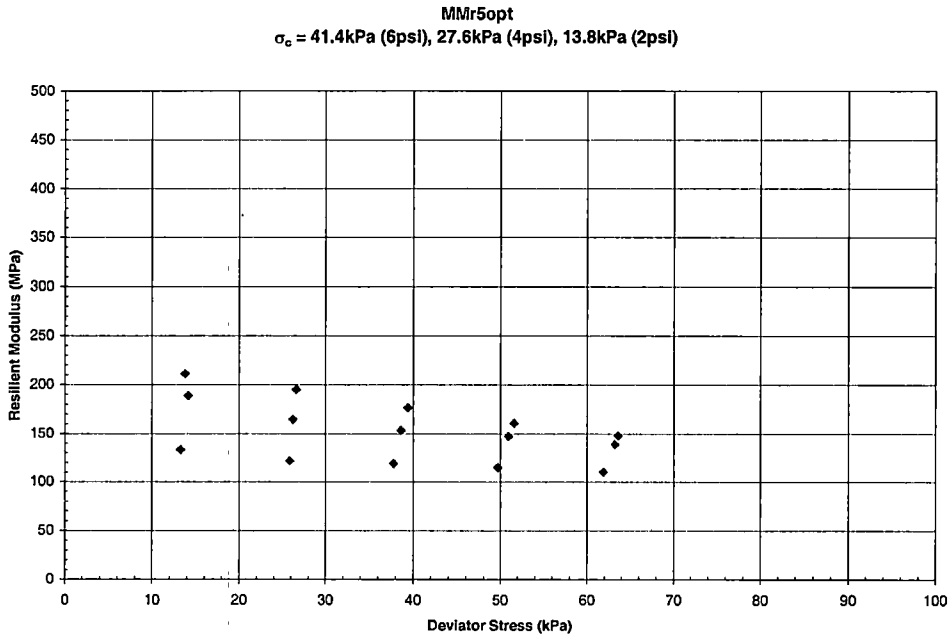

Graph B - 21 Resilient Modulus vs. Deviator Stress for McNairy County – MMr5opt

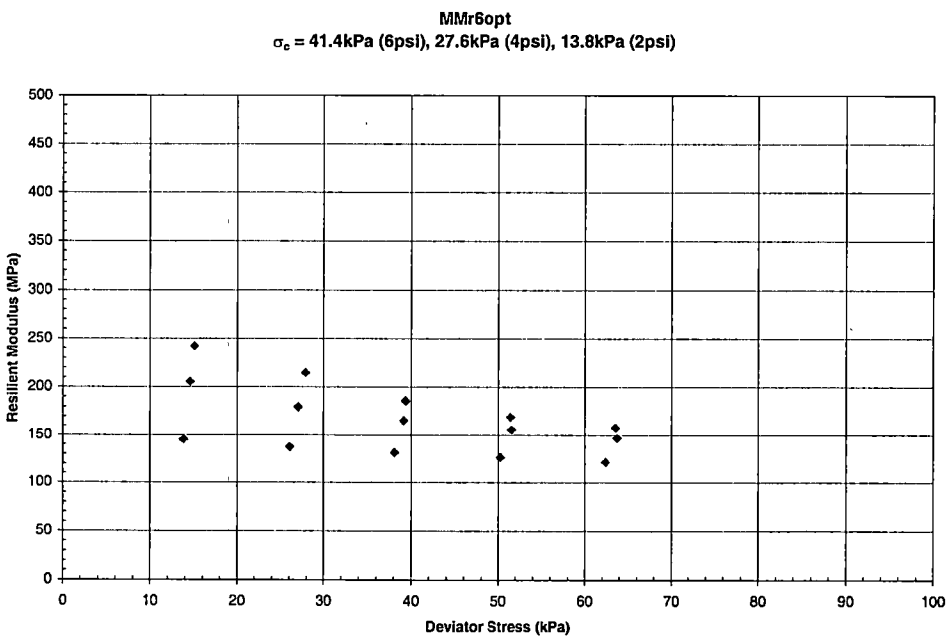

Graph B - 22 Resilient Modulus vs. Deviator Stress for McNairy County – MMr6opt

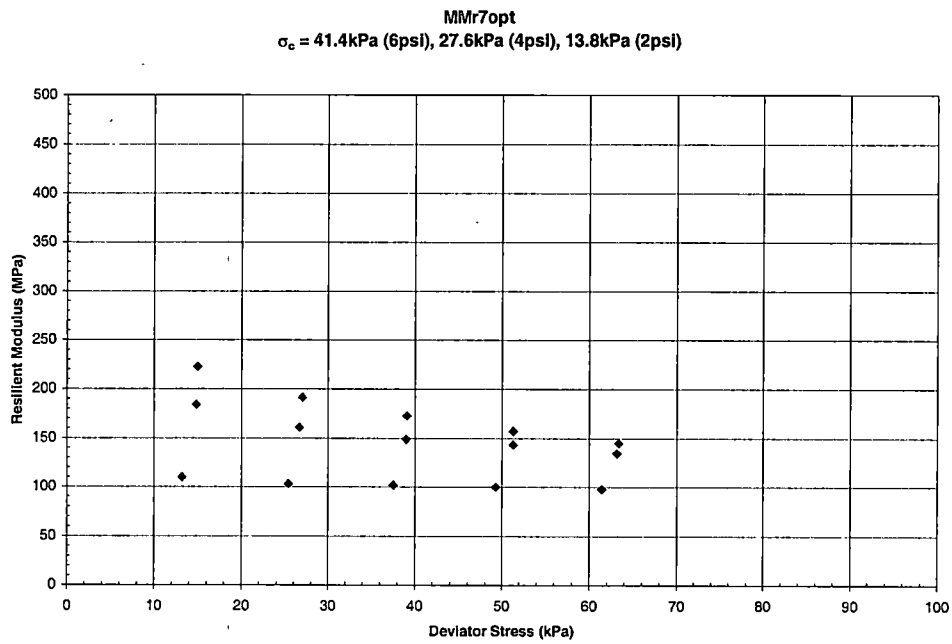

Graph B - 23 Resilient Modulus vs. Deviator Stress for McNairy County – MMr7opt

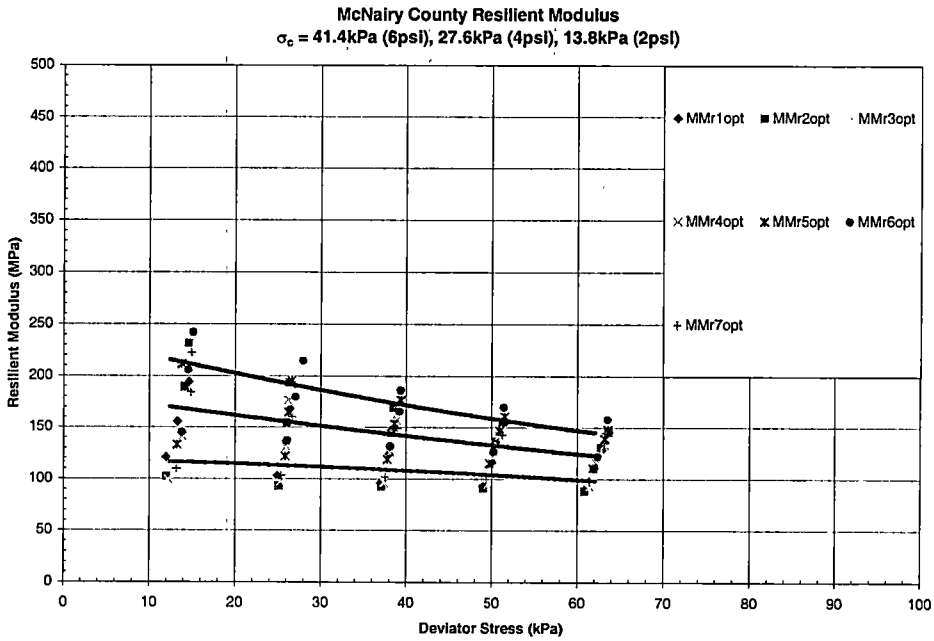

Graph B - 24 Resilient Modulus vs. Deviator Stress for McNairy County with Models

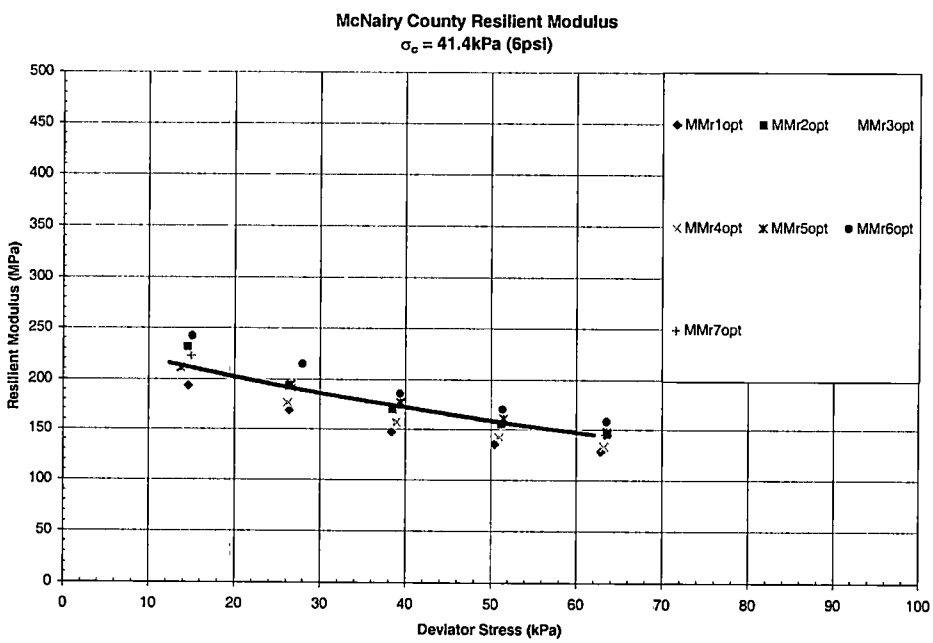

Graph B - 25 Resilient Modulus vs. Deviator Stress for McNairy County with Model, Confining Pressure = 41.4kPa (6psi)

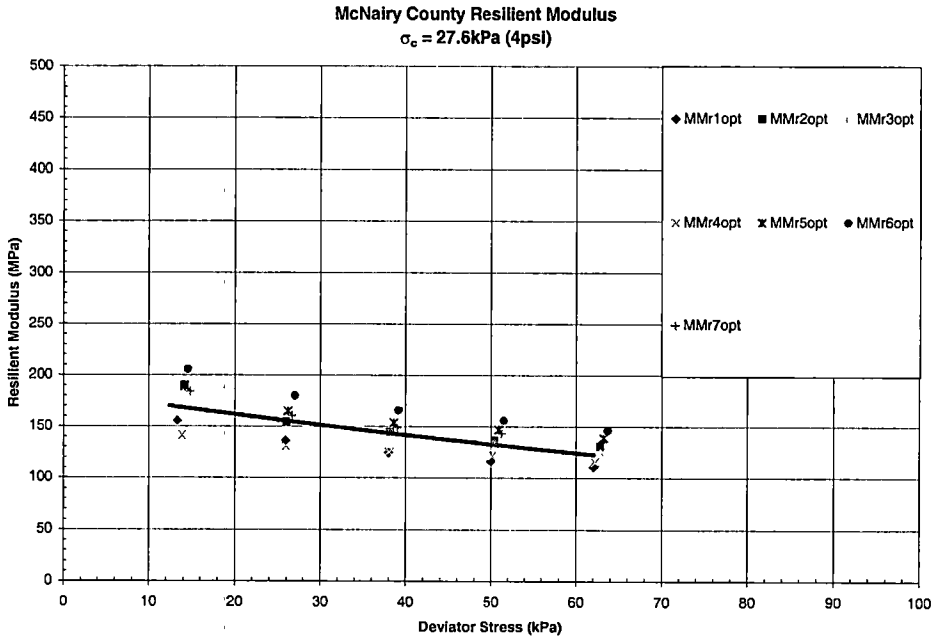

Graph B - 26 Resilient Modulus vs. Deviator Stress for McNairy County with Model, Confining Pressure = 27.6kPa (4psi)

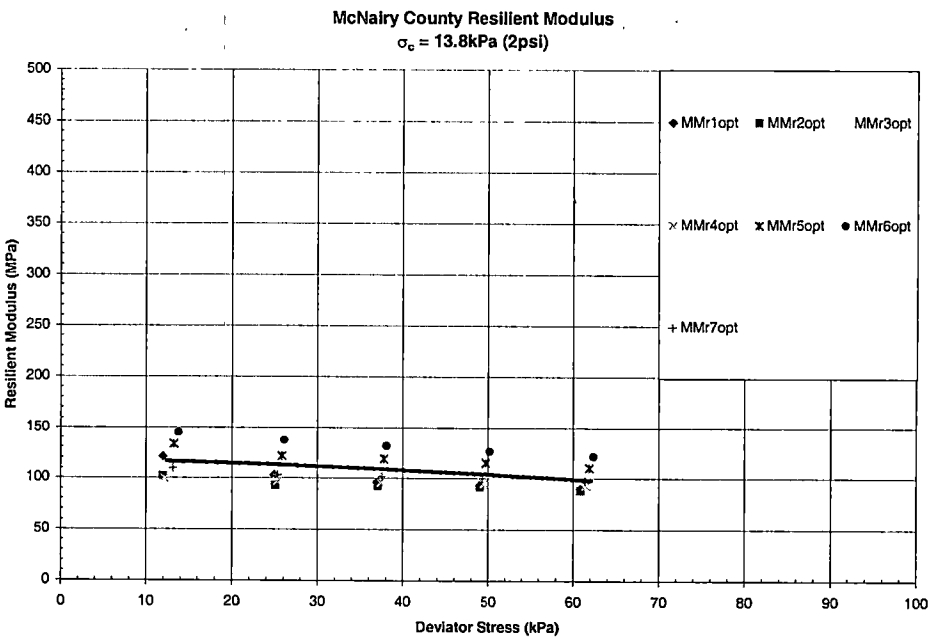

Graph B - 27 Resilient Modulus vs. Deviator Stress for McNairy County with Model, Confining Pressure = 13.8kPa (2psi)

Overton County

List B - 3 Overton County Resilient Modulus Sample Properties

Specimen Number	Dry Density (pcf)	Water Content (%)	Log - log model			
			K1	K2	K3	R^2
OMr1opt	108.7	15.8	1477	0.38409	-2.60998	0.98
OMr2opt	108.7	16.0	1508	0.63624	-3.50053	0.98
OMr3opt	108.9	15.9	1593	0.54086	-3.05916	0.96
OMr4opt	109.0	15.8	1617	0.80265	-3.63226	0.97
OMr5opt	109.2	15.7	1921	0.81363	-3.94172	0.98
OMr6opt	109.2	15.6	1938	0.60081	-3.19445	0.97
OMr7opt	109.6	15.2	2031	0.66612	-3.81761	0.95
OMr8opt	109.8	15.0	1890	0.70085	-3.01777	0.98
Ave.	109.1	15.6	1747	0.64316	-3.34669	0.97
Standard Deviation	0.4	0.3	220	0.14029	0.45321	

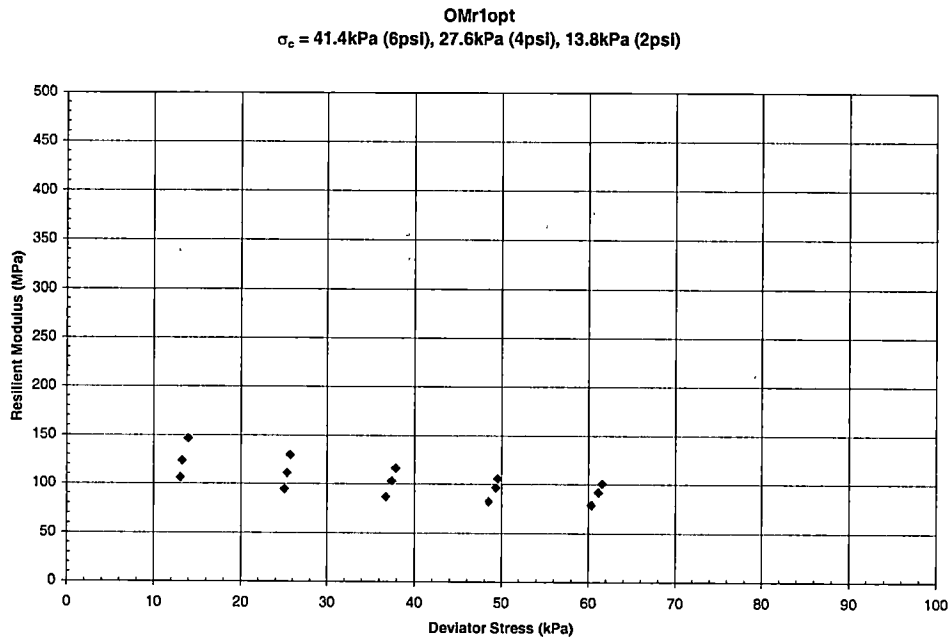

Graph B - 28 Resilient Modulus vs. Deviator Stress for Overton County – OMr1opt

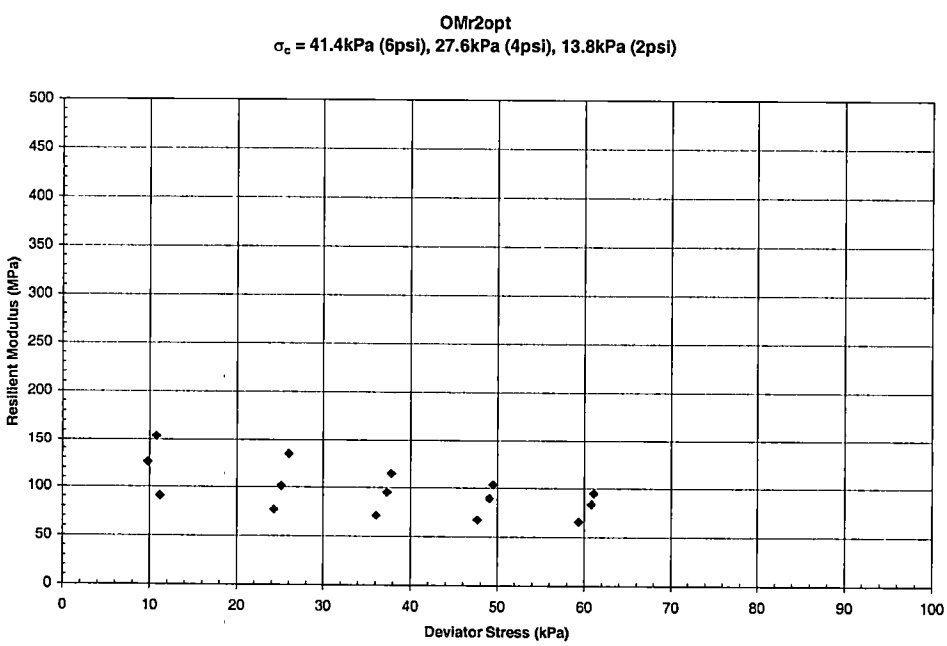

Graph B - 29 Resilient Modulus vs. Deviator Stress for Overton County – OMr2opt

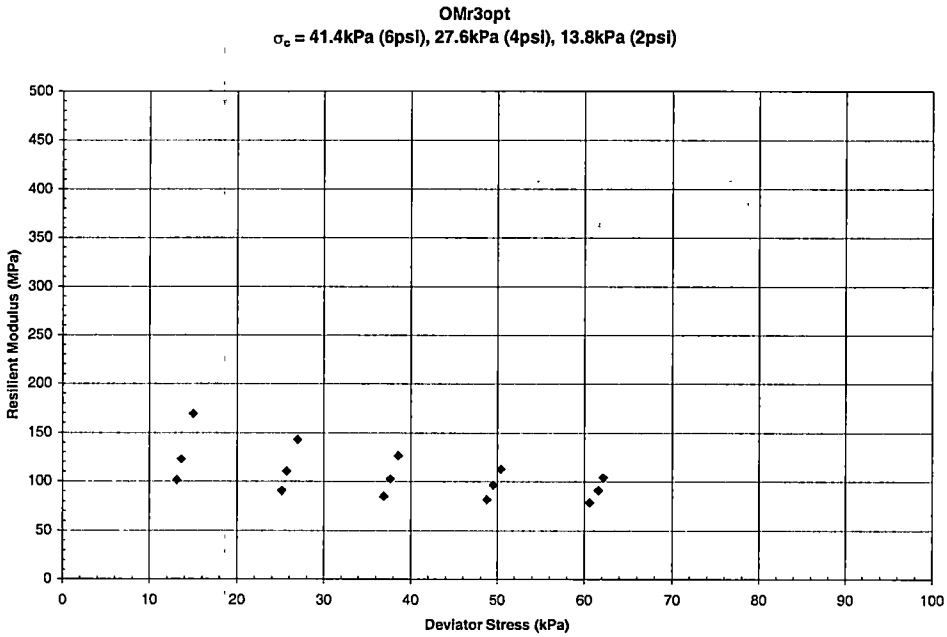

Graph B - 30 Resilient Modulus vs. Deviator Stress for Overton County – OMr3opt

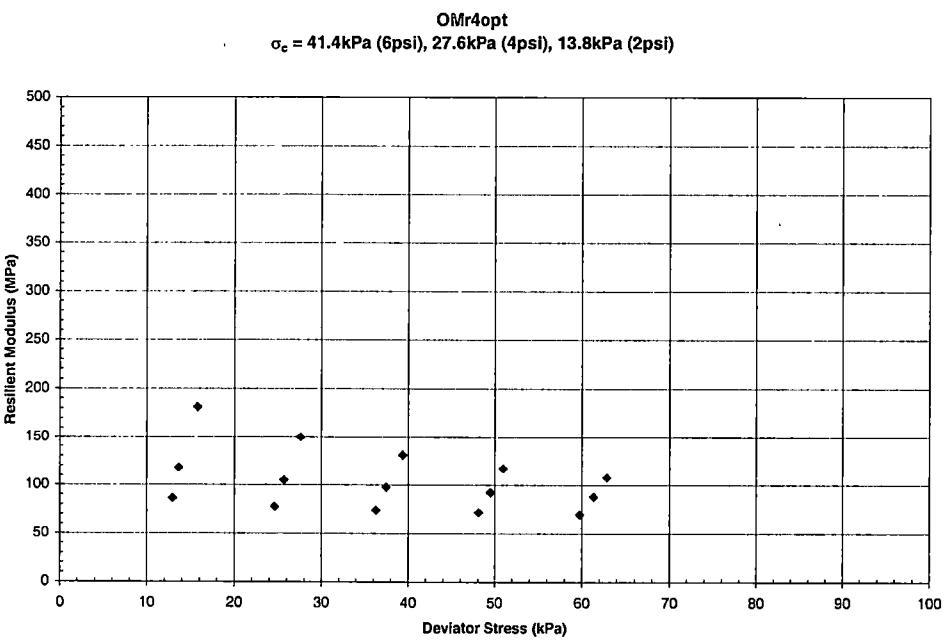

Graph B - 31 Resilient Modulus vs. Deviator Stress for Overton County – OMr4opt

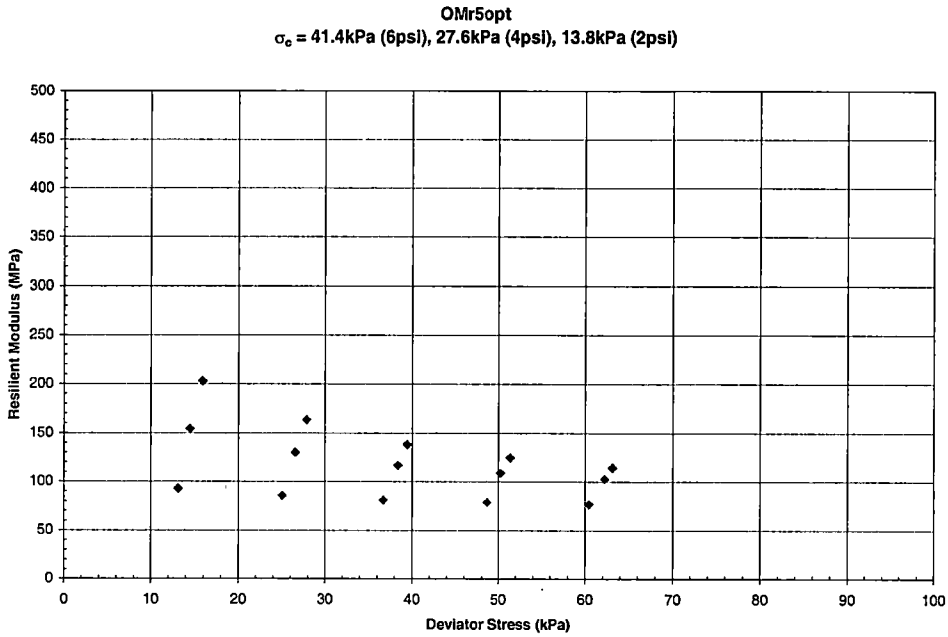

Graph B - 32 Resilient Modulus vs. Deviator Stress for Overton County – OMr5opt

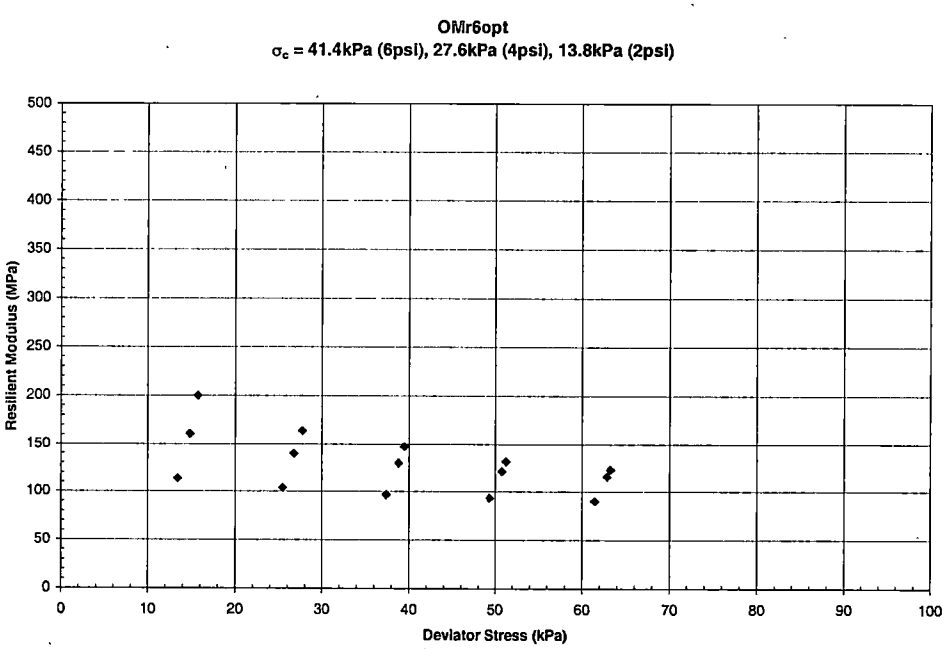

Graph B - 33 Resilient Modulus vs. Deviator Stress for Overton County – OMr6opt

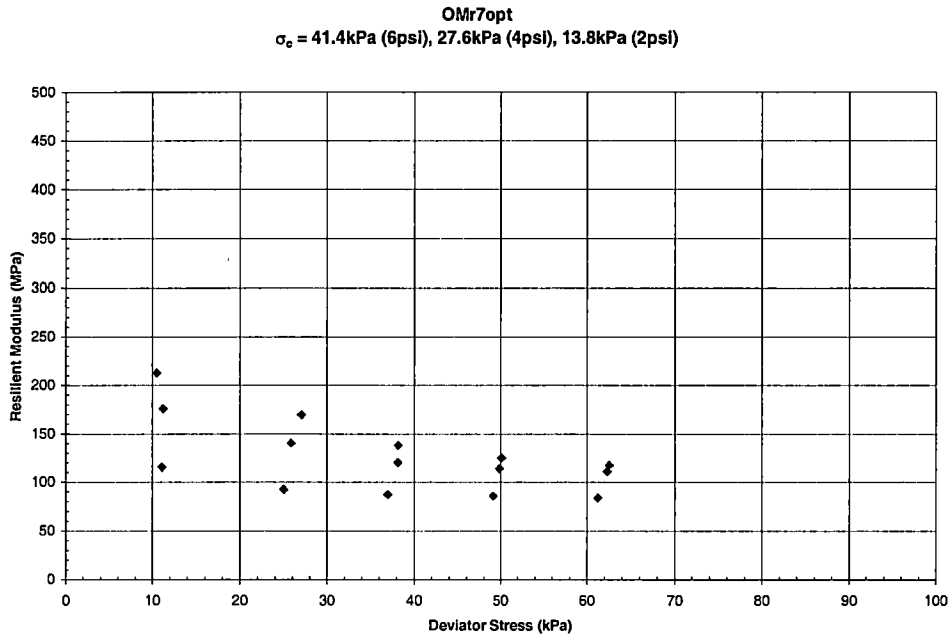

Graph B - 34 Resilient Modulus vs. Deviator Stress for Overton County – OMr7opt

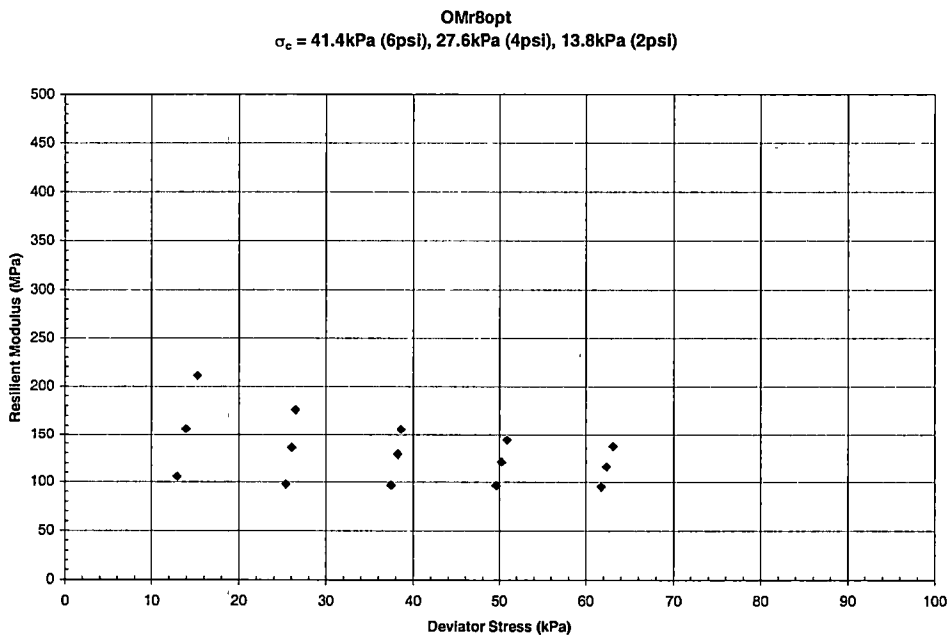

Graph B - 35 Resilient Modulus vs. Deviator Stress for Overton County – OMr8opt

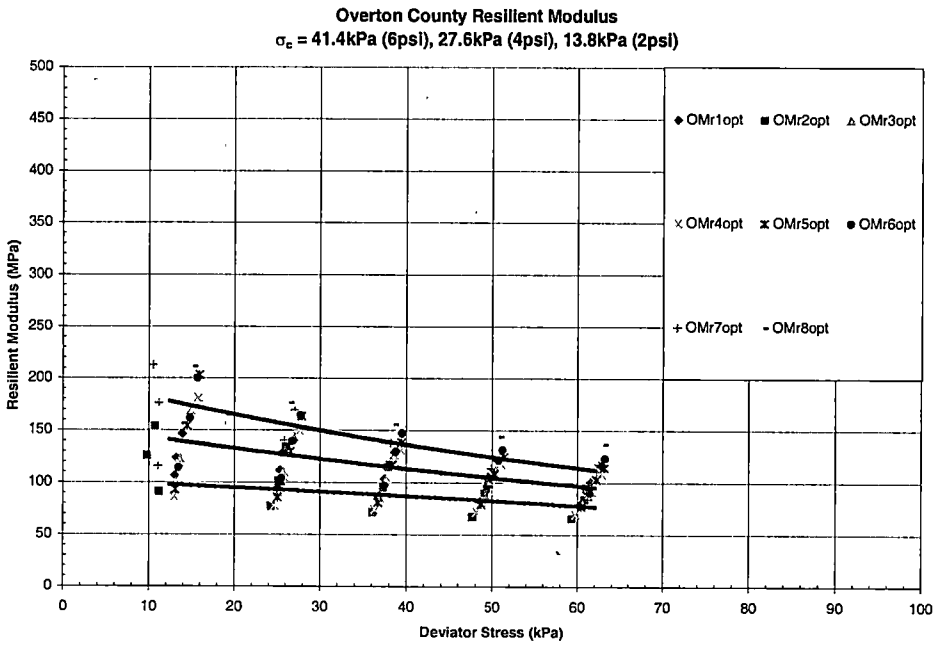

Graph B - 36 Resilient Modulus vs. Deviator Stress for Overton County with Models

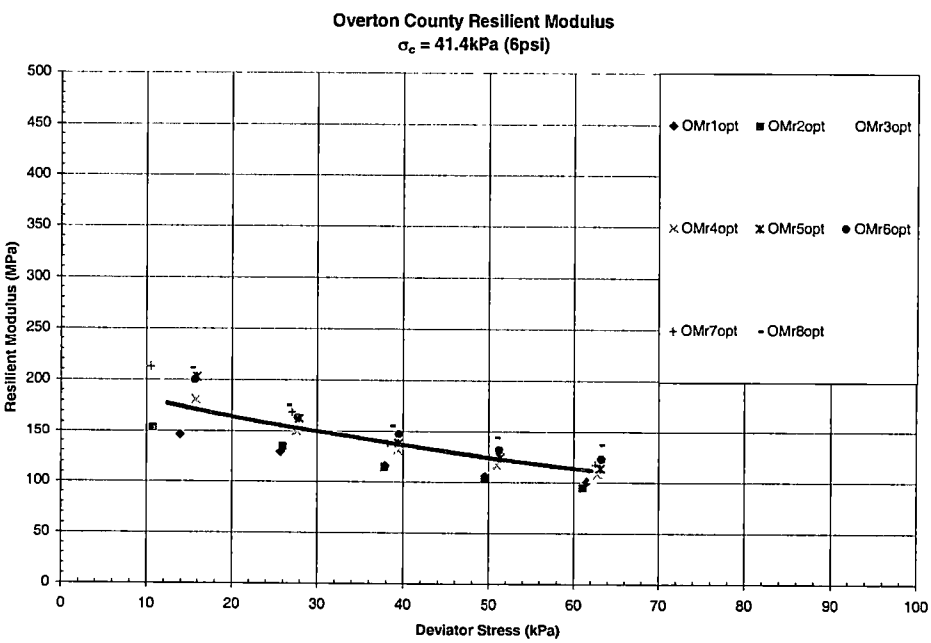

Graph B - 37 Resilient Modulus vs. Deviator Stress for Overton County with Model, Confining Pressure = 41.4kPa (6psi)

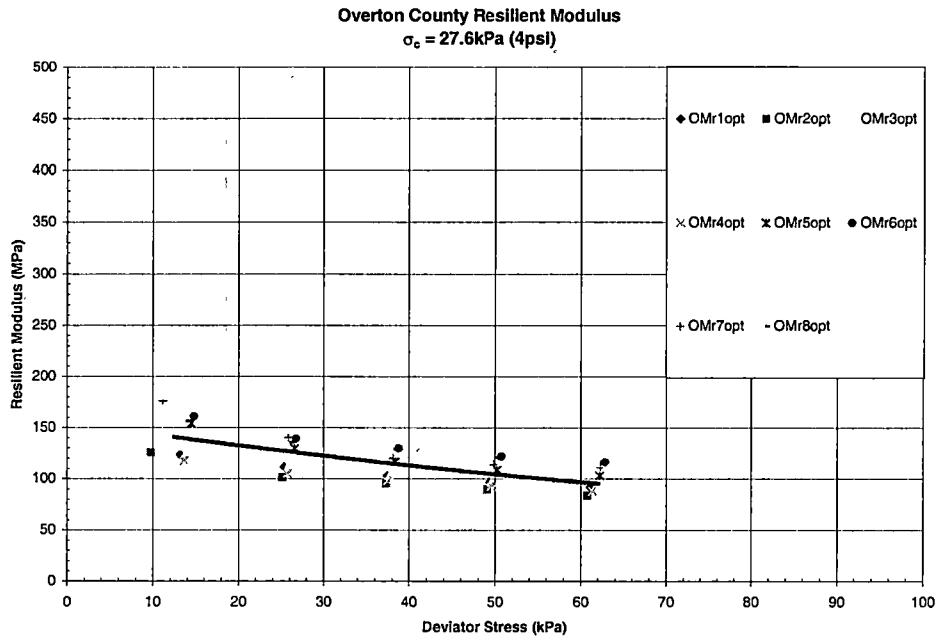

Graph B - 38 Resilient Modulus vs. Deviator Stress for Overton County with Model, Confining Pressure = 27.6kPa (4psi)

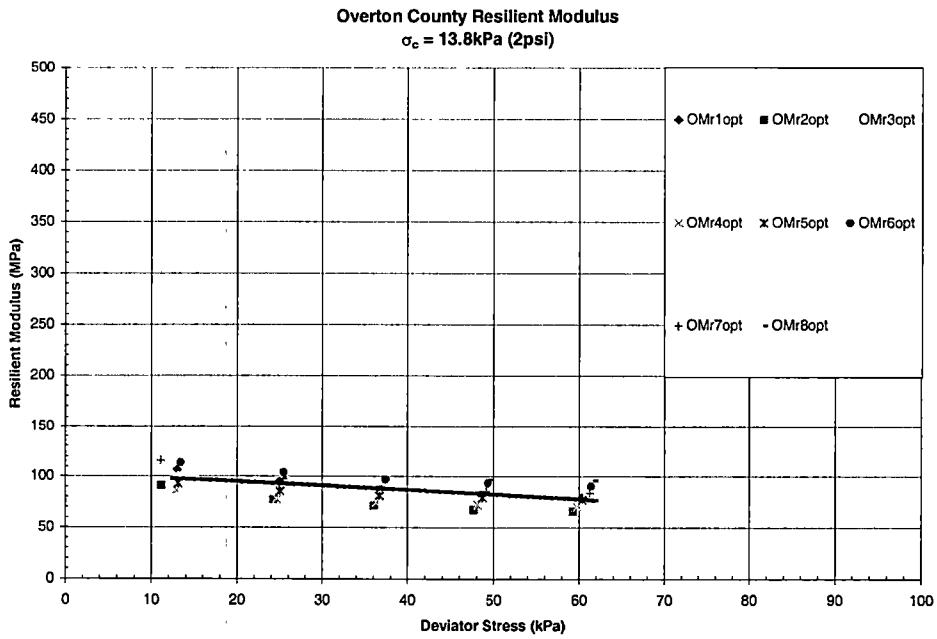

Graph B - 39 Resilient Modulus vs. Deviator Stress for Overton County with Model, Confining Pressure = 13.8kPa (2psi)

Sumner County

List B - 4 Sumner County Resilient Modulus Sample Properties

Specimen Number	Dry Density (pcf)	Water Content (%)	Log - log model			
			K1	K2	K3	R^2
SMr1opt	103.2	17.4	1501	0.61031	-3.58914	0.98
SMr2opt	104.2	16.6	1599	0.61976	-3.43206	0.95
SMr3opt	104.2	16.6	1419	0.55660	-3.00497	0.99
SMr4opt	103.9	16.8	1619	0.62870	-3.53473	0.98
SMr5opt	103.9	16.9	1427	0.65674	-3.35038	0.98
SMr6opt	104.0	16.7	1361	0.52077	-2.78180	0.97
SMr7opt	103.8	17.0	1681	0.53172	-3.13708	0.98
SMr8opt	103.7	17.1	1643	0.58982	-3.35425	0.96
Ave.	103.9	16.9	1531	0.58930	-3.27305	0.97
Standard Deviation	0.3	0.3	120	0.04863	0.27721	

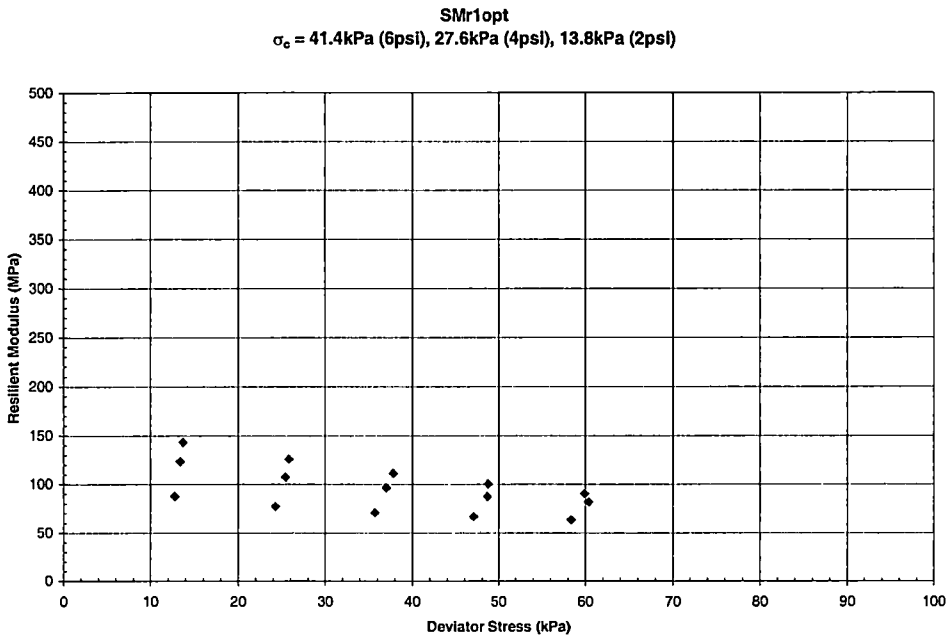

Graph B - 40 Resilient Modulus vs. Deviator Stress for Sumner County – SMr1opt

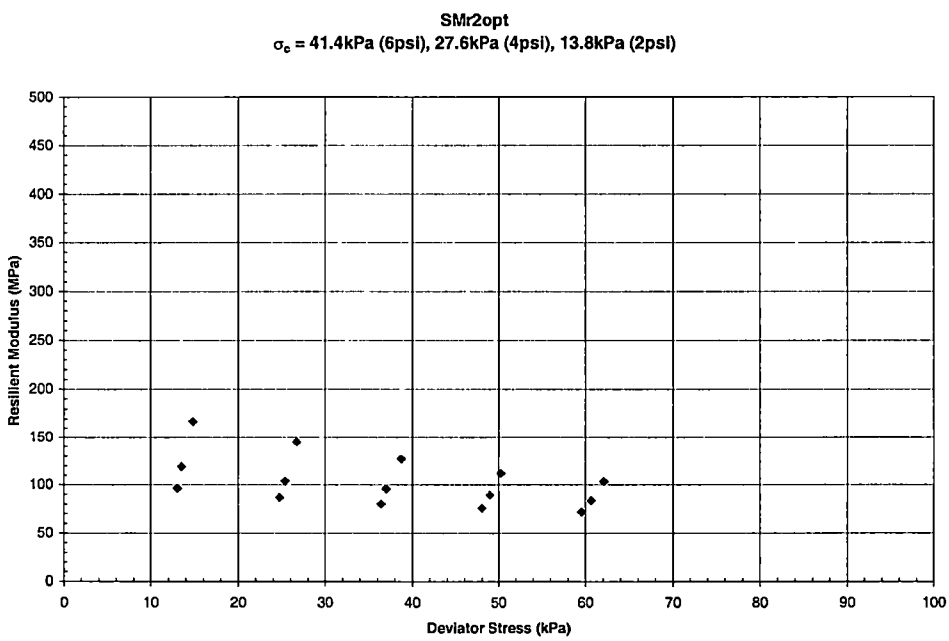

Graph B - 41 Resilient Modulus vs. Deviator Stress for Sumner County – SMr2opt

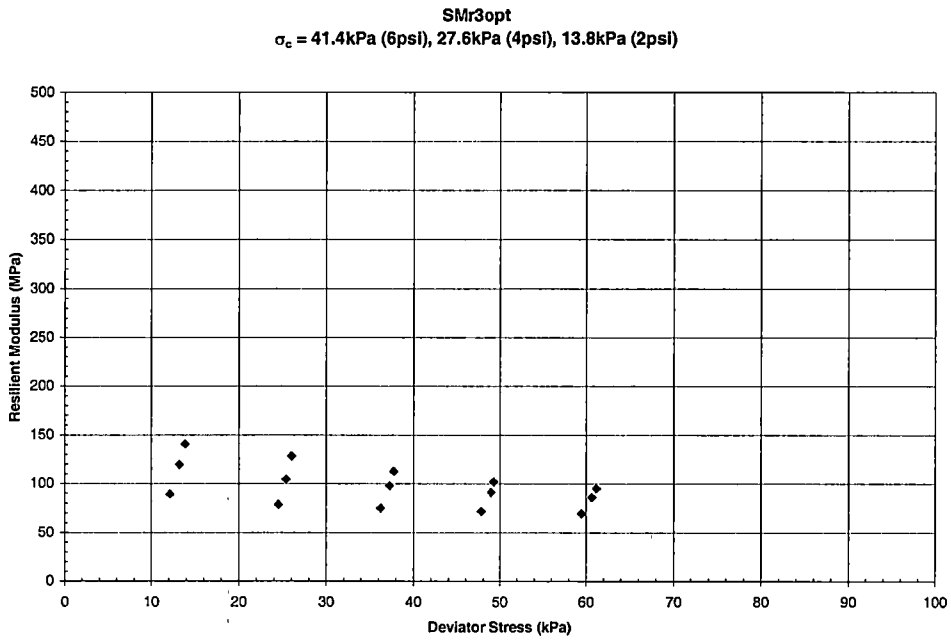

Graph B - 42 Resilient Modulus vs. Deviator Stress for Sumner County – SMr3opt

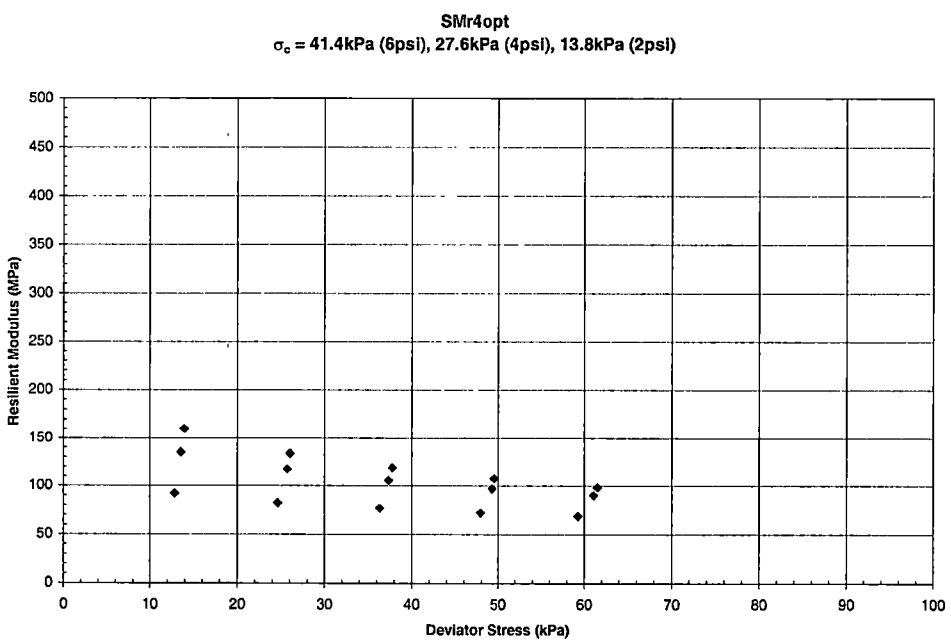

Graph B - 43 Resilient Modulus vs. Deviator Stress for Sumner County – SMr4opt

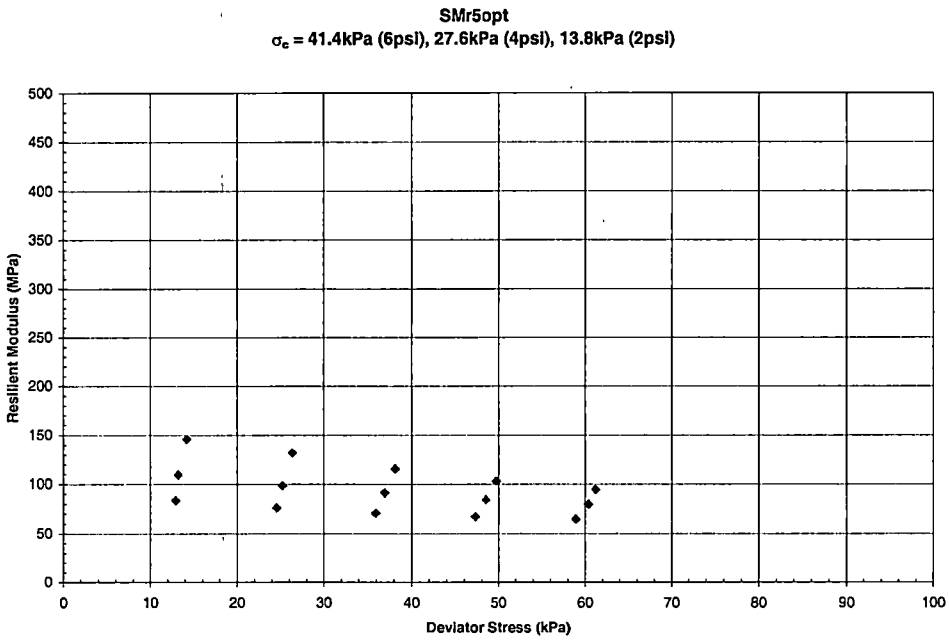

Graph B - 44 Resilient Modulus vs. Deviator Stress for Sumner County – SMr5opt

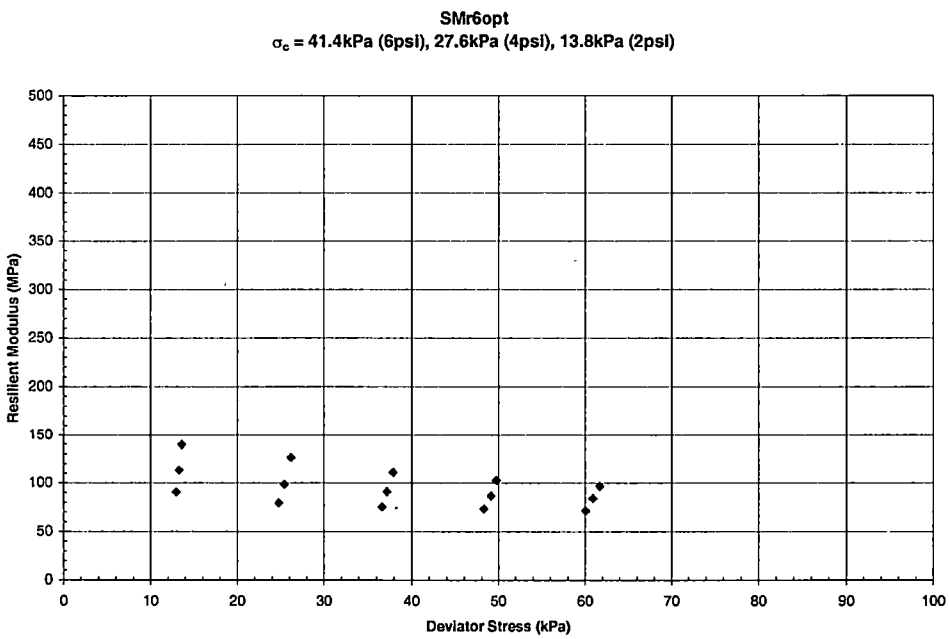

Graph B - 45 Resilient Modulus vs. Deviator Stress for Sumner County – SMr6opt

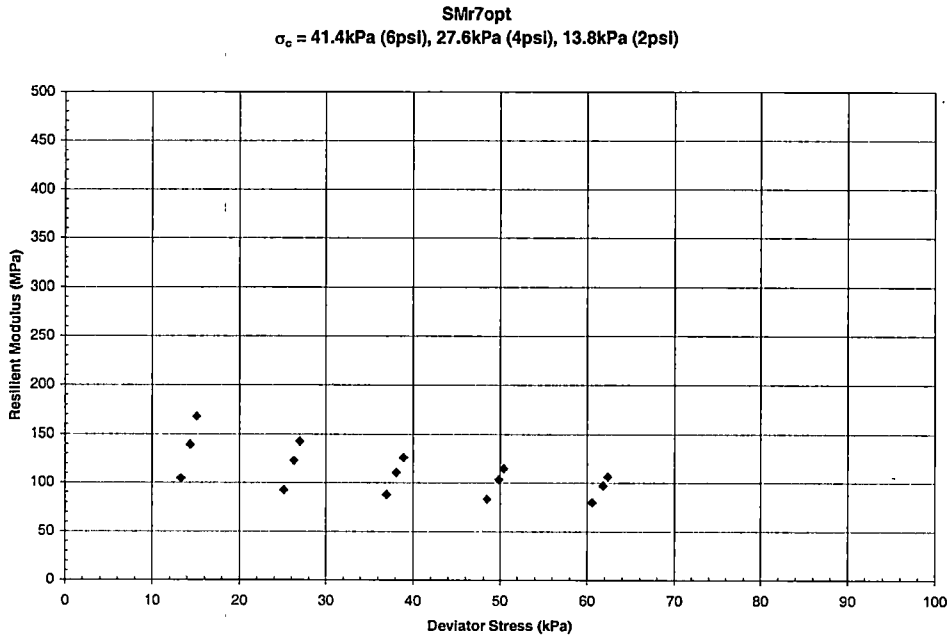

Graph B - 46 Resilient Modulus vs. Deviator Stress for Sumner County – SMr7opt

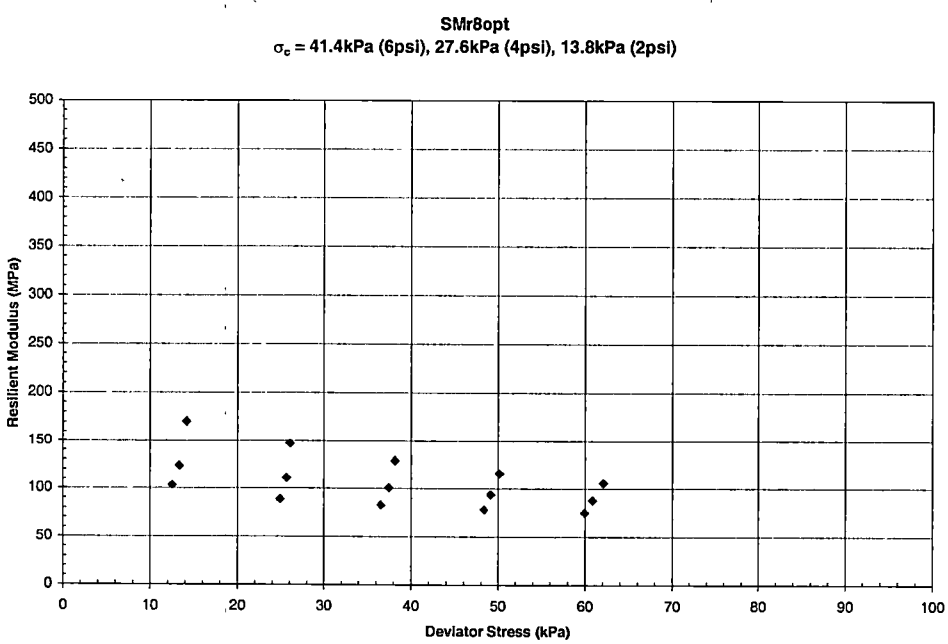

Graph B - 47 Resilient Modulus vs. Deviator Stress for Sumner County – SMr8opt

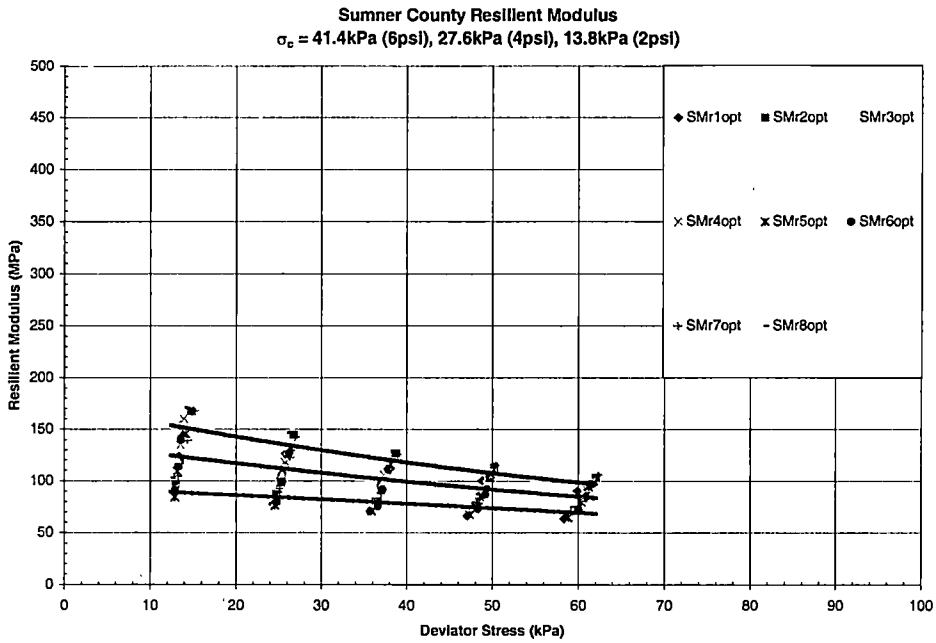

Graph B - 48 Resilient Modulus vs. Deviator Stress for Sumner County with Models

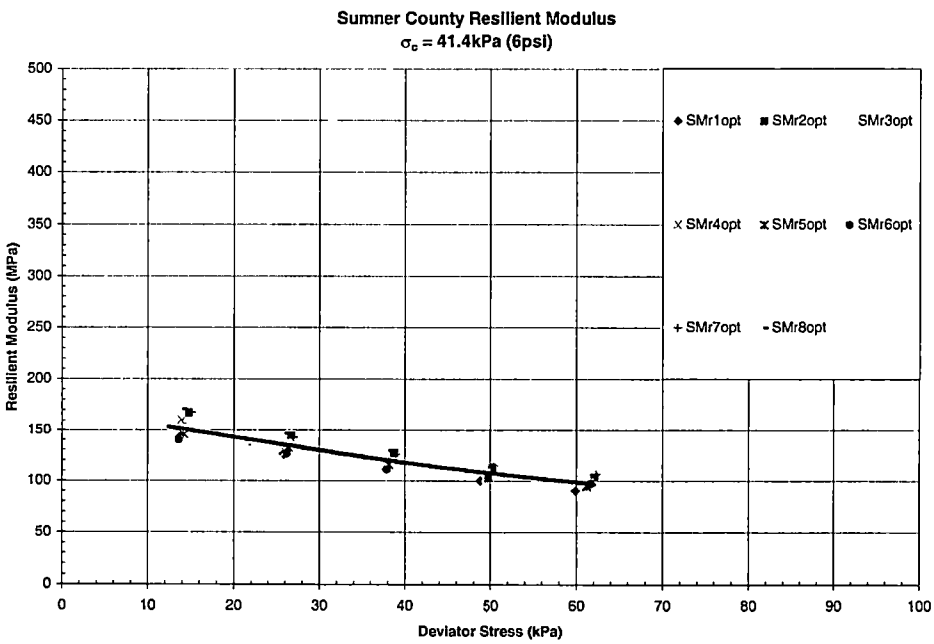

Graph B - 49 Resilient Modulus vs. Deviator Stress for Sumner County with Model, Confining Pressure = 41.4kPa (6psi)

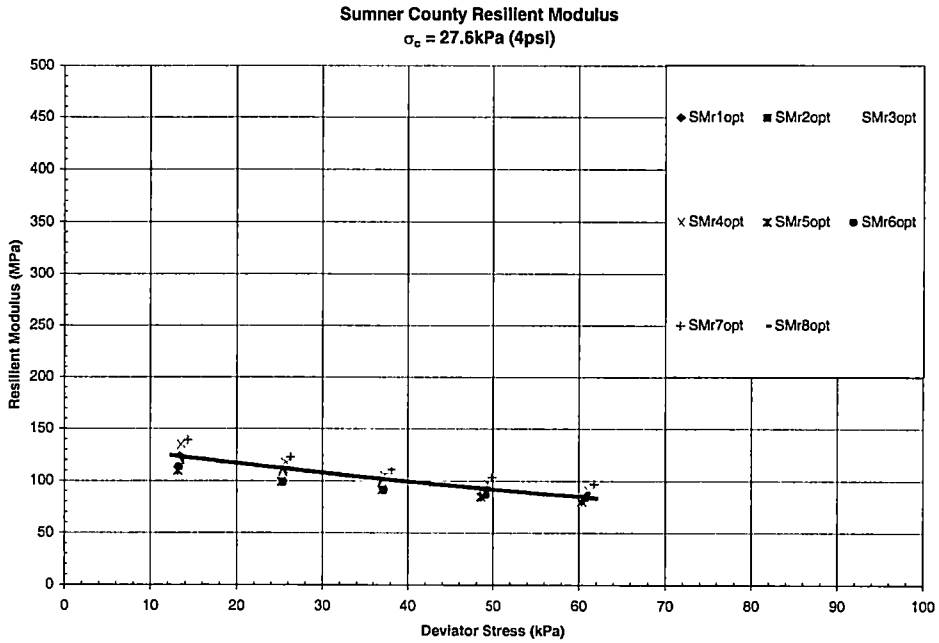

Graph B - 50 Resilient Modulus vs. Deviator Stress for Sumner County with Model, Confining Pressure = 27.6kPa (4psi)

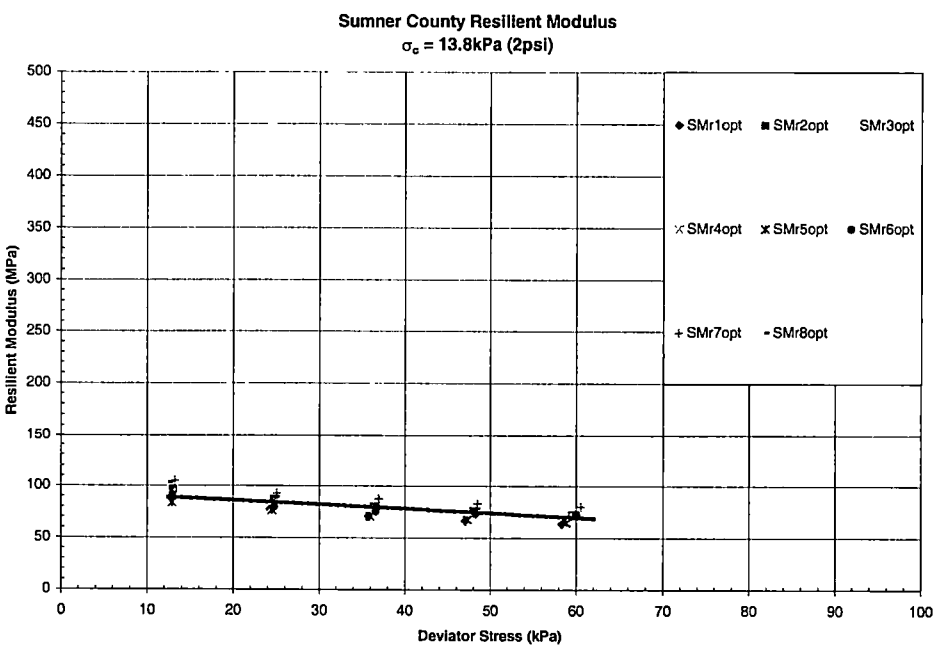

Graph B - 51 Resilient Modulus vs. Deviator Stress for Sumner County with Model, Confining Pressure = 13.8kPa (2psi)

Appendix C ATM Data

ATM

List C - 1 ATM Specimen Properties

Specimen Number	Wet Density (pcf)	Dry Density (pcf)	Water Content (%)	Total Mass of Specimen (lb / kg)
Blount ATM #1	123.6	102.7	20.4	4.00 lb 1.814 kg
Blount ATM #2	122.7	101.8	20.6	3.97 lb 1.801kg
McNairy ATM #1	130.9	116.2	12.7	4.24 lb 1.922 kg
McNairy ATM #2	130.3	115.2	13.2	4.22 lb 1.913 kg
Overton ATM #1	127.6	110.2	15.8	4.13 lb 1.873 kg
Overton ATM #2	127.8	110.2	16.0	4.14 lb 1.876 kg
Sumner ATM #1	123.8	105.7	17.1	4.01 lb 1.817 kg
Sumner ATM #2	122.7	104.9	16.9	3.97 lb 1.801 kg

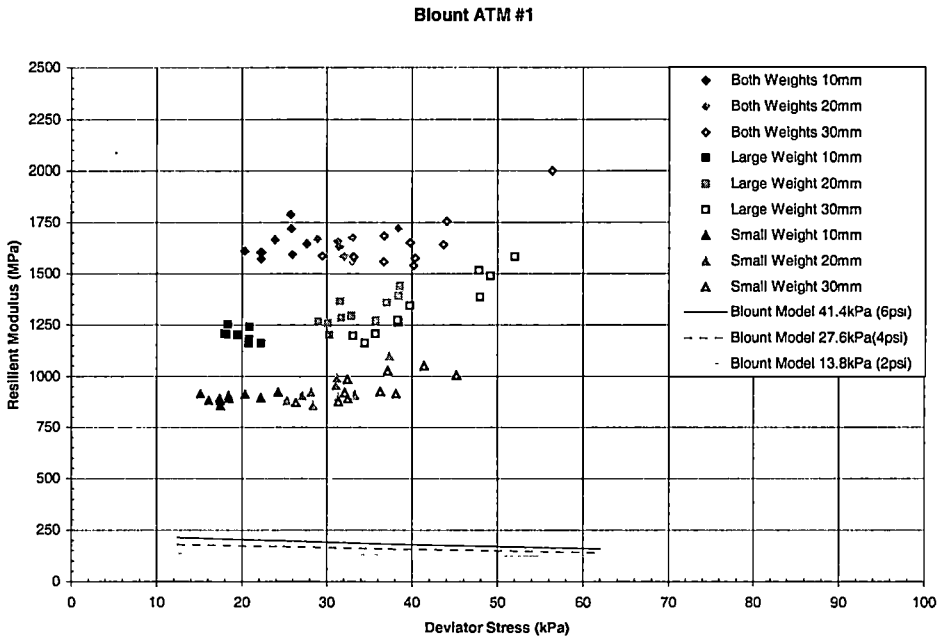

Graph C - 1 Resilient Modulus vs. Deviator Stress for Blount County Blount ATM #1 – Peak Acceleration

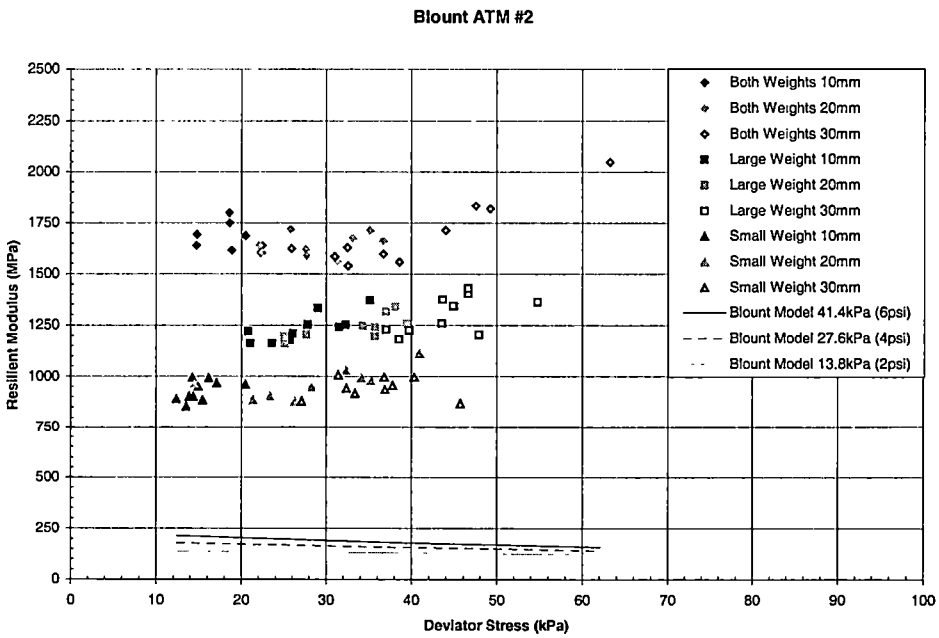

Graph C - 2 Resilient Modulus vs. Deviator Stress for Blount County Blount ATM #2 – Peak Acceleration

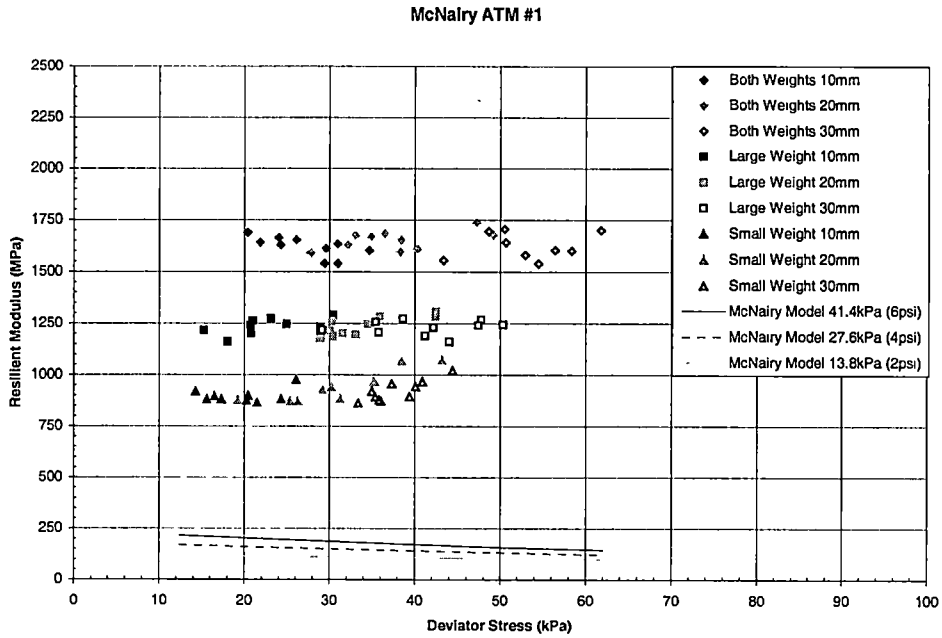

Graph C - 3 Resilient Modulus vs. Deviator Stress for McNairy County McNairy ATM #1 – Peak Acceleration

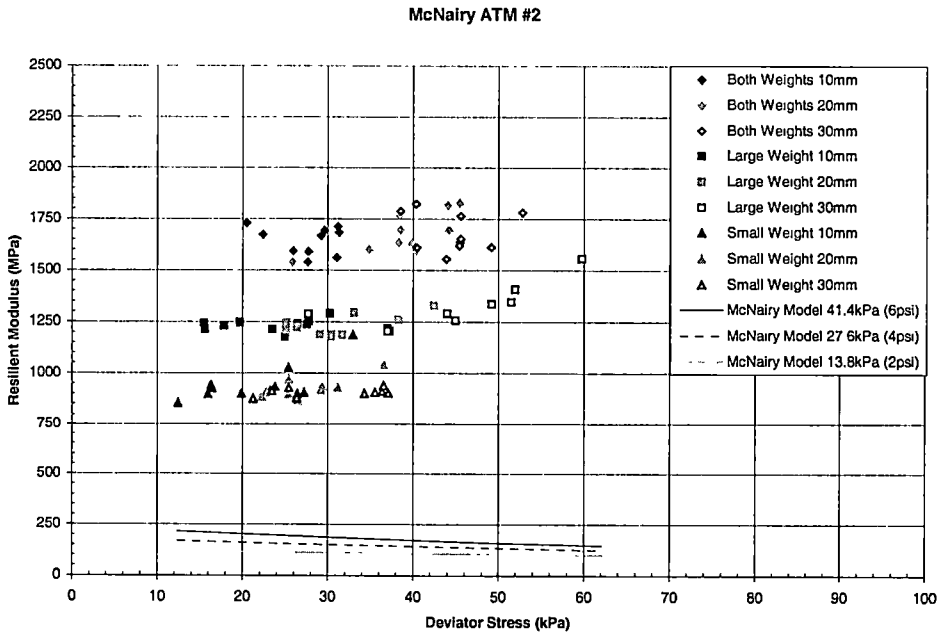

Graph C - 4 Resilient Modulus vs. Deviator Stress for McNairy County McNairy ATM#2 – Peak Acceleration

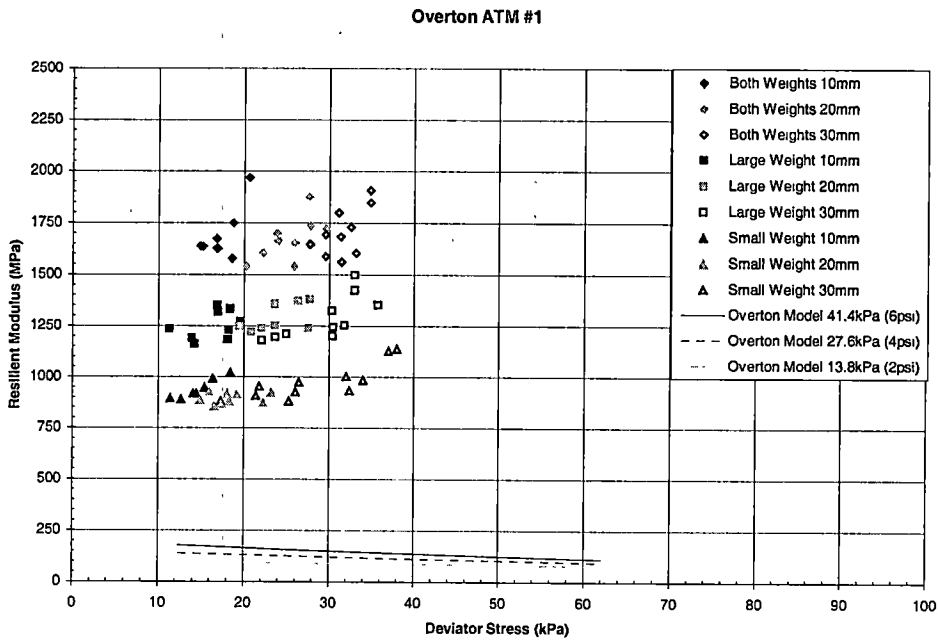

Graph C - 5 Resilient Modulus vs. Deviator Stress for Overton County Overton ATM #1 – Peak Acceleration

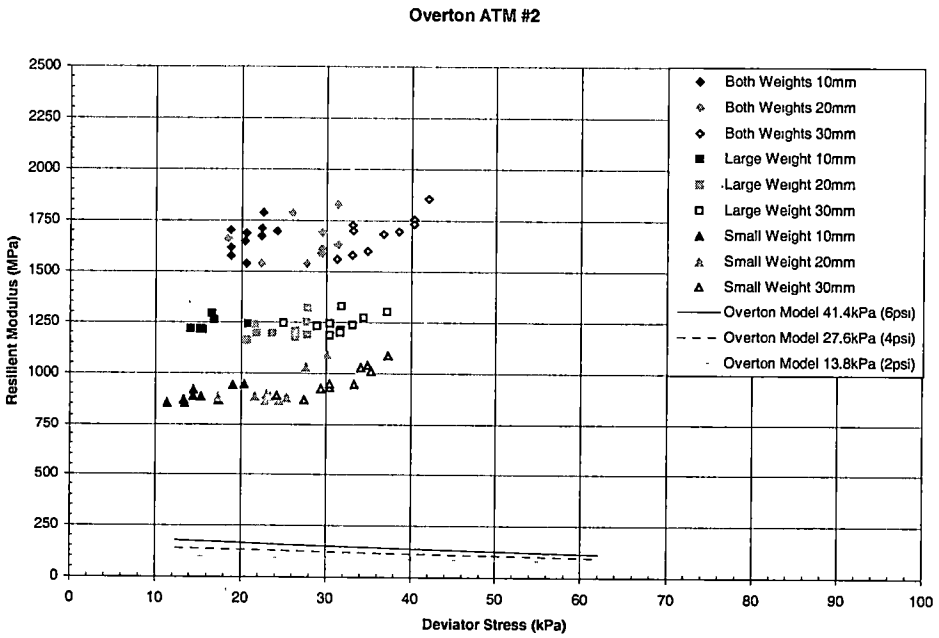

Graph C - 6 Resilient Modulus vs. Deviator Stress for Overton County Overton ATM #2 – Peak Acceleration

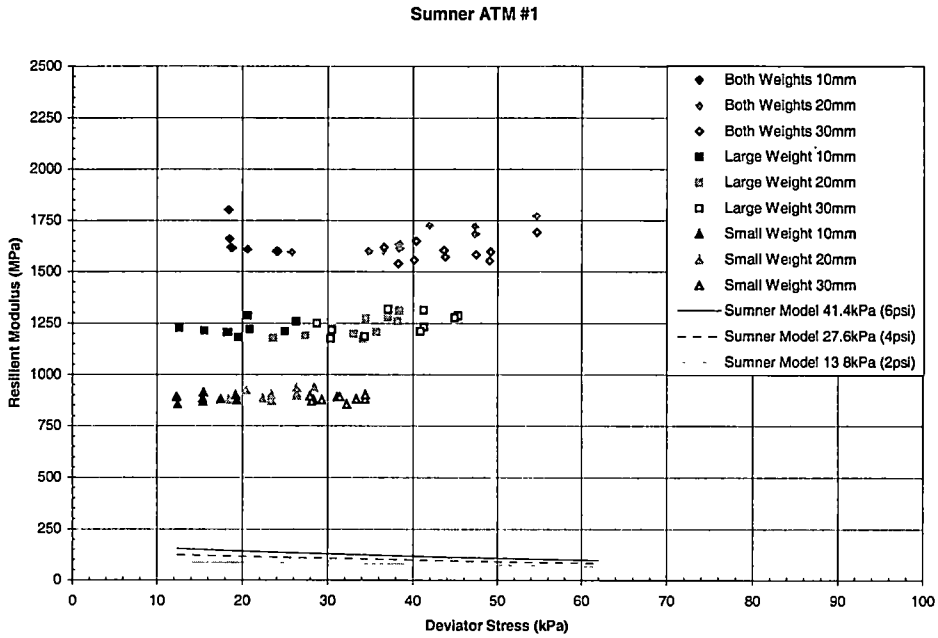

Graph C - 7 Resilient Modulus vs. Deviator Stress for Sumner County – Sumner ATM #1 – Peak Acceleration

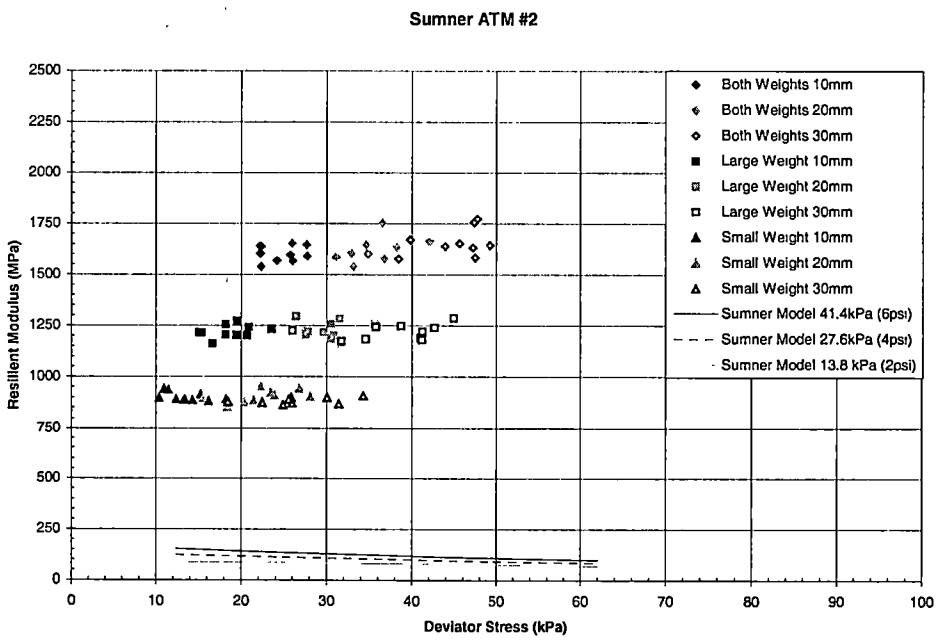

Graph C - 8 Resilient Modulus vs. Deviator Stress for Sumner County Sumner ATM #2 – Peak Acceleration

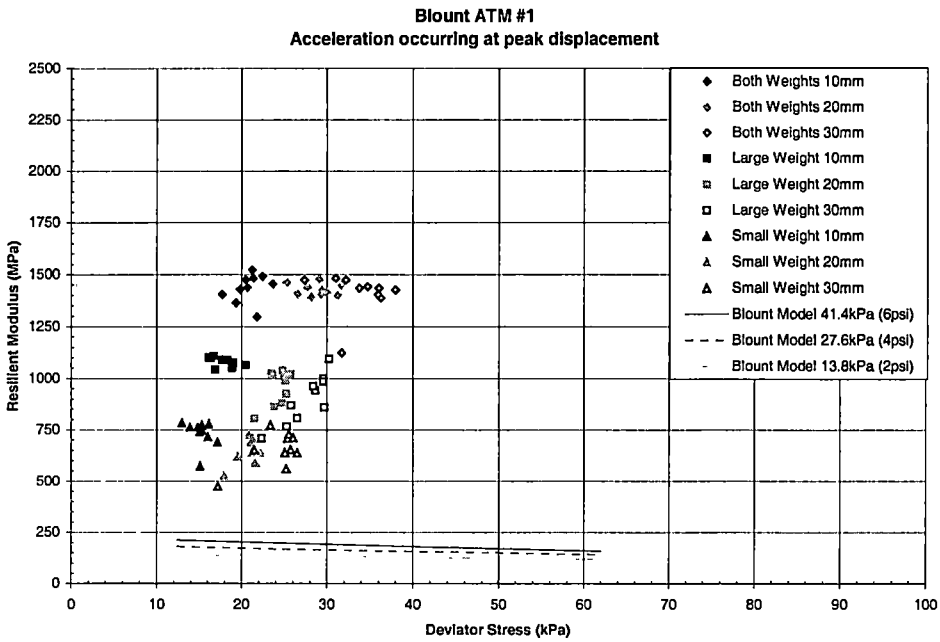

Graph C – 9 Resilient Modulus vs. Deviator Stress for Blount County Blount ATM #1 – Acceleration Occurring at Peak Displacement

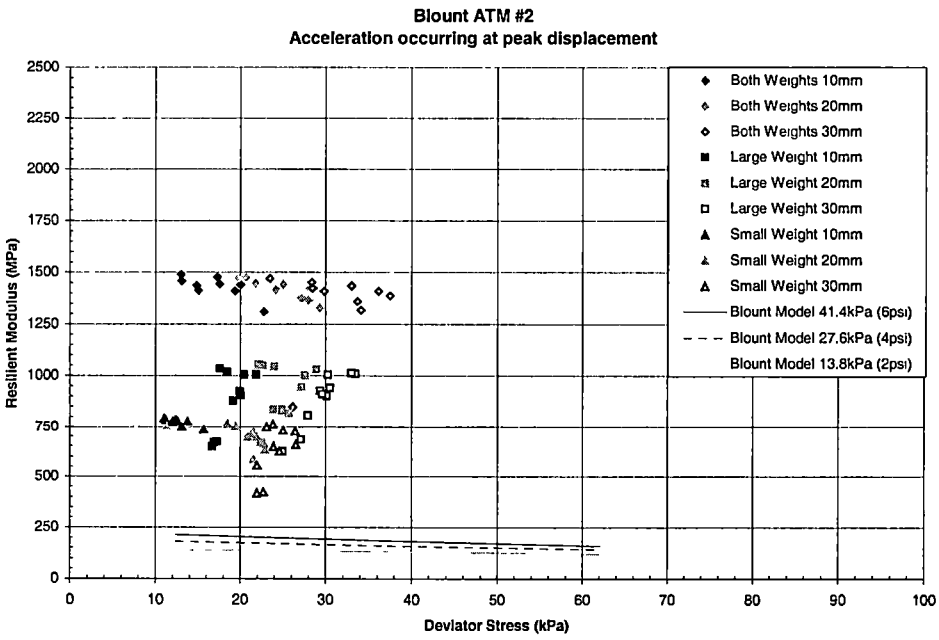

Graph C – 10 Resilient Modulus vs. Deviator Stress for Blount County Blount ATM #1 – Acceleration Occurring at Peak Displacement

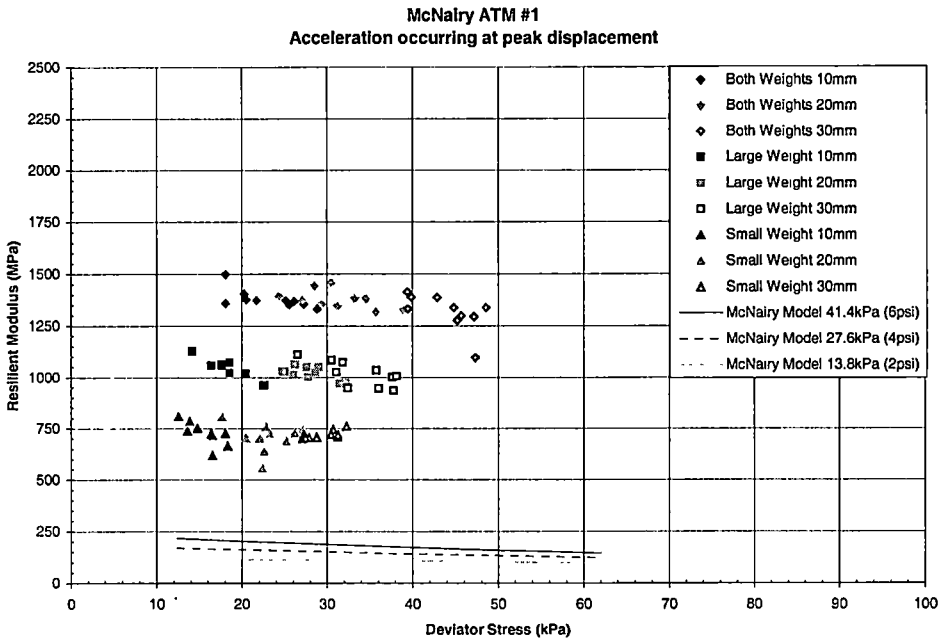

Graph C - 11 Resilient Modulus vs. Deviator Stress for McNairy County McNairy ATM #1 – Acceleration Occurring at Peak Displacement

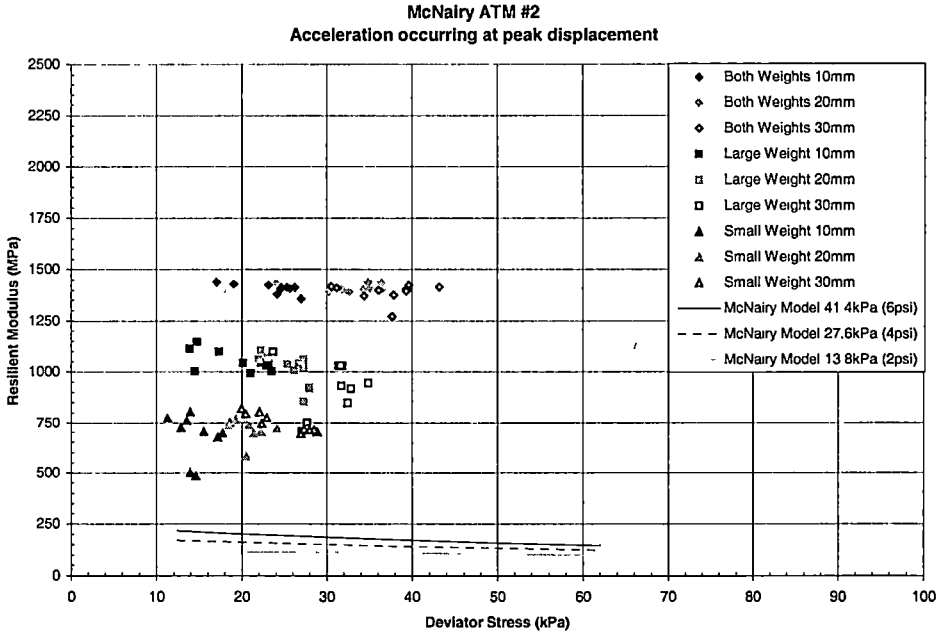

Graph C – 12 Resilient Modulus vs. Deviator Stress for McNairy County McNairy ATM #2 – Acceleration Occurring at Peak Displacement

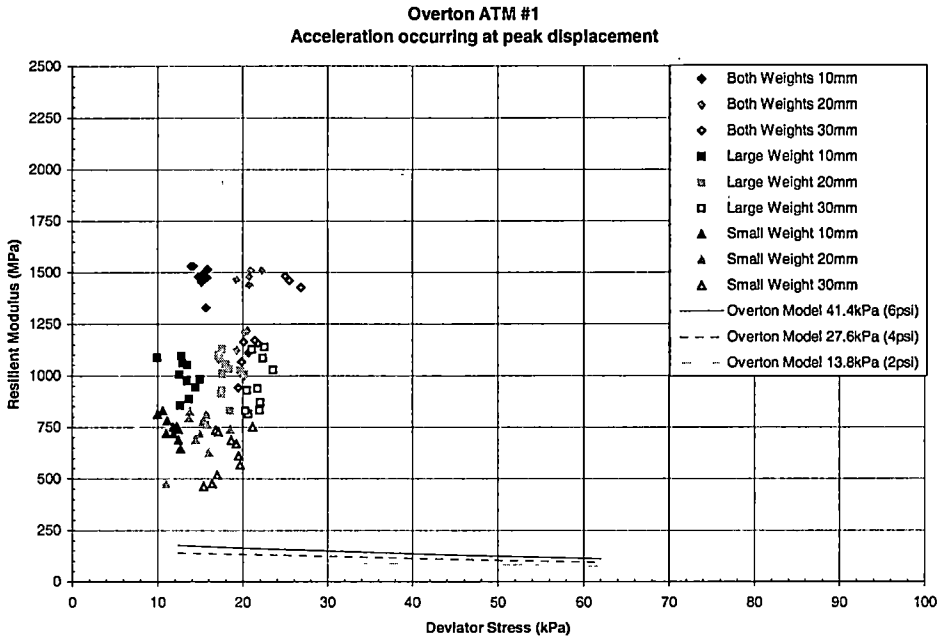

Graph C – 13 Resilient Modulus vs. Deviator Stress for Overton County Overton ATM #1 – Acceleration Occurring at Peak Displacement

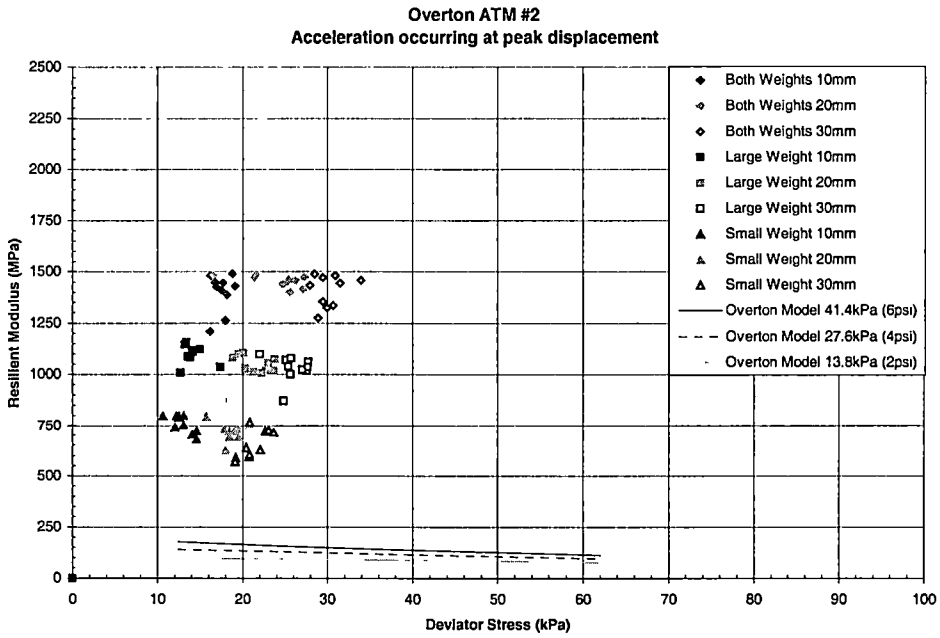

Graph C – 14 Resilient Modulus vs. Deviator Stress for Overton County Overton ATM #2 – Acceleration Occurring at Peak Displacement

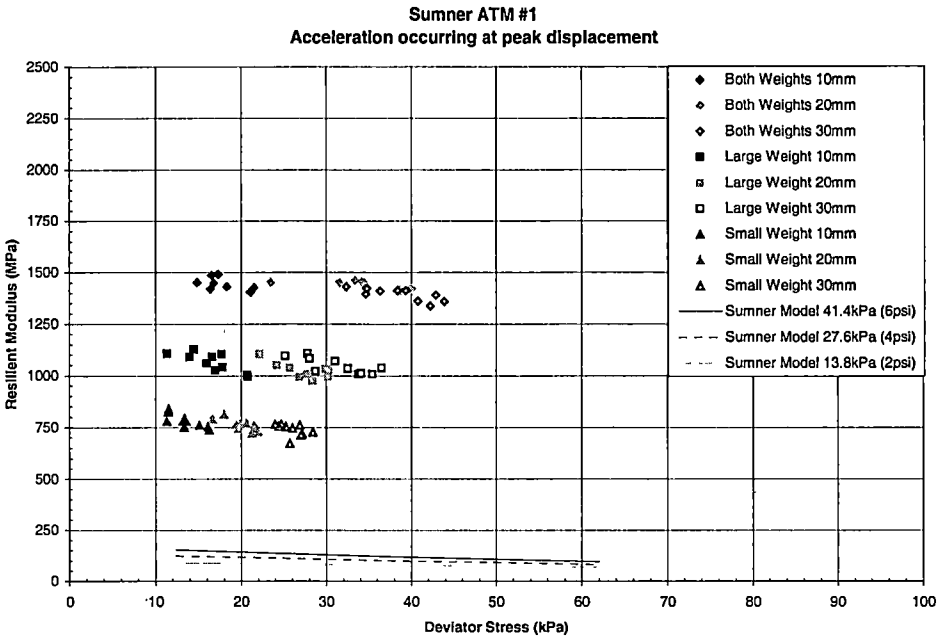

Graph C – 15 Resilient Modulus vs. Deviator Stress for Sumner County Sumner ATM #1 – Acceleration Occurring at Peak Displacement

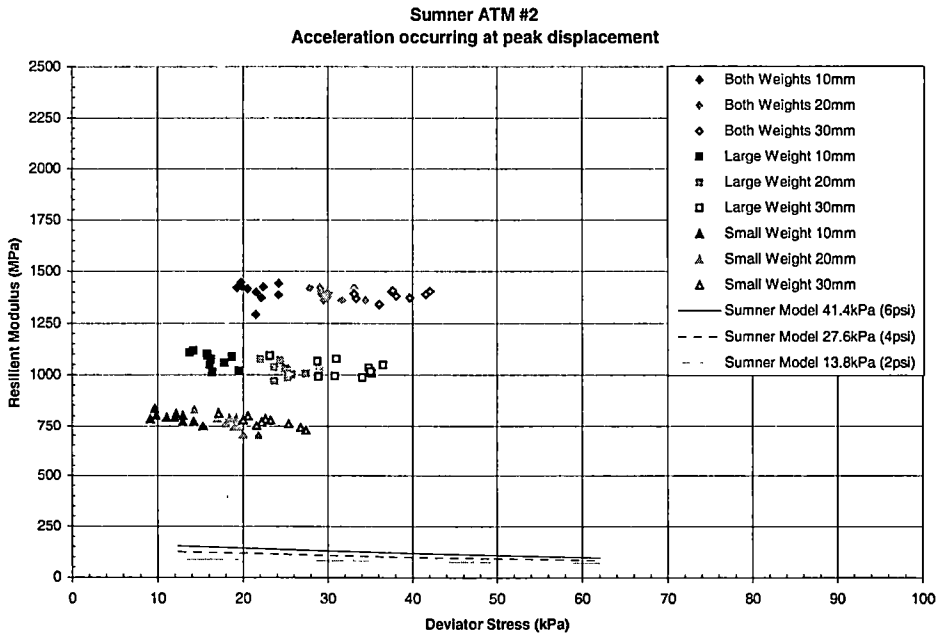

Graph C – 16 Resilient Modulus vs. Deviator Stress for Sumner County Sumner ATM #2 – Acceleration Occurring at Peak Displacement

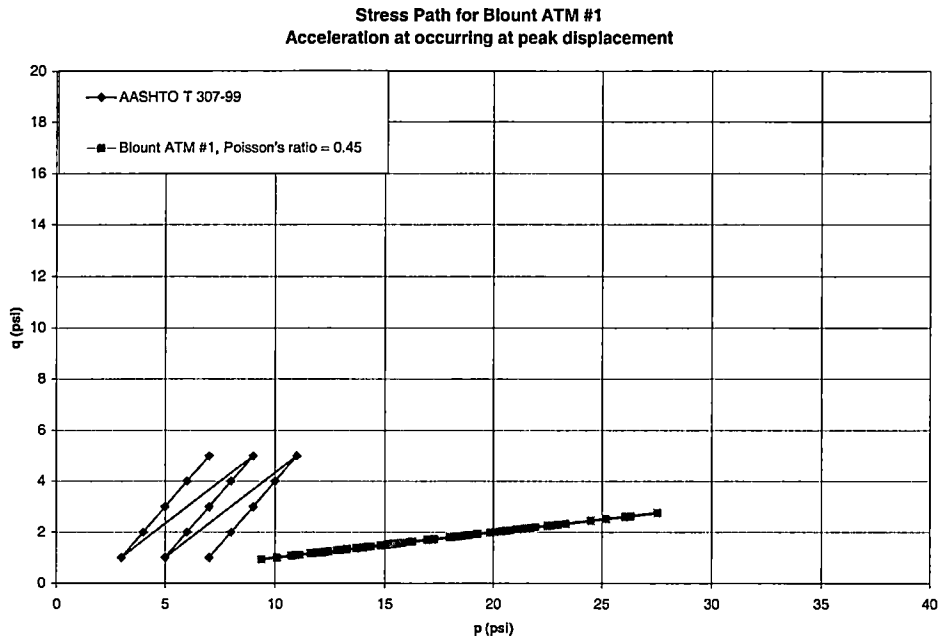

Graph C – 17 Stress Path for Blount ATM #1

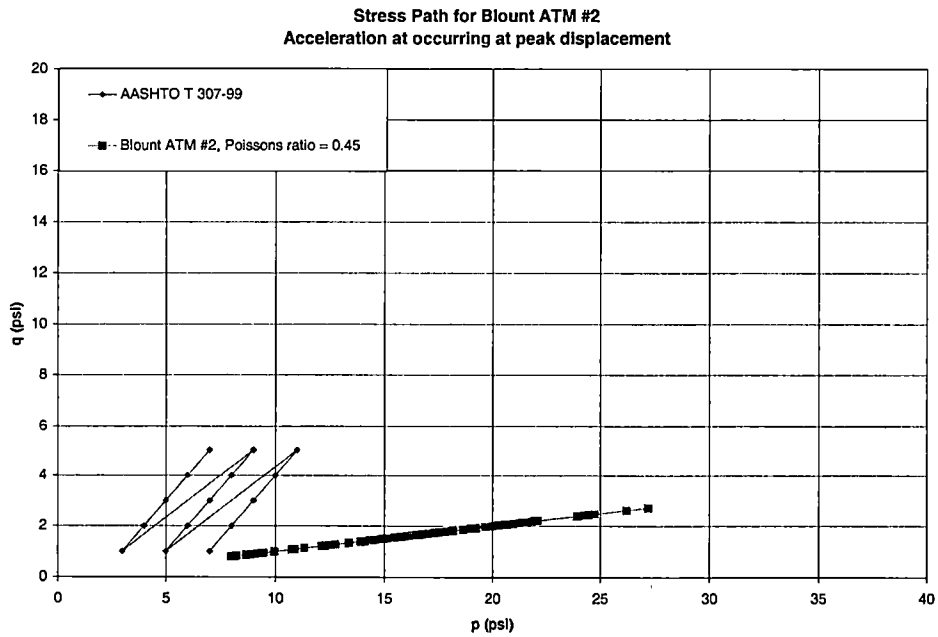

Graph C – 18 Stress Path for Blount ATM #2

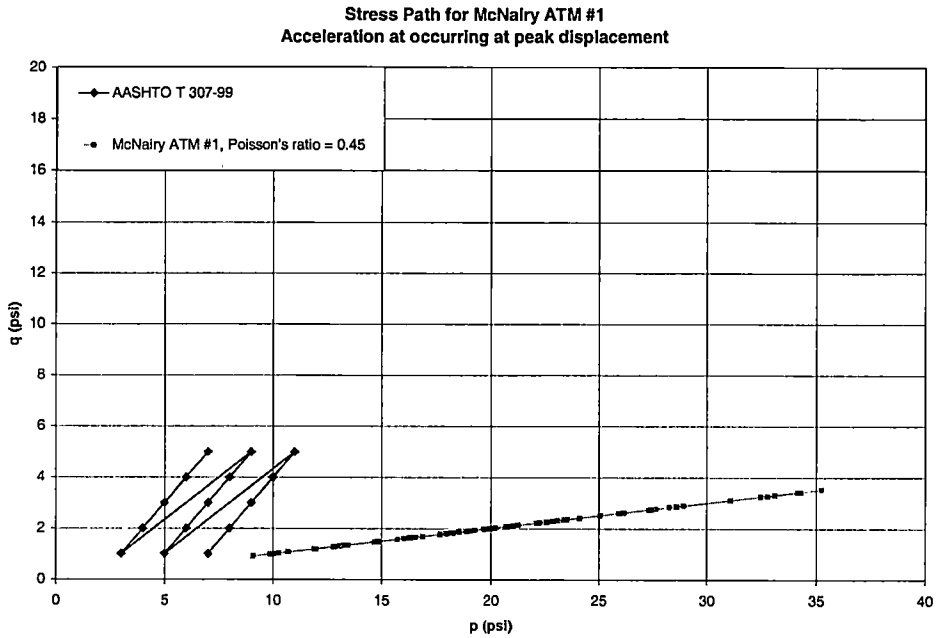

Graph C – 19 Stress Path for –McNairy ATM #1

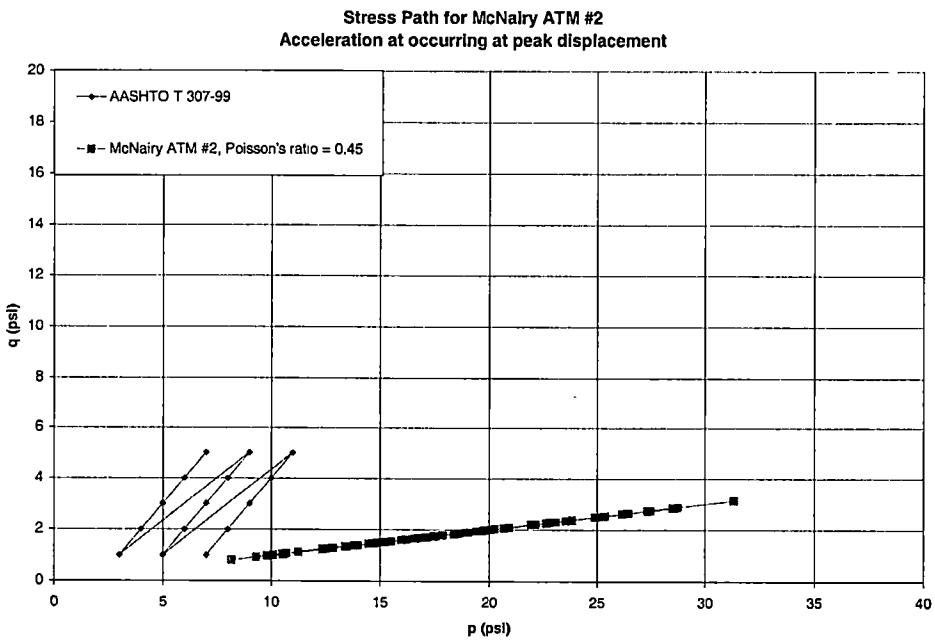

Graph C – 20 Stress Path for McNairy ATM #2

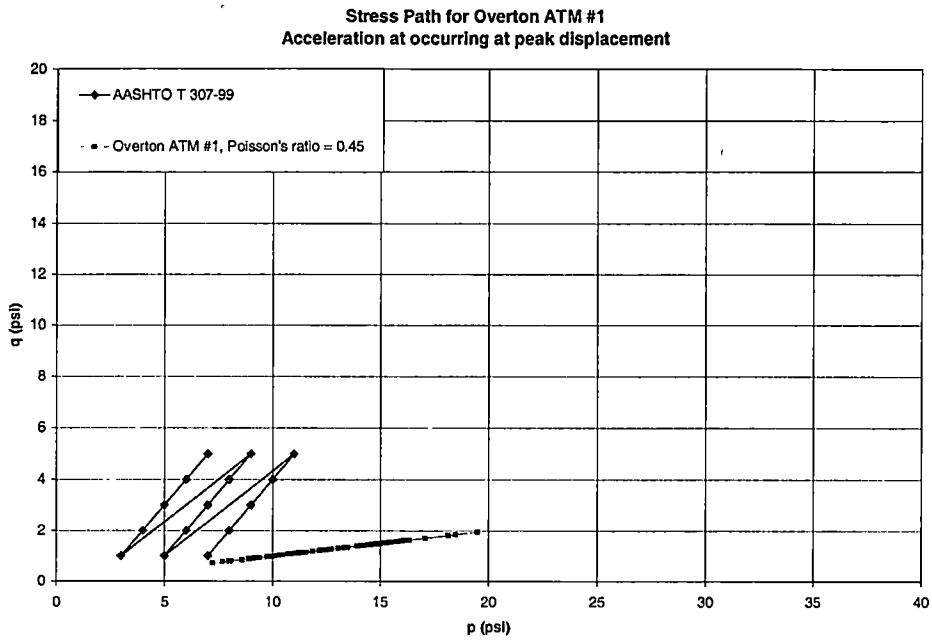

Graph C – 21 Stress Path for Overton ATM #1

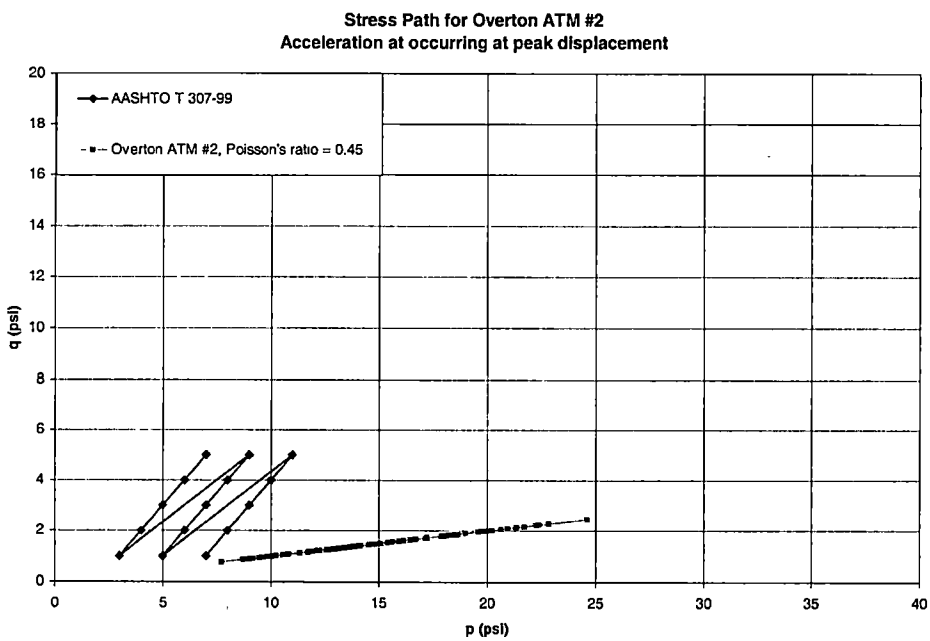

Graph C – 22 Stress Path for Overton ATM #2

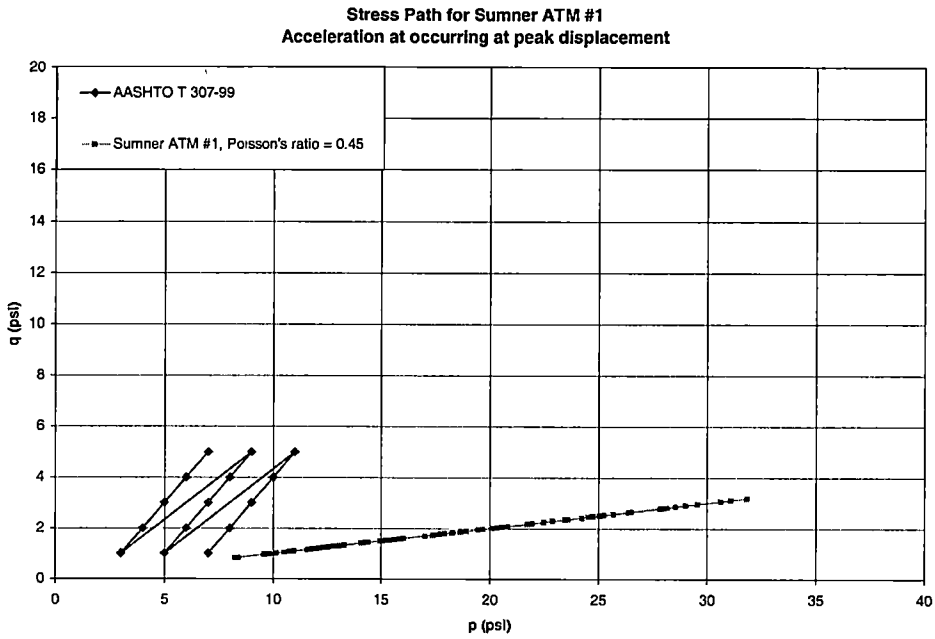

Graph C – 23 Stress Path for Sumner ATM #1

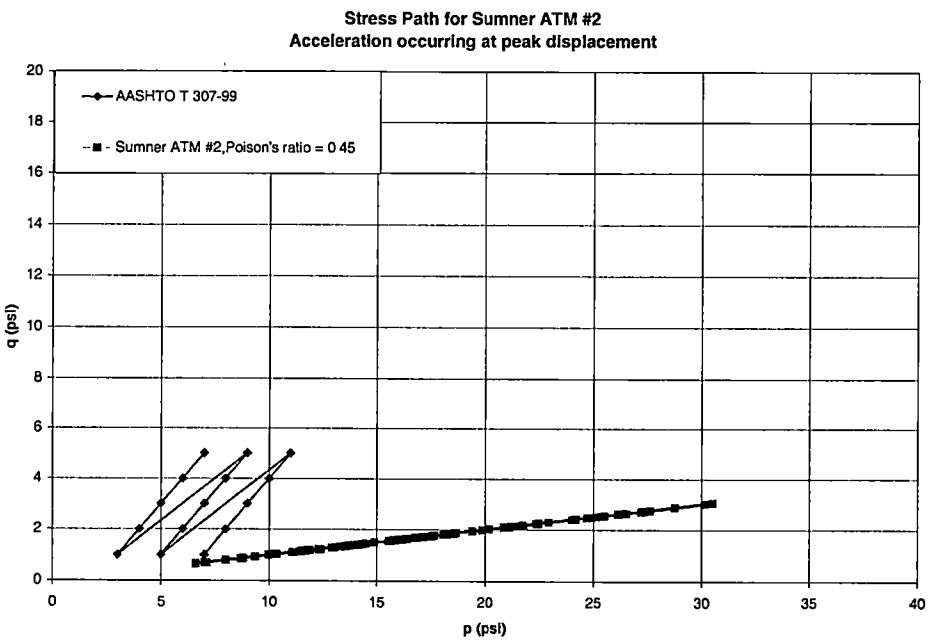

Graph C – 24 Stress Path for Sumner ATM #2

Appendix D MTS Template

MTS Template Introduction

The MTS test template was created in accordance with AASHTO T307-99, Determining the Resilient Modulus of Soils and Aggregate Materials, using TestWare-SX 4.0C. TestWare-SX 4.0C is used in the TestStar II operating system to write the test templates. A copy of the template can be found at the end of Appendix D.

A test template is broken up into 3 components; test procedure, steps, and processes. The test procedure is the actual test that is created from a group of steps. Steps contain the processes that control the test. Steps are a useful way to break up the test in a logical order.

Explanation of Test Template

Descriptions of the test processes can be found in the user's manual. This explanation is not meant to be used to explain setting up a template, but is written to briefly explain why certain steps were set up the way they were and describe problems that occurred along the way.

The first step (sample information) in the resilient modulus template asks the user for some basic information. The operator's name, date, specimen identification number, and specimen location are basic inputs used to identify the particular test at a later time.

The second step (sample check) is an operator event, which allows the operator to make sure that the sample is loaded properly and that the LVDT's have been zeroed out before the testing begins. Zeroing the LVDT's is not essential, since the calculations take the difference between peak and valley measurements as the deformation. If the LVDT's are zeroed, then system is set up to recognize and halt the test if the sample reaches 5

percent axial strain. Again, this is not an important step since the loads applied to the materials tested are small relative to their strength.

The third step (conditioning ramp) is a monotonic command ramp that applies a 5 lb force to the specimen. This ramp serves two purposes. The first is to have a negative force, compression, on the sample before the conditioning cycle begins. It should be noted that a negative sign indicates compression. Tension is positive. This step puts the MTS system in a force control mode. While in force control mode, the system is not affected by confining pressures applied to the sample. For this reason, any forces applied to the sample by the actuator correspond to deviator stresses. It has been observed that when the system was is in displacement control, the confining pressure changes the amount of force on the sample by applying an additional downward pressure.

The fourth step is an operator event (confining pressure check 6 psi). Here the operator is asked to apply a confining cell pressure of 6 psi. It can be observed at this point that the load on the sample does not change.

The fifth step (conditioning cycle) is composed of all the processes associated with the conditioning cycle. Three data limit detectors are placed in this step. A strain detector is applied, since the testing method states that the test must be terminated if the sample reaches 5 percent strain during any part of the test. To monitor the strain a value of -0.41 in. of actuator displacement is used, because this just exceeds the amount of deflection causing 5 percent strain in an 8 in. specimen. This value is relative to the start of the actuator displacement. A detector is set up for LVDT A and B so they will not exceed their capacity of 0.2 in. This value is absolute since they are both zeroed at the

beginning of the test.

Included in the fifth step is a file playback command. This command defines the magnitude and shape of the loading pulse. The file playback command is created in Excel and is saved with an .sfp extension. The file is composed of two haversine segments and a hold segment to model the pulse hold waveform described in the standard procedure. A copy of the conditioning file playback command is shown in List D-1.

It was desired to have the SAC (spectrum amplitude control) activated for the file playback command. The SAC function is an algorithm that monitors the command signal and feedback signal end levels in a table. The difference is monitored by the system and it continuously adjusts the over-programming to make the two coincide. When setting up the test template initially, this is how the SAC function was set up. The first time the test was performed, the "create a new SAC table" button was used. After the first test, the file can then be loaded and saved for following tests. Default table limits are set to the particular loading sequences peak and valley forces. In the case of the conditioning cycle, the upper force limit is -5 lbf and the lower force limit is -50.3 lbf. Applying the table limits optimizes the table for the test. The table limits must be set to exceed both of these end levels, because TestStar does not apply any over-programming to end levels outside the SAC table limits. The error tolerance is set for 2 lbf. This acts as a counter to let the user know how many times the feedback signal falls outside of the table limits. The standard method says that the accuracy of the loading must be plus or minus 2.25 lbf for a specimen with a 3.90 in. diameter. Since the specimens made are 4.0 in., the required accuracy is reduced. Therefore, the 2 lbf is a conservative counter.

As was mentioned above, the SAC function was desired in the test template, but was not used. The SAC function was not used because noise in the force signal made the system work too hard to compensate for the fluctuation in the loading. MTS technical support was contacted about the problem and a service call was made, but they were not able to offer a solution. At this time, the noise is believed to be due to cell pressure. Graph D-1 shows a typical force versus command signal over time. It was observed that the signal is much smoother when there is no confining pressure. The higher the confining pressure, the more noise there is in the signal. Also, as the deviator stress is increased during the test the noise generally increases.

Test sequences 1-5 are set up like the conditioning sequence. Each sequence has its own file playback file. The playback files are shown in Lists D-2 through D-6. The only exception to the setup of the testing sequences to that of the conditioning sequence is that there is data collection added to the sequences. Data is set to collect peak (minimum) and valley (maximum) forces. The valley/peak function is used to capture the valley force point, which is where the maximum displacement of the sample is assumed to occur. The peak is then collected which is where the maximum rebound of the specimen is assumed to occur. The displacement, force, and deformation of both LVDT's are measured. From these data points, the actual applied deviator stress can be calculated along with the recoverable deformation.

After the test is completed, the data collected is saved as a *.dat file. This file is opened up in Excel. The values are copied and pasted into another Excel file that has macros built in to make the necessary calculations and charts.

Shape	Time	Level_Data1
none	sec	lbf
haversine	0.05	-50.3
haversine	0.05	-5
step	0.9	-5

List D - 1 File Playback Command for Conditioning Sequence

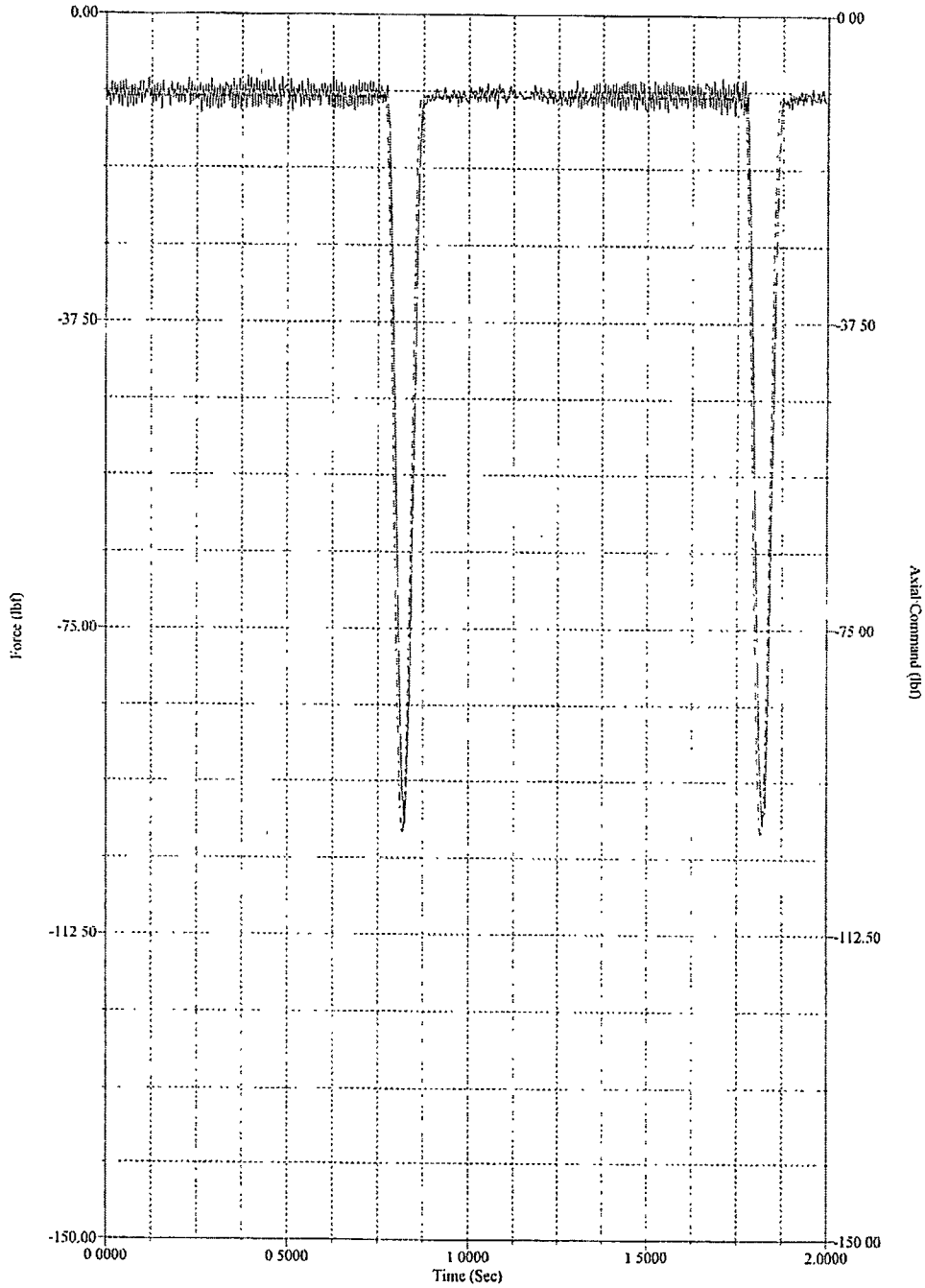

Graph D - 1 Typical Force versus Command Signal for Sequence 4

Shape	Time	Level_Data1
none	sec	lbf
haversine	0.05	-25.1
haversine	0.05	-2.5
step	0.9	-2.5

List D - 2 File Playback Command for Sequences 1, 6, and11

Shape	Time	Level_Data1
none	sec	lbf
haversine	0.05	-50.3
haversine	0.05	-5
step	0.9	-5

List D - 3 File Playback Command for Sequences 2,7, and 12

Shape	Time	Level_Data1
none	sec	lbf
haversine	0.05	-75.4
haversine	0.05	-7.5
step	0.9	-7.5

List - 4 File Playback Command for Sequences 3,8, and 13

Shape	Time	Level_Data1
none	sec	lbf
haversine	0.05	-100.5
haversine	0.05	-10.1
step	0.9	-10.1

List D - 5 File Playback Command for Sequences 4,9, and 14

Shape	Time	Level_Data1
none	sec	lbf
haversine	0.05	-125.7
haversine	0.05	-12.6
step	0.9	-12.6

List D - 6 File Playback Command for Sequences 5,10, and 15

Resilient Modulus Test Template

```
TestWare-SX

Procedure Name    = Resilient Modulus Final1nosac 1.1 Default Procedure
File Specification = D:\TS2\twsx\Resilient Modulus\Resilient Modulus
Final1nosac 1.1.000
Software Version = 4.0C
Printout Date     = 5/21/01 9:29:39 AM

Data File Options
     File Format       = Plain Text File
     Log Events        = Yes
     Include Procedure Description = No

Recovery Options
     Autosave disabled.

Sample Information : Step
     Step Done Trigger 1 = Sample information

     Sample information : Operator Information
          Start Trigger     = Step Start
          End Trigger       = <none>
          Form fields
               Label             = Resilient Modulus AASHTO TP46-94
               Default Entry     =
               Type              = String
               Attribute         = Non-Editable

               Label             = Operator Name
               Default Entry     = Jason Cathey
               Type              = String
               Attribute         = Non-Blank

               Label             = Date
               Default Entry     =
               Type              = String
               Attribute         = Non-Blank

               Label             = Specimen I.D.
               Default Entry     =
               Type              = String
               Attribute         = None

               Label             = Specimen Location
               Default Entry     =
               Type              = String
               Attribute         = Non-Blank


Sample Check : Step
     Step Done Trigger 1 = Check Sample Before Loading Ramp
```

```
     Check Sample Before Loading Ramp : Operator Event
          Start Trigger     = Step Start
          End Trigger       = <none>
          Button ID         = Button 1
          Single Shot       = Yes
          Button Label      = OK
          Description       = Sample loaded and ready for testing.Zero
LVDT's.
          Grab Focus        = Yes


Conditioning Ramp : Step
     Step Done Trigger 1 = Conditioning Ramp

     Conditioning Ramp : Monotonic Command
          Start Trigger     = Step Start
          End Trigger       = <none>
          Segment Shape     = Ramp
          Rate              = 0.9999999 ( lbf/Sec )
          Axial
               Control Mode      = Force  sg
               End level         = -5 ( lbf )


Confining Pressure Check 6 psi : Step
     Step Done Trigger 1 = Set Confining Pressure to 6 psi

     Set Confining Pressure to 6 psi : Operator Event
          Start Trigger     = Step Start
          End Trigger       = <none>
          Button ID         = Button 1
          Single Shot       = Yes
          Button Label      = OK
          Description       = Set Confining Pressure to 6 psi
          Grab Focus        = Yes


Conditioning Cycle : Step
     Step Done Trigger 1 = Conditioning Load

     Strain Detection : Data Limit Detector
          Start Trigger     = Step Start
          End Trigger       = <none>
          Data Channel      = Displacement
          Limit Value       = -0.41 ( in )
          Limit Value is    = Relative
          Detector Options  = Less than Limit Value
          Trigger Option    = Trigger Once

     LVDT A Limit Detector : Data Limit Detector
          Start Trigger     = Step Start
          End Trigger       = <none>
          Data Channel      = LVDT A
          Limit Value       = -0.2 ( in )
```

```
          Limit Value is    = Absolute
          Detector Options = Either Transition
          Trigger Option    = Trigger Once

     LVDT B Limit Detector : Data Limit Detector
          Start Trigger     = Step Start
          End Trigger       = <none>
          Data Channel      = LVDT B
          Limit Value       = -0.2 ( in )
          Limit Value is    = Absolute
          Detector Options = Either Transition
          Trigger Option    = Trigger Once

     Conditioning Load : File Playback Command
          Start Trigger     = Step Start
          End Trigger       = <none>
          File Name...      = D:\TS2\twsx\Resilient Modulus\Resilient
Modulus Sequences\Conditioning.sfp
          Passes            = 1000
          Time Multiplier   = 100 ( % )
          Compensation      = None
          Axial
               Control Mode      = Force  sg
               Level Reference   = 0 ( lbf )
               Level Multiplier = 100 ( % )


Confining Pressure Check 6psi (2) : Step
     Step Done Trigger 1 = Set Confining Pressure to 6 psi

     Set Confining Pressure to 6 psi : Operator Event
          Start Trigger     = Step Start
          End Trigger       = <none>
          Button ID         = Button 1
          Single Shot       = Yes
          Button Label      = OK
          Description       = Set Confining Pressure to 6 psi
          Grab Focus        = Yes


Sequence 1 Ramp : Step
     Step Done Trigger 1 = Sequence 1 Ramp

     Sequence 1 Ramp : Monotonic Command
          Start Trigger     = Step Start
          End Trigger       = <none>
          Segment Shape     = Ramp
          Rate              = 0.5 ( lbf/Sec )
          Axial
               Control Mode      = Force  sg
               End level         = -2.5 ( lbf )


Sequence 1 : Step
```

```
Step Done Trigger 1 = Sequence 1

Strain Detection : Data Limit Detector
     Start Trigger    = Step Start
     End Trigger      = <none>
     Data Channel     = Displacement
     Limit Value      = -0.41 ( in )
     Limit Value is   = Relative
     Detector Options = Less than Limit Value
     Trigger Option   = Trigger Once

LVDT A Limit Detector : Data Limit Detector
     Start Trigger    = Step Start
     End Trigger      = <none>
     Data Channel     = LVDT A
     Limit Value      = -0.2 ( in )
     Limit Value is   = Absolute
     Detector Options = Either Transition
     Trigger Option   = Trigger Once

LVDT B Limit Detector : Data Limit Detector
     Start Trigger    = Step Start
     End Trigger      = <none>
     Data Channel     = LVDT B
     Limit Value      = -0.2 ( in )
     Limit Value is   = Absolute
     Detector Options = Either Transition
     Trigger Option   = Trigger Once

Data Acquistion : Data Acquisition
     Start Trigger    = Step Start
     End Trigger      = Sequence 1
     Mode             = Valley / Peak
     Buffer Type      = Continuous
     Master Channel   = Force
     Slave Channel 1  = Displacement
     Slave Channel 2  = LVDT A
     Slave Channel 3  = LVDT B
     Data Header      = Sequence 1 Data
     Sensitivity      = 10 ( lbf )
     Buffer Size      = 500

Sequence 1 : File Playback Command
     Start Trigger    = Step Start
     End Trigger      = <none>
     File Name...     = D:\TS2\twsx\Resilient Modulus\Resilient
Modulus Sequences\Sequence 1.sfp
     Passes           = 100
     Time Multiplier  = 100 ( % )
     Compensation     = None
     Axial
          Control Mode     = Force  sg
          Level Reference  = 0 ( lbf )
          Level Multiplier = 100 ( % )
```

```
Sequence 2 : Step
     Step Done Trigger 1 = Sequence 2

     Strain Detection : Data Limit Detector
          Start Trigger    = Step Start
          End Trigger      = <none>
          Data Channel     = Displacement
          Limit Value      = -0.41 ( in )
          Limit Value is   = Relative
          Detector Options = Less than Limit Value
          Trigger Option   = Trigger Once

     LVDT A Limit Detector : Data Limit Detector
          Start Trigger    = Step Start
          End Trigger      = <none>
          Data Channel     = LVDT A
          Limit Value      = -0.2 ( in )
          Limit Value is   = Absolute
          Detector Options = Either Transition
          Trigger Option   = Trigger Once

     LVDT B Limit Detector : Data Limit Detector
          Start Trigger    = Step Start
          End Trigger      = <none>
          Data Channel     = LVDT B
          Limit Value      = -0.2 ( in )
          Limit Value is   = Absolute
          Detector Options = Either Transition
          Trigger Option   = Trigger Once

     Data Acquistion : Data Acquisition
          Start Trigger    = Step Start
          End Trigger      = Sequence 2
          Mode             = Valley / Peak
          Buffer Type      = Continuous
          Master Channel   = Force
          Slave Channel 1  = Displacement
          Slave Channel 2  = LVDT A
          Slave Channel 3  = LVDT B
          Data Header      = Sequence 2 Data
          Sensitivity      = 10 ( lbf )
          Buffer Size      = 500

     Sequence 2 : File Playback Command
          Start Trigger    = Step Start
          End Trigger      = <none>
          File Name...     = D:\TS2\twsx\Resilient Modulus\Resilient
Modulus Sequences\Sequence 2.sfp
          Passes           = 100
          Time Multiplier  = 100 ( % )
          Compensation     = None
          Axial
```

```
                Control Mode      = Force  sg
                Level Reference   = 0 ( lbf )
                Level Multiplier = 100 ( % )


Sequence 3 : Step
     Step Done Trigger 1 = Sequence 3

     Strain Detection : Data Limit Detector
          Start Trigger    = Step Start
          End Trigger      = <none>
          Data Channel     = Displacement
          Limit Value      = -0.41 ( in )
          Limit Value is   = Relative
          Detector Options = Less than Limit Value
          Trigger Option   = Trigger Once

     LVDT A Limit Detector : Data Limit Detector
          Start Trigger    = Step Start
          End Trigger      = <none>
          Data Channel     = LVDT A
          Limit Value      = -0.2 ( in )
          Limit Value is   = Absolute
          Detector Options = Either Transition
          Trigger Option   = Trigger Once

     LVDT B Limit Detector : Data Limit Detector
          Start Trigger    = Step Start
          End Trigger      = <none>
          Data Channel     = LVDT B
          Limit Value      = -0.2 ( in )
          Limit Value is   = Absolute
          Detector Options = Either Transition
          Trigger Option   = Trigger Once

     Data Acquistion : Data Acquisition
          Start Trigger    = Step Start
          End Trigger      = Sequence 3
          Mode             = Valley / Peak
          Buffer Type      = Continuous
          Master Channel   = Force
          Slave Channel 1  = Displacement
          Slave Channel 2  = LVDT A
          Slave Channel 3  = LVDT B
          Data Header      = Sequence 3 Data
          Sensitivity      = 10 ( lbf )
          Buffer Size      = 500

     Sequence 3 : File Playback Command
          Start Trigger    = Step Start
          End Trigger      = <none>
          File Name...     = D:\TS2\twsx\Resilient Modulus\Resilient
Modulus Sequences\Sequence 3.sfp
          Passes           = 100
```

```
          Time Multiplier  = 100 ( % )
          Compensation     = None
          Axial
               Control Mode     = Force  sg
               Level Reference  = 0 ( lbf )
               Level Multiplier = 100 ( % )


Sequence 4 : Step
     Step Done Trigger 1 = Sequence 4

     Strain Detection : Data Limit Detector
          Start Trigger    = Step Start
          End Trigger      = <none>
          Data Channel     = Displacement
          Limit Value      = -0.41 ( in )
          Limit Value is   = Relative
          Detector Options = Less than Limit Value
          Trigger Option   = Trigger Once

     LVDT A Limit Detector : Data Limit Detector
          Start Trigger    = Step Start
          End Trigger      = <none>
          Data Channel     = LVDT A
          Limit Value      = -0.2 ( in )
          Limit Value is   = Absolute
          Detector Options = Either Transition
          Trigger Option   = Trigger Once

     LVDT B Limit Detector : Data Limit Detector
          Start Trigger    = Step Start
          End Trigger      = <none>
          Data Channel     = LVDT B
          Limit Value      = -0.2 ( in )
          Limit Value is   = Absolute
          Detector Options = Either Transition
          Trigger Option   = Trigger Once

     Data Acquistion : Data Acquisition
          Start Trigger    = Step Start
          End Trigger      = Sequence 4
          Mode             = Valley / Peak
          Buffer Type      = Continuous
          Master Channel   = Force
          Slave Channel 1  = Displacement
          Slave Channel 2  = LVDT A
          Slave Channel 3  = LVDT B
          Data Header      = Sequence 4 Data
          Sensitivity      = 10 ( lbf )
          Buffer Size      = 500

     Sequence 4 : File Playback Command
          Start Trigger    = Step Start
          End Trigger      = <none>
```

```
          File Name...      = D:\TS2\twsx\Resilient Modulus\Resilient
Modulus Sequences\Sequence 4.sfp
          Passes            = 100
          Time Multiplier   = 100 ( % )
          Compensation      = None
          Axial
               Control Mode      = Force  sg
               Level Reference   = 0 ( lbf )
               Level Multiplier  = 100 ( % )


Sequence 5 : Step
     Step Done Trigger 1 = Sequence 5

     Strain Detection : Data Limit Detector
          Start Trigger     = Step Start
          End Trigger       = <none>
          Data Channel      = Displacement
          Limit Value       = -0.41 ( in )
          Limit Value is    = Relative
          Detector Options  = Less than Limit Value
          Trigger Option    = Trigger Once

     LVDT A Limit Detector : Data Limit Detector
          Start Trigger     = Step Start
          End Trigger       = <none>
          Data Channel      = LVDT A
          Limit Value       = -0.2 ( in )
          Limit Value is    = Absolute
          Detector Options  = Either Transition
          Trigger Option    = Trigger Once

     LVDT B Limit Detector : Data Limit Detector
          Start Trigger     = Step Start
          End Trigger       = <none>
          Data Channel      = LVDT B
          Limit Value       = -0.2 ( in )
          Limit Value is    = Absolute
          Detector Options  = Either Transition
          Trigger Option    = Trigger Once

     Data Acquistion : Data Acquisition
          Start Trigger     = Step Start
          End Trigger       = Sequence 5
          Mode              = Valley / Peak
          Buffer Type       = Continuous
          Master Channel    = Force
          Slave Channel 1   = Displacement
          Slave Channel 2   = LVDT A
          Slave Channel 3   = LVDT B
          Data Header       = Sequence 5 Data
          Sensitivity       = 10 ( lbf )
          Buffer Size       = 500
```

```
     Sequence 5 : File Playback Command
          Start Trigger    = Step Start
          End Trigger      = <none>
          File Name...     = D:\TS2\twsx\Resilient Modulus\Resilient
Modulus Sequences\Sequence 5.sfp
          Passes           = 100
          Time Multiplier  = 100 ( % )
          Compensation     = None
          Axial
               Control Mode     = Force  sg
               Level Reference  = 0 ( lbf )
               Level Multiplier = 100 ( % )


Confining Pressure Check 4 psi : Step
     Step Done Trigger 1 = Set Confining Pressure to 4 psi

     Set Confining Pressure to 4 psi : Operator Event
          Start Trigger    = Step Start
          End Trigger      = <none>
          Button ID        = Button 1
          Single Shot      = Yes
          Button Label     = OK
          Description      = Set Confining Pressure to 4 psi
          Grab Focus       = Yes


Sequence 6 Ramp : Step
     Step Done Trigger 1 = Sequence 6 Ramp

     Sequence 6 Ramp : Monotonic Command
          Start Trigger    = Step Start
          End Trigger      = <none>
          Segment Shape    = Ramp
          Rate             = 0.5 ( lbf/Sec )
          Axial
               Control Mode     = Force  sg
               End level        = -2.5 ( lbf )


Sequence 6 : Step
     Step Done Trigger 1 = Sequence 6

     Strain Detection : Data Limit Detector
          Start Trigger    = Step Start
          End Trigger      = <none>
          Data Channel     = Displacement
          Limit Value      = -0.41 ( in )
          Limit Value is   = Relative
          Detector Options = Less than Limit Value
          Trigger Option   = Trigger Once

     LVDT A Limit Detector : Data Limit Detector
          Start Trigger    = Step Start
```

```
          End Trigger       = <none>
          Data Channel      = LVDT A
          Limit Value       = -0.2 ( in )
          Limit Value is    = Absolute
          Detector Options  = Either Transition
          Trigger Option    = Trigger Once

     LVDT B Limit Detector : Data Limit Detector
          Start Trigger     = Step Start
          End Trigger       = <none>
          Data Channel      = LVDT B
          Limit Value       = -0.2 ( in )
          Limit Value is    = Absolute
          Detector Options  = Either Transition
          Trigger Option    = Trigger Once

     Data Acquistion : Data Acquisition
          Start Trigger     = Step Start
          End Trigger       = Sequence 6
          Mode              = Valley / Peak
          Buffer Type       = Continuous
          Master Channel    = Force
          Slave Channel 1   = Displacement
          Slave Channel 2   = LVDT A
          Slave Channel 3   = LVDT B
          Data Header       = Sequence 6 Data
          Sensitivity       = 10 ( lbf )
          Buffer Size       = 500

     Sequence 6 : File Playback Command
          Start Trigger     = Step Start
          End Trigger       = <none>
          File Name...      = D:\TS2\twsx\Resilient Modulus\Resilient
Modulus Sequences\Sequence 6.sfp
          Passes            = 100
          Time Multiplier   = 100 ( % )
          Compensation      = None
          Axial
               Control Mode      = Force  sg
               Level Reference   = 0 ( lbf )
               Level Multiplier  = 100 ( % )


Sequence 7 : Step
     Step Done Trigger 1 = Sequence 7

     Strain Detection : Data Limit Detector
          Start Trigger     = Step Start
          End Trigger       = <none>
          Data Channel      = Displacement
          Limit Value       = -0.41 ( in )
          Limit Value is    = Relative
          Detector Options  = Less than Limit Value
          Trigger Option    = Trigger Once
```

```
     LVDT A Limit Detector : Data Limit Detector
          Start Trigger    = Step Start
          End Trigger      = <none>
          Data Channel     = LVDT A
          Limit Value      = -0.2 ( in )
          Limit Value is   = Absolute
          Detector Options = Either Transition
          Trigger Option   = Trigger Once

     LVDT B Limit Detector : Data Limit Detector
          Start Trigger    = Step Start
          End Trigger      = <none>
          Data Channel     = LVDT B
          Limit Value      = -0.2 ( in )
          Limit Value is   = Absolute
          Detector Options = Either Transition
          Trigger Option   = Trigger Once

     Data Acquistion : Data Acquisition
          Start Trigger    = Step Start
          End Trigger      = Sequence 7
          Mode             = Valley / Peak
          Buffer Type      = Continuous
          Master Channel   = Force
          Slave Channel 1  = Displacement
          Slave Channel 2  = LVDT A
          Slave Channel 3  = LVDT B
          Data Header      = Sequence 7 Data
          Sensitivity      = 10 ( lbf )
          Buffer Size      = 500

     Sequence 7 : File Playback Command
          Start Trigger    = Step Start
          End Trigger      = <none>
          File Name...     = D:\TS2\twsx\Resilient Modulus\Resilient
Modulus Sequences\Sequence 7.sfp
          Passes           = 100
          Time Multiplier  = 100 ( % )
          Compensation     = None
          Axial
               Control Mode     = Force  sg
               Level Reference  = 0 ( lbf )
               Level Multiplier = 100 ( % )


Sequence 8 : Step
     Step Done Trigger 1 = Sequence 8

     Strain Detection : Data Limit Detector
          Start Trigger    = Step Start
          End Trigger      = <none>
          Data Channel     = Displacement
          Limit Value      = -0.41 ( in )
```

```
          Limit Value is    = Relative
          Detector Options = Less than Limit Value
          Trigger Option    = Trigger Once

     LVDT A Limit Detector : Data Limit Detector
          Start Trigger     = Step Start
          End Trigger       = <none>
          Data Channel      = LVDT A
          Limit Value       = -0.2 ( in )
          Limit Value is    = Absolute
          Detector Options = Either Transition
          Trigger Option    = Trigger Once

     LVDT B Limit Detector : Data Limit Detector
          Start Trigger     = Step Start
          End Trigger       = <none>
          Data Channel      = LVDT B
          Limit Value       = -0.2 ( in )
          Limit Value is    = Absolute
          Detector Options = Either Transition
          Trigger Option    = Trigger Once

     Data Acquistion : Data Acquisition
          Start Trigger     = Step Start
          End Trigger       = Sequence 8
          Mode              = Valley / Peak
          Buffer Type       = Continuous
          Master Channel    = Force
          Slave Channel 1   = Displacement
          Slave Channel 2   = LVDT A
          Slave Channel 3   = LVDT B
          Data Header       = Sequence 8 Data
          Sensitivity       = 10 ( lbf )
          Buffer Size       = 500

     Sequence 8 : File Playback Command
          Start Trigger     = Step Start
          End Trigger       = <none>
          File Name...      = D:\TS2\twsx\Resilient Modulus\Resilient
Modulus Sequences\Sequence 8.sfp
          Passes            = 100
          Time Multiplier   = 100 ( % )
          Compensation      = None
          Axial
               Control Mode      = Force  sg
               Level Reference   = 0 ( lbf )
               Level Multiplier = 100 ( % )


Sequence 9 : Step
     Step Done Trigger 1 = Sequence 9

     Strain Detection : Data Limit Detector
          Start Trigger     = Step Start
```

```
          End Trigger       = <none>
          Data Channel      = Displacement
          Limit Value       = -0.41 ( in )
          Limit Value is    = Relative
          Detector Options = Less than Limit Value
          Trigger Option    = Trigger Once

     LVDT A Limit Detector : Data Limit Detector
          Start Trigger     = Step Start
          End Trigger       = <none>
          Data Channel      = LVDT A
          Limit Value       = -0.2 ( in )
          Limit Value is    = Absolute
          Detector Options = Either Transition
          Trigger Option    = Trigger Once

     LVDT B Limit Detector : Data Limit Detector
          Start Trigger     = Step Start
          End Trigger       = <none>
          Data Channel      = LVDT B
          Limit Value       = -0.2 ( in )
          Limit Value is    = Absolute
          Detector Options = Either Transition
          Trigger Option    = Trigger Once

     Data Acquistion : Data Acquisition
          Start Trigger     = Step Start
          End Trigger       = Sequence 9
          Mode              = Valley / Peak
          Buffer Type       = Continuous
          Master Channel    = Force
          Slave Channel 1   = Displacement
          Slave Channel 2   = LVDT A
          Slave Channel 3   = LVDT B
          Data Header       = Sequence 9 Data
          Sensitivity       = 10 ( lbf )
          Buffer Size       = 500

     Sequence 9 : File Playback Command
          Start Trigger     = Step Start
          End Trigger       = <none>
          File Name...      = D:\TS2\twsx\Resilient Modulus\Resilient
Modulus Sequences\Sequence 9.sfp
          Passes            = 100
          Time Multiplier   = 100 ( % )
          Compensation      = None
          Axial
               Control Mode      = Force  sg
               Level Reference   = 0 ( lbf )
               Level Multiplier = 100 ( % )


Sequence 10 : Step
     Step Done Trigger 1 = Sequence 10
```

```
Strain Detection : Data Limit Detector
     Start Trigger    = Step Start
     End Trigger      = <none>
     Data Channel     = Displacement
     Limit Value      = -0.41 ( in )
     Limit Value is   = Relative
     Detector Options = Less than Limit Value
     Trigger Option   = Trigger Once

LVDT A Limit Detector : Data Limit Detector
     Start Trigger    = Step Start
     End Trigger      = <none>
     Data Channel     = LVDT A
     Limit Value      = -0.2 ( in )
     Limit Value is   = Absolute
     Detector Options = Either Transition
     Trigger Option   = Trigger Once

LVDT B Limit Detector : Data Limit Detector
     Start Trigger    = Step Start
     End Trigger      = <none>
     Data Channel     = LVDT B
     Limit Value      = -0.2 ( in )
     Limit Value is   = Absolute
     Detector Options = Either Transition
     Trigger Option   = Trigger Once

Data Acquistion : Data Acquisition
     Start Trigger    = Step Start
     End Trigger      = Sequence 10
     Mode             = Valley / Peak
     Buffer Type      = Continuous
     Master Channel   = Force
     Slave Channel 1  = Displacement
     Slave Channel 2  = LVDT A
     Slave Channel 3  = LVDT B
     Data Header      = Sequence 10 Data
     Sensitivity      = 10 ( lbf )
     Buffer Size      = 500

Sequence 10 : File Playback Command
     Start Trigger    = Step Start
     End Trigger      = <none>
     File Name...     = D:\TS2\twsx\Resilient Modulus\Resilient
Modulus Sequences\Sequence 10.sfp
     Passes           = 100
     Time Multiplier  = 100 ( % )
     Compensation     = None
     Axial
          Control Mode     = Force  sg
          Level Reference  = 0 ( lbf )
          Level Multiplier = 100 ( % )
```

```
Confining Pressure Check 2 psi : Step
     Step Done Trigger 1 = Set Confining Pressure to 2 psi

     Set Confining Pressure to 2 psi : Operator Event
          Start Trigger    = Step Start
          End Trigger      = <none>
          Button ID        = Button 1
          Single Shot      = Yes
          Button Label     = OK
          Description      = Set Confining Pressure to 2 psi
          Grab Focus       = Yes


Sequence 11 Ramp : Step
     Step Done Trigger 1 = Sequence 11 Ramp

     Sequence 11 Ramp : Monotonic Command
          Start Trigger    = Step Start
          End Trigger      = <none>
          Segment Shape    = Ramp
          Rate             = 0.5 ( lbf/Sec )
          Axial
               Control Mode     = Force  sg
               End level        = -2.5 ( lbf )


Sequence 11 : Step
     Step Done Trigger 1 = Sequence 11

     Strain Detection : Data Limit Detector
          Start Trigger    = Step Start
          End Trigger      = <none>
          Data Channel     = Displacement
          Limit Value      = -0.41 ( in )
          Limit Value is   = Relative
          Detector Options = Less than Limit Value
          Trigger Option   = Trigger Once

     LVDT A Limit Detector : Data Limit Detector
          Start Trigger    = Step Start
          End Trigger      = <none>
          Data Channel     = LVDT A
          Limit Value      = -0.2 ( in )
          Limit Value is   = Absolute
          Detector Options = Either Transition
          Trigger Option   = Trigger Once

     LVDT B Limit Detector : Data Limit Detector
          Start Trigger    = Step Start
          End Trigger      = <none>
          Data Channel     = LVDT B
          Limit Value      = -0.2 ( in )
          Limit Value is   = Absolute
```

```
          Detector Options = Either Transition
          Trigger Option   = Trigger Once

     Data Acquistion : Data Acquisition
          Start Trigger    = Step Start
          End Trigger      = Sequence 11
          Mode             = Valley / Peak
          Buffer Type      = Continuous
          Master Channel   = Force
          Slave Channel 1  = Displacement
          Slave Channel 2  = LVDT A
          Slave Channel 3  = LVDT B
          Data Header      = Sequence 11 Data
          Sensitivity      = 10 ( lbf )
          Buffer Size      = 500

     Sequence 11 : File Playback Command
          Start Trigger    = Step Start
          End Trigger      = <none>
          File Name...     = D:\TS2\twsx\Resilient Modulus\Resilient
Modulus Sequences\Sequence 11.sfp
          Passes           = 100
          Time Multiplier  = 100 ( % )
          Compensation     = None
          Axial
               Control Mode     = Force  sg
               Level Reference  = 0 ( lbf )
               Level Multiplier = 100 ( % )


Sequence 12 : Step
     Step Done Trigger 1 = Sequence 12

     Strain Detection : Data Limit Detector
          Start Trigger    = Step Start
          End Trigger      = <none>
          Data Channel     = Displacement
          Limit Value      = -0.41 ( in )
          Limit Value is   = Relative
          Detector Options = Less than Limit Value
          Trigger Option   = Trigger Once

     LVDT A Limit Detector : Data Limit Detector
          Start Trigger    = Step Start
          End Trigger      = <none>
          Data Channel     = LVDT A
          Limit Value      = -0.2 ( in )
          Limit Value is   = Absolute
          Detector Options = Either Transition
          Trigger Option   = Trigger Once

     LVDT B Limit Detector : Data Limit Detector
          Start Trigger    = Step Start
          End Trigger      = <none>
```

```
          Data Channel      = LVDT B
          Limit Value       = -0.2 ( in )
          Limit Value is    = Absolute
          Detector Options  = Either Transition
          Trigger Option    = Trigger Once

     Data Acquistion : Data Acquisition
          Start Trigger     = Step Start
          End Trigger       = Sequence 12
          Mode              = Valley / Peak
          Buffer Type       = Continuous
          Master Channel    = Force
          Slave Channel 1   = Displacement
          Slave Channel 2   = LVDT A
          Slave Channel 3   = LVDT B
          Data Header       = Sequence 12 Data
          Sensitivity       = 10 ( lbf )
          Buffer Size       = 500

     Sequence 12 : File Playback Command
          Start Trigger     = Step Start
          End Trigger       = <none>
          File Name...      = D:\TS2\twsx\Resilient Modulus\Resilient
Modulus Sequences\Sequence 12.sfp
          Passes            = 100
          Time Multiplier   = 100 ( % )
          Compensation      = None
          Axial
               Control Mode      = Force  sg
               Level Reference   = 0 ( lbf )
               Level Multiplier  = 100 ( % )


Sequence 13 : Step
     Step Done Trigger 1 = Sequence 13

     Strain Detection : Data Limit Detector
          Start Trigger     = Step Start
          End Trigger       = <none>
          Data Channel      = Displacement
          Limit Value       = -0.41 ( in )
          Limit Value is    = Relative
          Detector Options  = Less than Limit Value
          Trigger Option    = Trigger Once

     LVDT A Limit Detector : Data Limit Detector
          Start Trigger     = Step Start
          End Trigger       = <none>
          Data Channel      = LVDT A
          Limit Value       = -0.2 ( in )
          Limit Value is    = Absolute
          Detector Options  = Either Transition
          Trigger Option    = Trigger Once
```

```
     LVDT B Limit Detector : Data Limit Detector
          Start Trigger    = Step Start
          End Trigger      = <none>
          Data Channel     = LVDT B
          Limit Value      = -0.2 ( in )
          Limit Value is   = Absolute
          Detector Options = Either Transition
          Trigger Option   = Trigger Once

     Data Acquistion : Data Acquisition
          Start Trigger    = Step Start
          End Trigger      = Sequence 13
          Mode             = Valley / Peak
          Buffer Type      = Continuous
          Master Channel   = Force
          Slave Channel 1  = Displacement
          Slave Channel 2  = LVDT A
          Slave Channel 3  = LVDT B
          Data Header      = Sequence 13 Data
          Sensitivity      = 10 ( lbf )
          Buffer Size      = 500

     Sequence 13 : File Playback Command
          Start Trigger    = Step Start
          End Trigger      = <none>
          File Name...     = D:\TS2\twsx\Resilient Modulus\Resilient
Modulus Sequences\Sequence 13.sfp
          Passes           = 100
          Time Multiplier  = 100 ( % )
          Compensation     = None
          Axial
               Control Mode     = Force  sg
               Level Reference  = 0 ( lbf )
               Level Multiplier = 100 ( % )


Sequence 14 : Step
     Step Done Trigger 1 = Sequence 14

     Strain Detection : Data Limit Detector
          Start Trigger    = Step Start
          End Trigger      = <none>
          Data Channel     = Displacement
          Limit Value      = -0.41 ( in )
          Limit Value is   = Relative
          Detector Options = Less than Limit Value
          Trigger Option   = Trigger Once

     LVDT A Limit Detector : Data Limit Detector
          Start Trigger    = Step Start
          End Trigger      = <none>
          Data Channel     = LVDT A
          Limit Value      = -0.2 ( in )
          Limit Value is   = Absolute
```

```
          Detector Options = Either Transition
          Trigger Option   = Trigger Once

     LVDT B Limit Detector : Data Limit Detector
          Start Trigger    = Step Start
          End Trigger      = <none>
          Data Channel     = LVDT B
          Limit Value      = -0.2 ( in )
          Limit Value is   = Absolute
          Detector Options = Either Transition
          Trigger Option   = Trigger Once

     Data Acquistion : Data Acquisition
          Start Trigger    = Step Start
          End Trigger      = Sequence 14
          Mode             = Valley / Peak
          Buffer Type      = Continuous
          Master Channel   = Force
          Slave Channel 1  = Displacement
          Slave Channel 2  = LVDT A
          Slave Channel 3  = LVDT B
          Data Header      = Sequence 14 Data
          Sensitivity      = 10 ( lbf )
          Buffer Size      = 500

     Sequence 14 : File Playback Command
          Start Trigger    = Step Start
          End Trigger      = <none>
          File Name...     = D:\TS2\twsx\Resilient Modulus\Resilient
Modulus Sequences\Sequence 14.sfp
          Passes           = 100
          Time Multiplier  = 100 ( % )
          Compensation     = None
          Axial
               Control Mode     = Force  sg
               Level Reference  = 0 ( lbf )
               Level Multiplier = 100 ( % )


Sequence 15 : Step
     Step Done Trigger 1 = Sequence 15

     Strain Detection : Data Limit Detector
          Start Trigger    = Step Start
          End Trigger      = <none>
          Data Channel     = Displacement
          Limit Value      = -0.41 ( in )
          Limit Value is   = Relative
          Detector Options = Less than Limit Value
          Trigger Option   = Trigger Once

     LVDT A Limit Detector : Data Limit Detector
          Start Trigger    = Step Start
          End Trigger      = <none>
```

```
          Data Channel      = LVDT A
          Limit Value       = -0.2 ( in )
          Limit Value is    = Absolute
          Detector Options = Either Transition
          Trigger Option    = Trigger Once

     LVDT B Limit Detector : Data Limit Detector
          Start Trigger     = Step Start
          End Trigger       = <none>
          Data Channel      = LVDT B
          Limit Value       = -0.2 ( in )
          Limit Value is    = Absolute
          Detector Options = Either Transition
          Trigger Option    = Trigger Once

     Data Acquistion : Data Acquisition
          Start Trigger     = Step Start
          End Trigger       = Sequence 15
          Mode              = Valley / Peak
          Buffer Type       = Continuous
          Master Channel    = Force
          Slave Channel 1   = Displacement
          Slave Channel 2   = LVDT A
          Slave Channel 3   = LVDT B
          Data Header       = Sequence 15 Data
          Sensitivity       = 10 ( lbf )
          Buffer Size       = 500

     Sequence 15 : File Playback Command
          Start Trigger     = Step Start
          End Trigger       = <none>
          File Name...      = D:\TS2\twsx\Resilient Modulus\Resilient
Modulus Sequences\Sequence 15.sfp
          Passes            = 100
          Time Multiplier   = 100 ( % )
          Compensation      = None
          Axial
               Control Mode      = Force  sg
               Level Reference   = 0 ( lbf )
               Level Multiplier = 100 ( % )
```

1

Appendix E ATM Derivation

Idealized Model for the ATM

The resilient modulus of a soil can be calculated by analyzing the ATM as a single degree of freedom (SDOF) mass-spring model as shown in Graphic E-1. To calculate the resilient modulus from the data gathered by the ATM, several simplifying assumptions must be made for the model to work (Li 1992, Drumm, et al. 1996).

1. The base of the sample is a rigid, fixed boundary.
2. Friction between the sample and cylinder wall can be neglected.
3. Displacement, velocity, and acceleration in the soil sample are distributed linearly along the height of the sample, from maximum at the top to zero at the bottom.
4. The falling weight load is applied by a rigid block of circular cross section of the same diameter as the soil specimen with mass, m_o, and drop height, h_o. The hammer can be assumed to be rigid with respect to the soil because the modulus of the aluminum used in the hammer is about 100 times greater than that of soil.
5. The total mass of the spring system is $m = m_o + F_m m_1$, where m_1 is the mass of the soil and F_m is the mass participation factor of the soil. From previous work with the ATM, F_m has been assumed to be 0.5.
6. A spring with vertical stiffness, k, and an equivalent lumped mass, $F_m m_1$, represents the soil.

Newton's law is used to set up the differential equation which describes the motion of the weight (Wylie 1979):

$$\sum F = ma \qquad \text{(E1)}$$

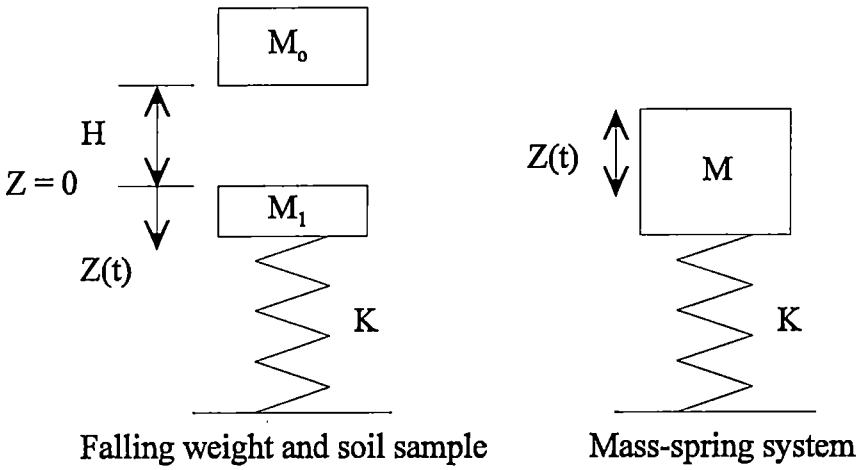

Graphic E-1 ATM SDOF Mass-Spring Model

The mass, m, of the weight is:

$$m = \frac{w}{g} \tag{E-2}$$

where

$\sum F$ = summation of forces

a = acceleration

w = weight

g= acceleration due to gravity

The spring is assumed to obey Hooke's Law, which is states that force is proportional to displacement:

$$F = kh_o \tag{E-3}$$

where

k = spring modulus

h_o = initial displacement of the spring

In equilibrium, the weight of the object is the force that stretches the spring (Graphic E-2). Equation E-3 can be written as:

$$w = kh_o \tag{E-4a}$$

or

$$h_o = \frac{w}{k} \tag{E-4b}$$

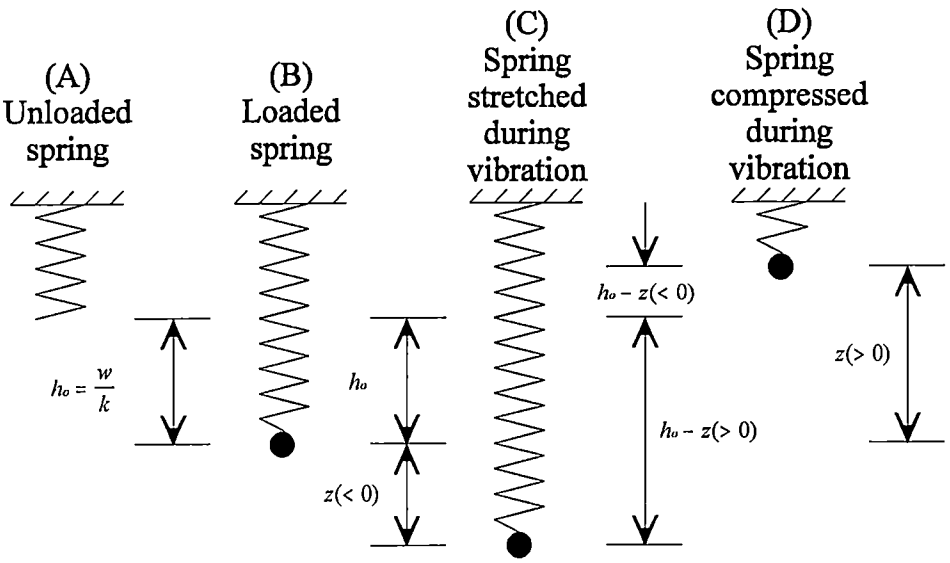

Graphic E-2 Simple Mass-Spring System

When the weight is set in motion, it moves in a vertical direction. When $z = h_o$, the system in equilibrium. The spring is therefore in the neutral starting position and the force exerted by the spring is zero. When the spring is moved from its equilibrium position, either up or down, the change in the spring length is $h_o - z$. Therefore the force of the spring at any position can be expressed as:

$$F_{sp} = k(h_o - z) \qquad \text{(E-5)}$$

Now using Newton's law the equation describing the motion can be written as (Wylie 1979):

$$\frac{w}{g}\frac{d^2z(t)}{dt^2} = F_{sp} + F_{fr} + F_{im} + F_{gr} = k(h_o - z) - c\frac{dz(t)}{dt} + F_o \cos \varpi t - w \qquad \text{(E-6)}$$

where

a = acceleration due to gravity = $\dfrac{d^2z(t)}{dt^2}$

F_{sp} = force the spring exerts on the weight

F_{fr} = force of friction

F_{im} = impressed forces from external sources

F_{gr} = force of gravity

By substituting the Equation E-4b into Equation E-6, the kh_o cancel out the -w, leaving:

$$\frac{w}{g}\frac{d^2z(t)}{dt^2} = -kz - c\frac{dz(t)}{dt} + F\cos\omega t \qquad \text{(E-7)}$$

Rearrange equation E-7:

$$\frac{w}{g}\frac{d^2z(t)}{dt^2} + c\frac{dz(t)}{dt} + kz = F\cos\omega t \qquad \text{(E-8)}$$

The idealized model for the ATM assumes free motion with no damping. Therefore the friction term and impressed force term can be removed from Equation E-8:

$$\frac{w}{g}\frac{d^2z(t)}{dt^2} + ky = 0 \qquad \text{(E-9)}$$

Multiply Equation E-9 by $\frac{g}{w}$:

$$\frac{d^2z(t)}{dt^2} + \frac{kg}{w}y = 0 \qquad \text{(E-10)}$$

The generalized solution for Equation E-10 can be found in most textbooks on differential equations and is as follows:

$$z(t) = A\cos\sqrt{\frac{kg}{w}}t + B\sin\sqrt{\frac{kg}{w}}t \qquad \text{(E-11)}$$

Substituting the undamped natural frequency, ω, as a constant into the equation aids in the rest of the derivation (Das 1993):

$$\omega = \sqrt{\frac{kg}{w}} = \sqrt{\frac{k}{m}} \tag{E-12}$$

$$z(t) = A\cos\omega t + B\sin\omega t \tag{E-13}$$

The initial conditions of the system are the initial static displacement and the initial velocity of the hammer after it collides with the spring at time t = 0:

$$z(0) = h_o = \frac{w}{k} \tag{E-14}$$

and

$$\left[\frac{dz(t)}{dt}\right]_{t=0} = v_1 \tag{E-15}$$

Solve Equation E-13 by using the initial conditions:

$$z(0) = A\cos\omega(0) + B\sin\omega(0) = \frac{mg}{k} \tag{E-16}$$

$$A = \frac{mg}{k} \tag{E-17}$$

The first derivative of Equation E-13 is the velocity:

$$\frac{dz(t)}{dt} = -A\omega\sin\omega t + B\omega\cos\omega t \tag{E-18}$$

$$\frac{dz(0)}{dt} = -A\omega \sin\omega(0) + B\omega \cos\omega(0) = v_1 \tag{E-19}$$

$$B = \frac{v_1}{\omega} = \frac{v_1}{\sqrt{\frac{k}{m}}} = v_1\sqrt{\frac{m}{k}} \tag{E-20}$$

Substituting Equations E-17 and E-20 into Equation E-13 and its derivatives, the final equations for displacement, velocity, and acceleration are found:

(Displacement)

$$z(t) = \frac{mg}{k}\cos\omega t + v_1\sqrt{\frac{m}{k}}\sin\omega t = h_o \cos\omega t + v_1\sqrt{\frac{m}{k}}\sin\omega t \tag{E-21}$$

(Velocity)

$$\frac{dz(t)}{dt} = -g\sqrt{\frac{m}{k}}\sin\omega t + v_1 \cos\omega t \tag{E-22}$$

(Acceleration)

$$\frac{d^2z(t)}{dt^2} = -g\cos\omega t - v_1\sqrt{\frac{k}{m}}\sin\omega t \tag{E-23}$$

In the work done by Li (1992), the initial velocity was defined as the velocity of the free falling hammer without energy losses:

$$v_1 = \sqrt{2gh} \tag{E-24}$$

where

h = drop height of the hammer

Substituting Equation E-24 into Equation E-21:

$$z(t) = h_o \cos\omega t + \sqrt{\frac{2ghm}{k}} \sin\omega t \tag{E-25}$$

If inertia is not considered, and h is the initial drop height of the sample. When h_o is much less than h ($h_o < h/5000$), the first term in Equation E-21 is less than 1/100 of the second term. Therefore, the first term of the equation can be cancelled out (Li 1992). The acceleration can then be written as:

$$\frac{d^2z(t)}{dt^2} = -v_1\sqrt{\frac{k}{m}} \sin\omega t \tag{E-26}$$

The maximum acceleration occurs when the sin(ωt) term equals one. The equation for the maximum acceleration is then:

$$A_p = \max\left[\frac{d^2z(t)}{dt^2}\right] = -v_1\sqrt{\frac{k}{m}} \tag{E-27}$$

where

A_p = the peak acceleration (or peak deceleration)

From the law of the conservation of energy, the initial velocity before impact, v_o, must equal the velocity just after the hammer impacts the soil, v_1:

$$\frac{1}{2}m_o v_o^{\,2} = \frac{1}{2}(m_o + F_m m_1)v_1^{\,2} \tag{E-28}$$

The initial velocity of the hammer just after it collides with the soil is then:

$$v_1 = \sqrt{\frac{m_o v_o^{\,2}}{m_o + F_m m_1}} = \sqrt{2gh\frac{m_o}{m_o + F_m m_1}} = \sqrt{2gh\frac{m_o}{m}} \tag{E-29}$$

By substituting Equation E-29 into Equation E-27, the spring stiffness, k, can be found based on the peak acceleration measured by the ATM:

$$k = \frac{(m_o + F_m m_1)^2 A_p^{\,2}}{2ghm_o} \tag{E-30}$$

It is assumed that the soil is compressed in a rigid cylinder such that the radial displacement is zero. Under these conditions, the constrained modulus, D, is determined for the system stiffness, k, as (Drumm, et al. 1996):

$$D = k\frac{L}{A_{\text{sec}}} = \frac{(m_o + F_m m_1)^2 A_p^{\,2}}{2ghm_o}\cdot\frac{L}{A_{\text{sec}}} \tag{E-31}$$

where

L = the total height of the soil sample

A_{sec} = the cross sectional area of the soil sample

Based on the theory of elasticity, a linear elastic material will have a linear relationship between stress and strain. The relationship for vertical compressive stress and lateral expansion for an elastic cylinder under a uniaxial stress can be expressed by Equations E-32 and E-33 (Lamb and Whitman, 1969):

$$E = \frac{\sigma_z}{\varepsilon_z} \tag{E-32}$$

$$\varepsilon_x = \varepsilon_y = -\nu\varepsilon_z \tag{E-33}$$

where

E = Young's modulus of elasticity

σ_z = vertical stress

ϵ_x, ϵ_y, ϵ_z = strains in the x, y, and z directions

ν = Poisson's ratio

Poisson's ratio is the relationship between lateral strain and axial strain and is expressed as (Gere and Timoshenko, 1990):

$$\nu = \frac{\varepsilon_x}{\varepsilon_z} \tag{E-34}$$

$$\nu = \frac{\varepsilon_y}{\varepsilon_z} \tag{E-35}$$

The generalized Hooke's law for three-dimensional stress consists of the triaxial equations (Gere and Timoshenko, 1990):

$$\varepsilon_x = \frac{1}{E}\left[\sigma_x - \nu(\sigma_y + \sigma_z)\right] \tag{E-36}$$

$$\varepsilon_y = \frac{1}{E}\left[\sigma_y - \nu(\sigma_z + \sigma_x)\right] \tag{E-37}$$

$$\varepsilon_z = \frac{1}{E}\left[\sigma_z - \nu(\sigma_x + \sigma_z\right] \tag{E-38}$$

For a state of confined compression, the strains in the x and y directions are zero and the constrained modulus, D, can be written as (Lamb and Whitman, 1969):

$$D = \frac{\sigma_z}{\varepsilon_z} = \frac{E(1-\nu)}{(1+\nu)(1-2\nu)} \tag{E-39}$$

By rearranging Equation E-39 and substituting the equations for constrained modulus (Equation E-31), the resilient modulus of the soil can be calculated:

(Resilient Modulus for Peak Method)

$$M_r = \frac{(1+\nu)(1-2\nu)}{(1-\nu)} D = \frac{(1+\nu)(1-2\nu)}{(1-\nu)} \cdot \frac{(m_o + F_m m_1)^2 A_p^{\ 2}}{2ghm_o} \cdot \frac{L}{A_{sec}} \qquad \text{(E-40)}$$

The resilient modulus of a sample is dependent on the deviator stress applied. The deviator stress can be derived in the following manner. For constrained compression, the radial stress can be expressed as (Lamb and Whitman, 1969):

$$\sigma_r = \sigma_x = \sigma_y = \frac{\nu}{1-\nu}\sigma_z \qquad \text{(E-41)}$$

where

σ_r = radial stress

The deviator stress for confined compression is:

$$\sigma_d = \sigma_1 - \sigma_3 = \sigma_z - \sigma_r \qquad \text{(E-42)}$$

where

σ_d = deviator stress

Substituting the radial stress equation (Equation E-41) into the equation for deviator stress (Equation E-42):

$$\sigma_d = \sigma_z - \frac{\nu}{1-\nu}\sigma_z \qquad \text{(E-43)}$$

Equation E-43 can be simplified:

$$\sigma_d = \sigma_z\left[1 - \frac{\nu}{1-\nu}\right] \qquad \text{(E-44)}$$

Then

$$\sigma_d = \sigma_z \left[\frac{1-\nu}{1-\nu} - \frac{\nu}{1-\nu} \right] \tag{E-45}$$

Finally

$$\sigma_d = \left[\frac{1-2\nu}{1-\nu} \right] \sigma_z \tag{E-46}$$

The vertical stress applied by the hammer to the soil is:

$$\sigma_z = \frac{A_p m_o}{A_{\text{sec}}} \tag{E-47}$$

Therefore the deviator stress can be calculated by using the peak acceleration from the ATM:

(Deviator Stress)

$$\sigma_d = \frac{1-2\nu}{1-\nu} \cdot \frac{A_p m_o}{A_{\text{sec}}} \tag{E-48}$$

A second way to calculate the resilient modulus of the soil is to use the area under the acceleration curve. The area underneath the acceleration curve from time zero to the peak acceleration can be measured. This area represents the velocity of the hammer. In this way, the velocity is not calculated but actually measured using the ATM, reducing

the amount of error in the underlying assumptions. The area underneath the curve replaces the velocity term in Equation E-40:

(Resilient Modulus for Area Method)

$$M_r = \frac{(1+\nu)(1-2\nu)}{(1-\nu)} \cdot \frac{(m_o + F_m m_1)^2 A_p^{\,2}}{Area^2 m_o} \cdot \frac{L}{A_{sec}} \qquad \text{(E-49)}$$

References

Das, B.M. (1993). "*Principles of soil dynamics.*" PWS-KENT Publishing Company, Boston.

Drumm, E.C., Li., Z., Reeves, J.S., and Madgett, M.R. (1996). "Alternative test method for resilient modulus of fine-grained subgrades." *Geotechnical Testing Journal*, ASTM, Vol 19, No. 2, 141-154.

Gere, J.M., and Timoshenko, S.P. (1990). "*Mechanics of materials 3rd* edition." PWS-KENT Publishing Company, Boston.

Lamb, T.W., and Whitman, R.V. (1969). "*Soil Mechanics.*" John Wiley and Sons, New York.

Li, Z. (1992). "An alternative test method for resilient modulus of fine grained subgrades," Thesis presented in partial fulfillment of the requirements for the Master of Science Degree, Department of Civil Engineering, University of Tennessee, Knoxville, TN.

Wylie, C.R. (1979). "*Differential Equations.*" McGraw-Hill Book Company, Inc., New York.

Appendix F ATM Integration

To verify that the ATM program calculates the correct maximum displacement, an artificial time-acceleration history was input into a signal file. The artificial signal, which is similar in period and amplitude to actual ATM signals, is a sine function shown in Graph F-1. The function starts at time equal to zero and continues to 0.0023 sec. The sine function can be described by the following equation:

$$a = 588.600 \sin(1365.91t) \tag{F-1a}$$

or

$$a = C_1 \sin(C_2 t) \tag{F-1b}$$

Where

$C_1 = 588.600$ m/sec^2 = maximum acceleration

$C_2 = 1365.91$

Integrating Equation F-1b from 0 to 0.00230 sec yields the velocity:

$$v = \int_0^{0.0023} C_1 \sin(C_2 t) dt \tag{F-2}$$

$$v = -\frac{1}{C_2} C_1 \cos(C_2 t) + C_v \tag{F-3}$$

C_v is found by solving equation F-3 for the for v(0.00115) = 0 m/sec.

$C_v = 3.03843X10^{-10}$

Integrating Equation F-3 from time 0 to 0.0023 sec yields the displacement:

$$d = \int_0^{0.0023} \left(-\frac{1}{C_2} C_1 \cos(C_2 t) + C_v \right) dt \tag{F-4}$$

$$d = -\frac{1}{C_2^{\,2}} C_1 \sin(C_2 t) + C_v t + C_d \tag{F-6}$$

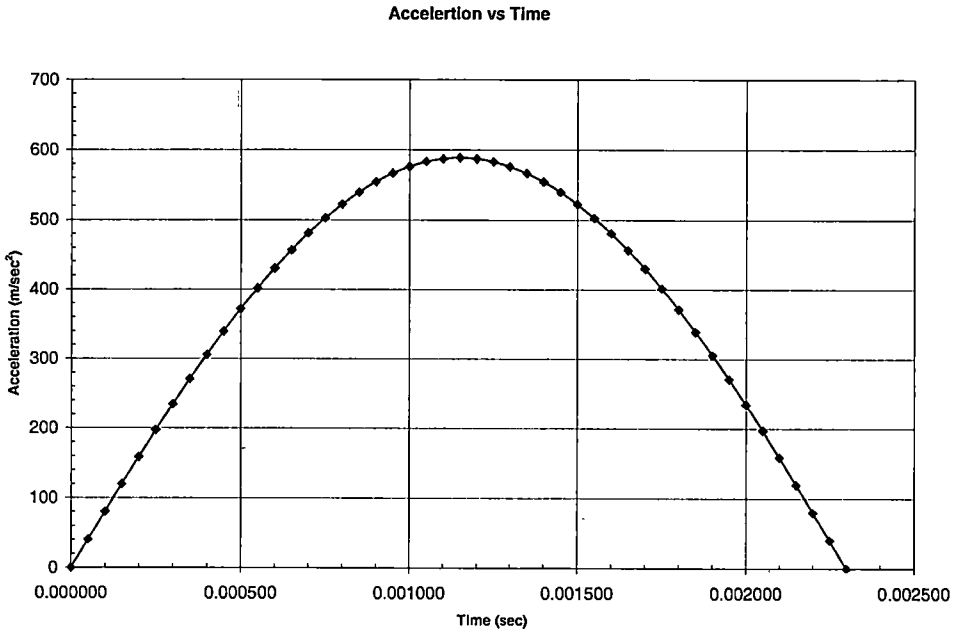

Graph F-1 Artificial Signal Used for Verification

Since the d(0) = 0, the C_d term is equal to zero and the final equation for displacement is:

$$d = -\frac{1}{C_2^{\,2}} C_1 \sin(C_2 t) + C_v t \qquad \text{(F-7)}$$

The maximum displacement from Equation F-7 is found by solving the equation from time when the velocity is zero. The velocity is zero at 0.00115 sec. The maximum displacement from the closed-form solution is $d_{\max} = 3.15483x10^{-4} m$.

The closed-form sine function, shown in Graph F-2, was then input into the ATM program to obtain the maximum displacement. The ATM code converts voltage to acceleration before the integration begins. The maximum displacement was found to be $1.5042x10^{-6}$ m, occurring at 0.00110 sec. The displacement from the ATM did not agree with the closed-form solution. It was suspected that the sampling rate of 0.00005 sec was the cause of the discrepancy. The displacement was recalculated for the sampling rate divided by 3 and by 30. The results are shown as "ATM solution with $\Delta\delta_{max}$" in List F-1. As can be seen from the list, the increased sampling rate reduced the displacement. The value appears to be converging to zero, which suggests an unstable integration scheme. Decreasing the sampling interval should make the approximate solution converge to the closed-form solution. The same integration technique used in the ATM program was then reproduced using Microsoft Excel. The results of the analysis are also shown in List F-1 under the heading "Excel solution with $\Delta\delta_{max}$." The Excel results are of the same order of magnitude as the ATM values and have the same trend of decreasing displacement with increased sampling rate. These findings lead to the conclusion that the results in Chapter 4 were in error.

	Displacement (m)				
Sampling Rate (sec)	Closed Form Solution	Excel Solution with v_o	Excel Solution with $\Delta\delta_{max}$	ATM Solution with v_o	ATM Solution with $\Delta\delta_{max}$
5.00×10^{-5}	3.1548×10^{-4}	3.1524×10^{-4}	1.4698×10^{-6}	3.1833×10^{-4}	1.5042×10^{-6}
1.67×10^{-5}	3.1548×10^{-5}	3.1546×10^{-4}	1.6348×10^{-7}	3.0881×10^{-4}	1.6218×10^{-7}
1.67×10^{-6}	3.1548×10^{-6}	3.1548×10^{-4}	1.6350×10^{-9}	3.0634×10^{-4}	1.6028×10^{-9}

List F-1 Displacements for the Sinusoidal Closed-Form Solution

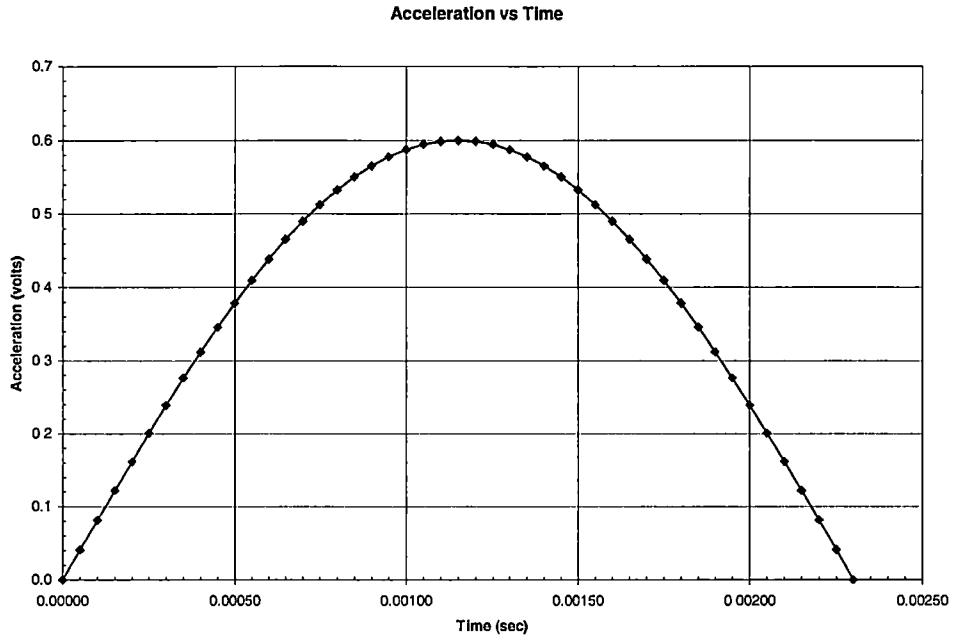

Graph F-2 Artificial Signal Used for Verification in ATM

The ATM used an integration technique that found the maximum change in displacement, not the peak displacement of the sample. In the integration technique, a plot of change in velocity versus time was made. This was accomplished by using the Trapezoidal Rule described in Chapter 4. The change in velocity versus time curve was then integrated to produce a change in displacement versus time curve. The largest value from the change in displacement curve was recorded as the maximum displacement, when in fact it is the maximum change in displacement. This technique was used because it did not require an initial velocity.

A better approach to integrating the sinusoidal curve is to integrate the time-acceleration history and plot the time-velocity history. The time-velocity history can be graphed by assuming the initial velocity as the area underneath the time-acceleration curve from time zero to the time of peak acceleration. The closed form solution was reanalyzed in the ATM program and the Excel spreadsheet using this method. The results can be seen in List F-1 under the column heading "solution with v_o." The results from both approximations are very close to the closed-form solution and are not significantly affected by the selected sampling rate, which indicates that the default sampling rate is adequate for ATM data collection of time-acceleration histories.

Regardless of the hammer weight used in the ATM, all of the peak accelerations are close to the 0.6 volts used for the closed form solution. Using the displacement found in the closed-form and original ATM program, the resilient modulus for each solution can be calculated for this artificial time-history assuming that both hammer weights are used, that Poisson's ratio remains at 0.45, and that the correction factor stays at 0.30. Using the

erroneous displacement from the ATM, the modulus is determined to be 451 MPa and the correct modulus for the closed-form is determined to be 2.15 MPa. The small value of modulus from the closed-form indicates that more research needs to be done on the affect of the sample length and mass participation factor in order for the calculated value to agree with modulus values measured in the laboratory.

Vita

Jason Cathey was born in Nashville, Tennessee on January 20, 1976. He lived in Smyrna, Tennessee and graduated Smyrna High School in 1994. The author enrolled at the University of Tennessee, Knoxville in the fall of 1994 and graduated with a Bachelor of Science in Civil Engineering in May 1999. He later enrolled in the graduate program the following fall. There the author worked on a Master of Science Degree in Civil Engineering with an emphasis on Geotechnical Engineering.